Università degli Studi di Napoli Federico II

DOCTOR of PHILOSOPHY in
BIOLOGY
XXXVIII Cycle

Translational Control by RNA-Binding Proteins in Cell-Free Expression Systems

SUPERVISOR
Dr. Velia Siciliano

CANDIDATE
Dudu Boyvat

CO-SUPERVISOR
Prof. Caterina Missero

Ph.D. COORDINATOR
Prof. Sergio Esposito

Academic Year 2022-2025

Translational Control by RNA-Binding Proteins in Cell-Free Expression Systems

A THESIS
SUBMITTED TO THE DEPARTMENT OF BIOLOGY OF UNIVERSITÀ DEGLI STUDI DI NAPOLI FEDERICO II
FOR THE DEGREE OF
DOCTOR OF PHILOSOPHY

By
Dudu Boyvat
2025

Abstract

Cell-free systems provides a cost-effective and versatile platform for biosensor applications, offering rapid responses, simplified workflows, and enhanced stability compared to cell-based systems. However, despite these advantages, their regulatory flexibility (especially at the level of transcriptional repression) remains limited, limiting their dynamic range and robustness. To address this gap, this study investigates post-transcriptional control strategies based on RNA-binding proteins (RBPs) to enhance translational repression in vitro.

I designed and characterized genetic circuits regulated by the RBPs MS2-CNOT7 and L7Ae to assess their repression efficiencies in different cell-free systems, including rabbit reticulocyte lysate, E. coli lysate, and the reconstituted cell-free system. MS2-cNOT7 exhibited minimal repression in these contexts, while L7Ae showed measurable but variable repression, particularly in RRL. Based on these findings, I evaluated different genetic architectures and expression protocols in both E.coli lysate and the PURE system. My findings identified that as the most consistent platform for potent RBP-mediated suppression, particularly when combined with optimized backbone design and pre-incubation strategies.

Finally, I created an additional layer of translational control capable of responding to viral protease activity by integrating engineered L7Ae to make the protease-responsive module. This work provides a foundation for the development of in vitro protease biosensors and contributes to next-generation diagnostic platforms based on programmable, genetically encoded editing in cell-free systems.

Acknowledgement

I would like to express my deepest gratitude to my supervisor, Dr. Velia Siciliano, for her continuous guidance, support, and encouragement throughout my PhD journey. Her scientific insight, constructive feedback, and patience have been invaluable in shaping both my research and professional development.

I am also grateful to my postdoctoral supervisor, Dr. Lucia Casella, for her mentorship, enthusiasm, and constant willingness to share her expertise. Her dedication and attention to detail have greatly contributed to the progress and quality of my work. I am also thankful to Lucia for sharing Polda and Sisma's life, which consistently brought me joy and served as a small but meaningful source of happiness.

I would like to sincerely thank our technicians, Daniela, Fabiana, and Mario, for their constant help, kindness, and willingness to step in whenever needed. Their support not only made our work more efficient but also made daily lab life much easier and more enjoyable. I am truly grateful for their contribution to this project and the positive atmosphere in the lab.

I would also like to thank all the members of the SynBio and SYNSENSO teams for their collaboration, inspiring discussions, and for creating such a warm and supportive research environment. Working alongside such talented colleagues has truly been both a privilege and a joy. I am especially grateful to the SynBio and SYSENSO team for the unforgettable trips and tours we shared; memories will always be a treasure.

I want to express my deepest gratitude to my friends and family for their unconditional love, endless patience, and constant encouragement. Your belief in me has been my greatest source of strength and motivation throughout this entire journey. None of this would have been possible without you. You are truly the best family anyone could ever ask for. If I had the chance to choose my family all over again, I would choose you across every universe, at every moment. Thank you for always being by my side.

It may not be entirely conventional to thank a therapist in an academic thesis, yet I must acknowledge that finding the right therapist was one of the most meaningful discoveries I made during my doctoral process.

Finally, I want to express my deepest gratitude to my beloved friend Aybala, whom I lost so tragically in the earthquake on February 6, 2023. Aybala, your absence is felt every day, yet your presence remains a comforting whisper in my heart. Throughout this entire journey, I have felt you beside me, your strength, your unwavering support, your love, and hearing you laugh in my memories, supporting me through every challenge. The unexpected loss of you has left a void that nothing can fill. I miss you endlessly, and I will always remember you with your big laugh and your tight hugs that felt like they could break my ribs. That warmth lingers in my heart, along with the ache of missing you. I'm waiting for the day we will meet again. You will always be my best friend.

Table of Contents

List of Figures

List of Tables

List of Abbreviations

AA	Amino acid
ARCA	Anti-reverse cap analog
BB1	Backbone 1
BB2	Backbone 2
BYL	Tobacco by-2 lysate
CAR	Chimeric antigen receptor
CFME	Cell-free metabolic engineering
CFS	Cell-free system
CHO	Chinese hamster ovary
DBD	DNA binding domain
EGFP	Enhanced green fluorescent protein
FCE	Faustovirus capping enzyme
HBC	Hepatitis b core antigen
HTS	High-throughput screening
KT	Kink turn
LOD	Limit of detection
LUC	Luciferase
MCS	Multiple cloning site
ML	Machine learning
NCAA	Non-canonical amino acids
NLUC	Nanoluciferase
PLA	Polylactic acid
PURE	Protein synthesis using recombinant elements
RBP	RNA-binding protein
RLU	Relative light units

RRL	Rabbit reticulocyte lysate
RRM	RNA recognition motif
TCS	TEV cleavage site
TEV	Tobacco Etch Virus
TEVP	TEV protease
TL	Translation
TX	Transcription
UTR	Untranslated regions
VLP	Virus-like particles

To my family, who bring beauty to everything in this universe.

Bu evrendeki her şeye güzellik katan aileme.

Introduction

1.1 Synthetic Biology – Overview and Significance

The rise of synthetic biology at the beginning of the 21st century marked a significant transition to combining engineering and the life sciences, and it allowed us to view biological systems as programmable quantities (Cameron et al. 2014). It has become a rapidly growing field that is rooted in turning biological processes into mathematical models and using the concepts of electrical circuits in biological pathways (Khalil and Collins 2010). In contrast to classical genetic engineering, which typically focused on single-gene modifications, this new field pointed out the rational design of complex biological systems with predictable functions (Purnick and Weiss 2009). Synthetic biology focuses on engineering biological circuits, metabolic processes, and entire genomes in a predictable and modular manner (Weber and Fussenegger 2009). It is a discipline that combines the concepts from biology, engineering, and computer science to modify and reprogram living cells and systems for novel applications (Garner 2021).

The genetic switches and the oscillator represent some of the advancements in the field of regulatory circuits in synthetic biology. The circuits demonstrated the possibility of engineering cellular behavior in a logic of electrical circuits (Elowitz and Leibler 2000; Gardner et al. 2000). Over time, the applications of synthetic biology have diversified, extending from metabolic pathway engineering to disease treatment and environmental and healthcare solutions (Ruder et al. 2011).

Recent advancements in DNA synthesis, high-throughput sequencing, and computational modeling have sped up the design-build-test cycle, which is core to synthetic biology (Kelwick et al. 2014; Xiang et al. 2018). This acceleration enables the construction of more complex genetic systems.

Important achievements in the field include the production of pharmaceutical and important compounds such as the antimalarial precursor artemisinin, which shows the translational impact of engineered pathways (Paddon et al. 2013). Beyond industrial applications, synthetic biology has also provided a deep understanding of the design principles of natural regulatory networks, offering new insights into the complexity of cellular systems and helping to understand the biological systems (Cameron et al. 2014). Taken together, these advances highlight that integrating molecular biology and engineering is transforming

biotechnology and medicine in favour of humanity and the environment. (Alberts 2011) (**Fig. 1.1**).

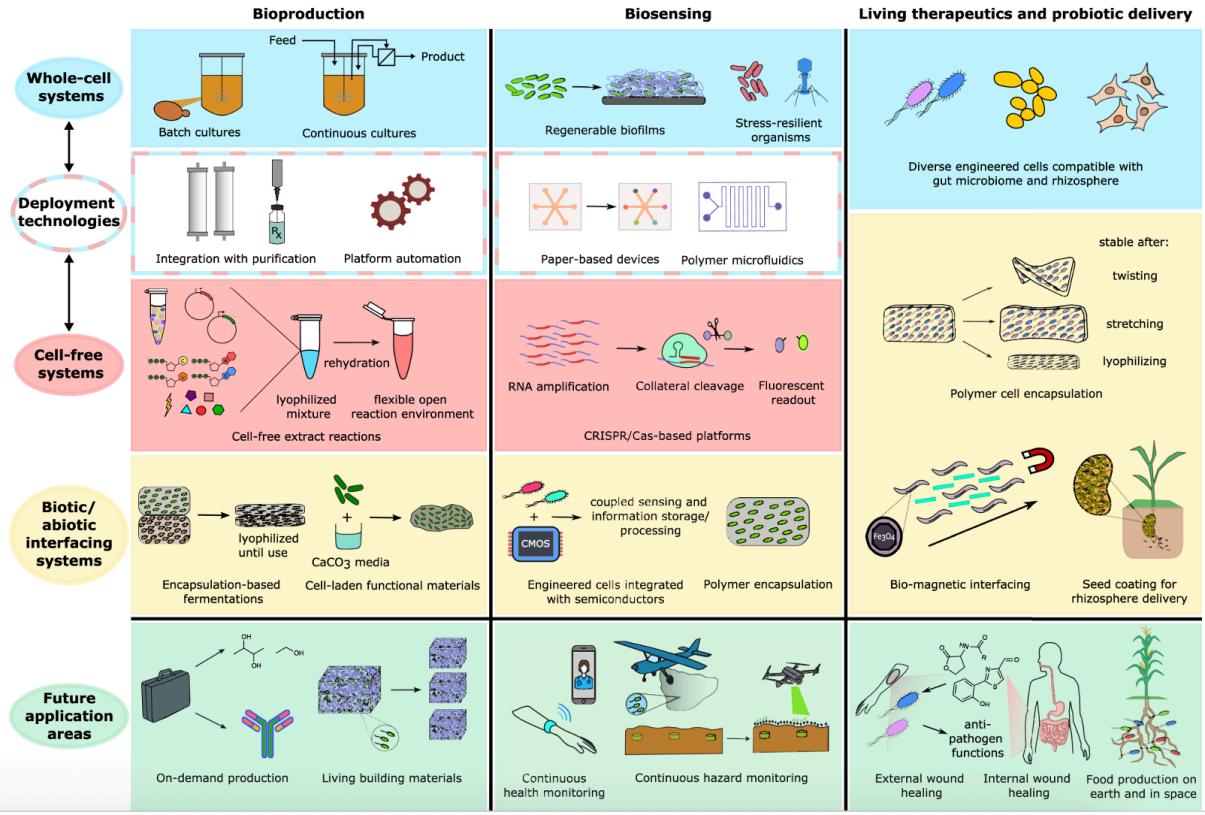

Figure 1.1 Design strategies for deploying synthetic biology systems outside the laboratory. This schematic illustrates system types (whole-cell, cell-free, and biotic/abiotic interfaces) and application areas (bioproduction, biosensing, living therapeutics, and probiotic delivery) in synthetic biology. Adapted from (Brooks and Alper 2021).

Synthetic biology offers a versatile framework that facilitates the early detection and prevention of diseases, along with the development of targeted and personalized treatments (Tan et al. 2021; Jain 2013). Lage and colleagues' development of a synthetic vaccine to help prevent infection with Leishmania infantum, which has an annual infection rate of about one million and a global death toll of up to 50,000 this is an important example of how synthetic biology can benefit healthcare as a prevention(Lage et al. 2020). In the field of diagnostics, synthetic biology presents considerable advancements and innovative tools that significantly improve detection capabilities. Synthetic biology facilitates the availability of diagnostic systems that function across various regulatory levels, including transcriptional and translational biosensors(Wang and Tan 2023). Additionally, it allows for the integration of dynamic behaviours, such as genetic oscillators, to improve signal processing capabilities, and

one recent example is Martorell and colleagues recently developed a biosensing platform for detecting norovirus in fecal samples (Martorell et al. 2025).

Biosensors are not only considered a diagnostic tool for disease but also widely used for environmental concerns. In environmental monitoring, these devices play an important role by identifying contaminants and pollutant substances, as a result, helping to assess ecological health more effectively (Fdez-Sanromán et al. 2025; Xiao et al. 2025). Biosensors, for instance, have been used extensively for the purpose of detecting pollutants in water and soil and food safety (Huang et al., n.d.; Zhang et al. 2022). These pollutants include heavy metals, pesticides, and pathogens. Biosensors offer a number of benefits, including sensitivity, portability, and real-time measurement technology (Rojas-Villacorta et al. 2022). Technological progress, such as the use of nanomaterials and microfluidic systems, has made biosensors work even better, allowing for continuous and on-site assessments of environmental quality(Siavashy et al. 2024).

Synthetic biology plays a key role in developing therapies such as chimeric antigen receptor (CAR) therapy. This approach involves engineering a patient's own immune cells and reintroducing them into the body, thereby minimizing the toxicity associated with immunotherapy(Clubb et al. 2023). In addition to this strategy, using and engineering microorganisms represents another important topic in synthetic biology, offering novel possibilities for treatment development. In addition to all those, synthetic biology also enables scientists to develop platforms for testing these preventive, diagnostic, and therapeutic products (Rooke 2013).

Synthetic biology offers a powerful advantage through the design of cellular systems that are capable of manufacturing important pharmaceuticals (Yan et al. 2023). Rather than relying on extraction from limited natural resources or complex chemical synthesis, these engineered systems redirect simple substrates toward the production of biologically active compounds by biotransformation (Sokolova et al. 2023). An example is the use of Saccharomyces cerevisiae, in which researchers have introduced an artificial biosynthetic pathway composed of multiple tailored genes to enable hydrocortisone biosynthesis (Feng et al. 2022). Approaches like this not only provide a more sustainable way to drug development but also expand access to molecules that are difficult to obtain. Advances in pathway engineering have made it possible to generate a wide range of pharmaceutical products with improved yield and scalability, showing the versatility of synthetic biology in therapeutic

innovation, in addition to supporting drug development, synthetic biology also helps researchers with drug delivery (Khalil and Collins 2010).

1.2 Cell-Free Systems: Principles and Development

Cell-free systems (CFS) have emerged as a significant platform in biotechnology and synthetic biology, providing a regulated environment for protein synthesis and metabolic reactions independent of living organisms. These systems offer an open and adjustable setup for studying gene expression, constructing biosensors, prototyping genetic circuits, and producing useful and important biomolecules by removing the complexities of cellular physiology (Garenne et al. 2021; Vilkhovoy et al. 2020).

In the middle of the 20th century, Nirenberg and Matthaei used crude *E. coli* extracts to decipher the genetic code, thereby demonstrating the potential of *in vitro* transcription and translation systems. This was the beginning of cell-free translation and transcription systems. (Nirenberg and Leder 1964). Over the following decades, cell-free extracts from rabbit reticulocytes, wheat germ, and *E. coli* became increasingly used for the purpose of conducting research on molecular biology. Later advancement was on protein synthesis using purified and defined components rather than crude lysates, which was made possible by the development of the PURE (Protein Synthesis Using Recombinant Elements) system in 2001 (Shimizu et al. 2001). It was a significant milestone in the field of protein synthesis. These improvements turned cell-free systems from basic research tools into flexible platforms for use in biotechnology and industry (**Fig. 1.2**).

The essential transcriptional and translational machinery, such as ribosomes, tRNAs, RNA polymerases, and translation factors, is supplied *in vitro* by cell-free systems in order for them to function(Cui et al., n.d.). Since they are not limited by the viability of the cell, they enable great flexibility in the control of reaction conditions, and they also allow us to incorporate unnatural factors. (Gao et al. 2019; Zhang et al. 2021). In addition, toxic proteins, membrane proteins, and other challenging products to express can be synthesized within cell-free systems compared to traditional living host organisms (Hodgman and Jewett 2012). Moreover, the open nature of these systems facilitates direct manipulation of metabolic fluxes, energy regeneration pathways, making them an attractive tool for systems biology and synthetic biology research (Kim and Swartz 2001; Silverman et al. 2020).

In recent years, cell-free systems have evolved into a robust technology with applications across multiple areas. Their application allows us to rapidly prototype genetic

circuits and reduces the optimization time from days to hours (Caschera 2025). And it greatly accelerates the design-build-test cycle in synthetic biology (Sun et al. 2013). There have been encouraging developments in the use of cell-free systems in industry, particularly due to their scalability and cost-efficiency, which make them valuable for optimizing the production of pharmaceuticals, therapeutic proteins, beneficial chemicals, and proteins that are difficult to express in cell-based systems (Vilkhovoy et al. 2020; Zawada et al. 2011). Moreover, the integration of automation and computational methods promotes the development of high-throughput, miniaturized systems, which leads to new possibilities for more sustainable and flexible biomanufacturing (Brookwell et al. 2021; Silverman et al. 2020).

These advancements are based on the critical processes of transcription and translation, which are performed *in vitro* outside of the cellular environment. A deep understanding of *in vitro* transcription and translation is critical to work with cell-free systems and their potential adaptation for a variety of biotechnological applications.

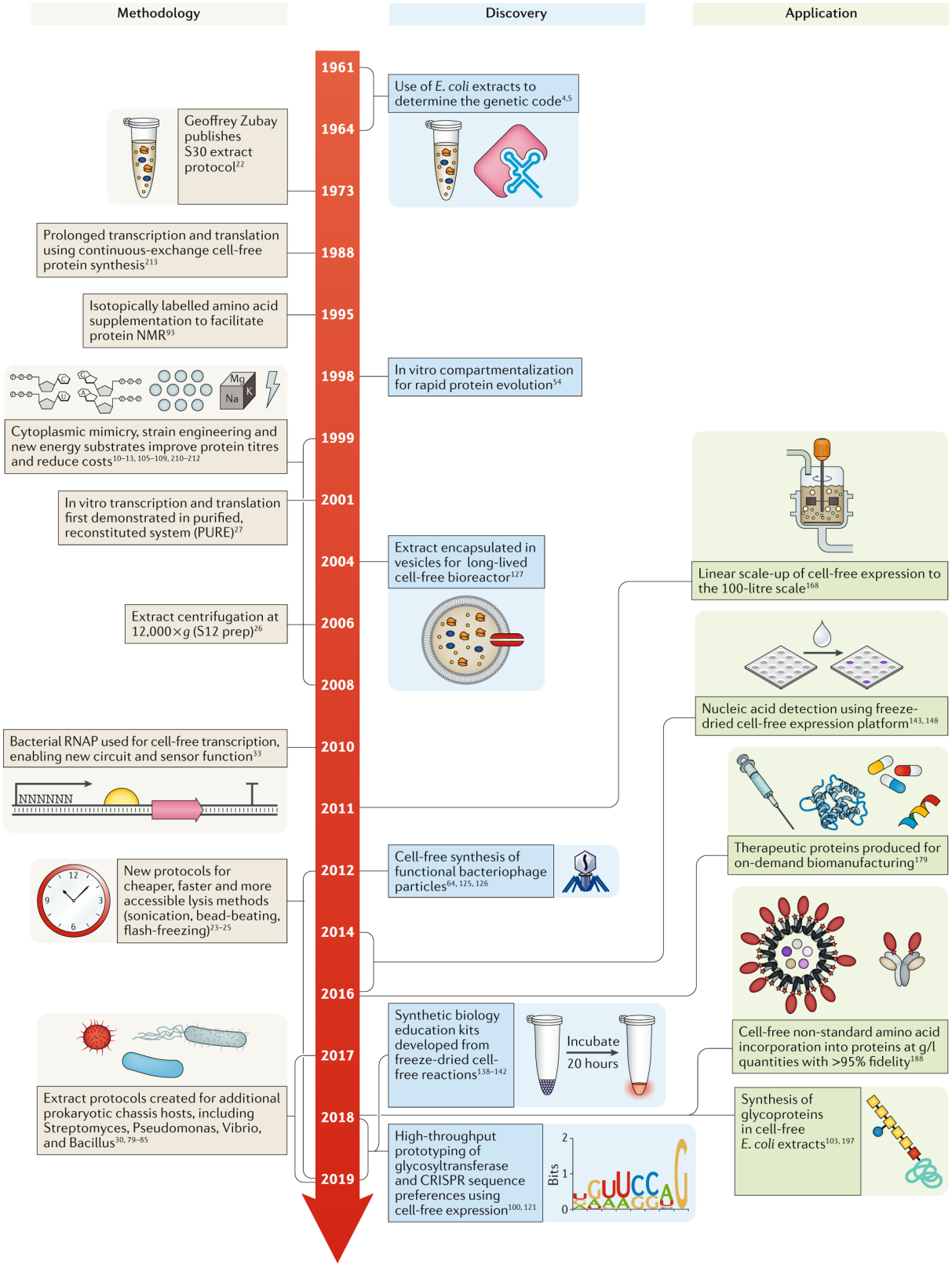

Figure 1.1 A chronological overview of cell-free gene expression systems. Emphasizing key practical improvements and innovations achieved in the last 20 years, adapted from (Silverman et al. 2020).

1.2.1 *In Vitro* Transcription (TX)

In vitro transcription (IVT) is a technique used to produce RNA from a DNA template outside the cell. This technique was first developed by the discovery of bacteriophage RNA polymerases like T7, T3, and SP6, and in a short time, it became one of the important molecular techniques (Milligan and Uhlenbeck 1989). IVT is decoupling the complexity of in vivo conditions and offering an independent system to produce RNA in a more controlled manner. This property is making the IVT widely used, particularly in research fields that require the synthesis of functional RNA, such as aptamers or the production of guide RNA in CRISPR-Cas studies (Gao and Zhao 2014; Famulok et al. 2007)

In recent years, advancements in mRNA vaccines and therapeutics have positioned IVT in a strategically significant role within the field of biomedicine. Investigation and inquiry into a specific subject matter (Sahin et al. 2014). During the COVID-19 pandemic, mRNA vaccines were rapidly introduced for clinical use, and it showed that it is possible to produce mRNA on an industrial scale with high purity. These developments also showed that IVT is not only useful for basic scientific research but also it is critically important for clinical studies and industrial applications. However, even if it's widely used, the method has several limitations in terms of purity and efficiency, such as contamination of double-stranded RNA (dsRNA) and possible by-products produced during the transcription, which may cause incomplete transcript production (Perenkov et al. 2023; Lenk et al. 2024). To overcome these limitations, different strategies are tested, such as designing RNA polymerase binding sites, optimizing the promoter sequences, and, most importantly, the reaction conditions (e.g., Magnesium ion concentration, temperature) make it possible to have increased yields and improved purity for IVT reactions (Samnuan et al. 2021; Perenkov et al. 2023; Kartje et al. 2020; Youssef et al. 2023). In addition, improving the purification step after the IVT (e.g., HPLC, cellulose-based chromatography) especially improves the dsRNA contamination (Weissman et al. 2013; Baiersdörfer et al. 2019). Also, implementation of computational methods, like in the other fields, is used to improve and optimize the IVT reaction (McMinn et al. 2024).

To deeply understand the IVT workflow, it starts with designing the DNA template. The stability and efficiency of synthesized RNA are strongly dependent on designing the structural elements. It can be defined by main structural elements, which are the promoter selection, 5' cap, UTRs, the open reading frame (ORF), and the 3' poly(A) tail. Depending on the RNA polymerase used, a proper promoter should be selected. 5' and 3' untranslated regions

(UTRs) should be designed carefully since they are critically important for initiation of the transcription and the stability of mRNA (Jia and Qian 2021).

5’ UTR is a critical element that affects and regulates translation. In eukaryotic systems, it changes between 100 and 200 nt. It is also stated that GC content and codon usage are effective in transcription initiation, stability, and the formation of secondary structure (McClellan 2000; Mordstein et al. 2020). Certain modifications, capping, can be implemented at the 5′ end of the transcripts, which is suggested to be necessary to obtain efficiently functioning RNA. The synthesized RNA can be capped with different methods. 5’ cap can be introduced via enzymatic reaction, post-transcriptionally, or the cap can be introduced co-transcriptionally with cap analogs. Enzymatic capping facilitates the addition of a m7G cap to the 5′-triphosphate ends of RNA through the action of vaccinia or Faustovirus Capping Enzyme (FCE) virus capping enzymes (VCE)(Ogino 2013; Chan et al. 2023). But it has the risk of reverse incorporation (Kuhn et al. 2010). To eliminate this risk, there are several synthetic caps, including an anti-reverse Cap analog known as ‘ARCA’ and a Cap dinucleotide referred to as CleanCap®(Tusup et al. 2019).

The 3' (UTR) is also crucial to increase the mRNA stability and translation efficiency. Poly (A) tail is also an important component of the 3’ UTR. The poly(A) tail plays a crucial role in providing stability to mRNA molecules, thereby significantly improving the efficiency of translation processes. It can be incorporated into the gene of interest while designing the DNA template, or it may be introduced after the transcription process through an alternative protocol (Sahin et al. 2014; Youssef et al. 2023). (Figure: Jia and Qian 2021)

1.2.2 *In Vitro* Transcription-Translation (TX/TL) Platforms

In vitro translation is a powerful biotechnological tool that translates RNA into DNA. Since it is an *in vitro* system, it doesn’t have the concerns that arise from cell-based systems’ complexity, such as the production of toxic proteins, hard-to-translate membrane proteins, or integration of unnatural amino acids to protein production (Gregorio et al. 2019). In addition to all these, it also enables us to have a fast and controlled protein synthesis (Sawasaki et al. 2002). Consequently, various parameters, including pH levels, ion concentrations, energy regeneration systems, and the presence of chaperone proteins, can be readily manipulated, allowing for studying the protein synthesis process. The *in vitro* translation system can be classified into lysate-based and reconstituted systems. Lysate-based systems can be cell lysates prepared from *E. coli,* rabbit reticulocytes, wheat germ, and human cells. Prokaryotic lysates generally offer higher yields, while eukaryotic lysates allow for post-translational

modifications (Thoring et al. 2019). A common challenge faced in lysate-based systems is the degradation of DNA or RNA templates, which occurs due to the activities of endogenous nucleases and proteases (McSweeney and Styczynski 2021; Schinn et al. 2016). Purified (Reconstituted) systems, also known as PURE (Protein Synthesis Using Recombinant Elements), provide a more regulated experimental setting since it is a recombinantly reconstituted systems, and they consist of defined and purified components, and the system is free from undesirable activities such as nucleases and proteases. This feature is particularly advantageous for sensitive experiments requiring high purity and controllability (Shimizu et al., 2001). Purified PURE systems offer higher purity and easier manipulation compared to lysate-based systems (Gregorio et al. 2019). Additionally *in vitro* translation system can be used to design an experiment in a couple or linked format. Coupled systems mean that transcription and translation can be performed in the same system (Starting from DNA→RNA→Protein). Linked systems use RNA as a starting template (RNA→Protein).

1.2.3.1 *E. coli* Cell-Free Lysates

The *E. coli* cell-free system is among the most commonly used and well-characterized platforms in the field (Garenne et al. 2021; Hunt et al. 2025). Its advantageous system stems from its rapid growth, ease of culture, and high protein production. The lysate was mostly produced using the BL21 strain, which is optimized for protein production, but recently different strains have been tested and optimized for lysate preparation (Henrich et al. 2015; Krinsky et al. 2016). In comparison to other cell-free lysates, particularly those derived from eukaryotic sources, the preparation process is more straightforward (Gregorio et al. 2019). Lysates are typically generated through S30-based methodologies, which use the polymerases, ribosomes, and other internal components derived from *E. coli.* Moreover, lysates can be further enhanced by incorporating additional T7 polymerase, which serves to elevate the transcription rate, particularly when utilized alongside robust promoter elements. (Shrestha et al. 2012). *E. coli* lysate not only contains molecular machinery, but also necessary enzymes related to energy metabolism. While protein synthesis quickly stops when ATP is depleted in traditional systems, energy regeneration systems in modern lysates keep ATP and GTP levels stable for several hours by using, e.g. the reuse of phosphoenolpyruvate, creatine phosphate, or glycolysis pathways, allowing for efficient protein production (Calhoun and Swartz 2005).

The ionic conditions in a cell-free system play a crucial role in many aspects, such as controlling the crowding (Ge and Xu 2020; Cross et al. 1999). The concentration of magnesium ions serves as a crucial factor influencing the balance between transcription and

translation within a cell-free system derived from *E. coli* (Kapasiawala and Murray 2024). In addition to ions, lysates also contain amino acids, nucleotides, coenzymes, and polyamines (e.g., spermidine) to improve translational activity(Atkins et al. 1975). However, some factors can reduce translation efficiency, such as nuclease and protease activity. These factors can cause degradation of mRNA or protein. RNAse and protease inhibitors can be used to prevent such damage. Another approach is to use genetically modified strains to remove the protease and RNAse genes to prepare more stable and high-yield lysate preparations.(Hong et al. 2015; Jiang et al. 2002). The full range of possible additions to cell-free lysates demonstrates the potential for improvement in these systems. For example, one of the drawbacks of the *E. coli*-based system is its inability to reproduce post-translational modifications. However, these limitations can be addressed by adding supplements such as chaperones or microsomes (Jin et al. 2019).

1.2.3.2 Rabbit Reticulocyte Lysates

Rabbit reticulocyte lysate (RRL) is a commonly used system containing mammalian translational machinery. RRL is prepared by using precursor rabbit erythrocytes and contains tRNAs, aminoacyl tRNA synthetase, and other translational machinery (Jackson and Hunt 1983). Since the lysate contains translational machinery such as eIF4, eIF2, and eIF3, this allows the system to start the translation by recognizing the 5' cap structure of the eukaryotic mRNAs (Pelham and Jackson 1976). This makes the system more efficient and proper for the translation of eukaryotic mRNA compared to prokaryotic systems. For the translation in RRL, ATP and GTP are necessary and supported with creatine phosphate and creatin kinase system for the energy regeneration (Favre and Muellhaupt 2005; Merrick 2010). This improves the translation time and yield. Endogenous mRNA is eliminated by treating the lysate with micrococcal nuclease, an endo-exonuclease that selectively degrades single-stranded nucleic acids (Pelham and Jackson 1976; Zemella et al. 2015).

Since RRL consists of eukaryotic machinery, it has better protein folding than prokaryotic lysates but still requires the addition of microsomes in order to support complex post-translational modification such as glycosylation (Shields and Blobel 1978; Dougherty and Parks 1991).

Rabbit reticulocyte lysate (RRL) cell-free systems ins an *in vitro* translation system, meaning that the system requires mRNA templates for translation. This requirement needs an extra step for RNA transcription and purification. The instability of mRNA significantly reduces protein yield, therefore RRL is considered a less efficient systems available compared

to the other cell-free lysates (Gregorio et al. 2019). Furthermore, RRL lysate production necessitates a complex and time-consuming extraction process, making large-scale synthesis challenging (Jackson and Hunt 1983).

1.2.3.3 PURE Systems

The PURE (Protein Synthesis Using Recombinant Elements) system is a significant advancement in the field since it is a cell-free protein synthesis system that is reconstructed from the individually produced components from *E. coli* (Shimizu et al. 2001). Shimizu and his colleagues developed this new system in 2001, contributing significantly to our understanding of protein synthesis processes. This system has a well-defined structure, with each component, around 36, going through a purification process, and the exact composition of these components is adjusted (Grasemann et al. 2021). The PURE system is made up of several essential components, including ribosomes, tRNAs, and aminoacyl-tRNA synthases. It also contains translation factors like T7 RNA polymerase, eIF2, and eIF3 (Whittaker 2013). Additionally, the system includes energy regeneration systems such as creatine kinase, creatine phosphate, and adenylate kinase, as well as purified components from *E. coli* (Whittaker 2013). Considering that all components must be reconstituted by combining them synthetically rather than using the living organism resources, it is a more labour-intensive and expensive system than the lysate-based system (Lavickova and Maerkl 2019; Grasemann et al. 2021). Additionally, proteins can be synthesized with modifications such as N-terminal acetylation and myristylation in PURE (Matsumoto et al. 2023). This process is possible with the addition of a modifying enzyme into to PURE system (e.g., N-acetyltransferase or N-myristoyltransferase) and allows the production of a modified protein in a controlled and one-step reaction (Matsumoto et al. 2023; 2025).

Recent studies show that the PURE system is evolving from a traditional energy system to more efficient, modular, and sustainable systems. The progress made in pyruvate-based ATP regeneration, the utilization of single-enzyme polyphosphate kinase, the incorporation of glycolysis, and the conversion of plastic waste into amino acids make these systems especially attractive for both foundational research and biotechnological studies and fully autonomous artificial cell construction (Rothschild et al. 2024; Yadav et al. 2025; Doerr et al. 2019; Nishikawa et al. 2024).

1.2.3.3 Other Cell-free systems

There are several lysate-based cell-free systems used for studies, such as wheat germ and CHO lysates. Depending on the purpose of the study, different lysates can be used and modified.

1.2.3.3.1 Wheat Germ Lysate

Wheat germ lysate is one of the cell-free systems that most closely resembles eukaryotic cell translation mechanisms. Its high throughput makes it ideal for producing difficult proteins, such as membrane proteins. It is also used extensively in protein labeling and structural genomics research(Harbers 2014). The benefits of this system include high success rates and rapid protein production.

1.2.3.3.2 Chinese Hamster Ovary Lysate

Lysates from Chinese Hamster Ovary (CHO) cells can perform post-translational modifications, particularly glycosylation. These systems are used for a variety of applications, including therapeutic protein production and antibody synthesis. Because CHO lysates contain microsomal structures, they can also be used to produce membrane proteins(Thoring et al. 2016)

1.2.3.3.3 *Leishmania tarentolae* Lysate

Leishmania tarentolae, a nonpathogenic protozoan, makes an ideal platform for cell-free protein expression. It is simple to culture and can be used to produce large protein libraries at a high rate (Kovtun et al. 2011). This system is ideal for the rapid production and labeling of eukaryotic proteins.

1.2.3.3.4 HeLa Lysate

The cell-free lysates obtained by using HeLa cells are mostly used to synthesize human-based proteins. This system can perform post-translational modifications and is suitable to produce therapeutic proteins. On the other hand, additional components may be required to make modifications, such as glycosylation (Yadavalli and Sam-Yellowe 2015)

1.2.3.3.5 *Pichia pastoris* Lysate

Pichia pastoris cell-free lysates are particularly well-suited for eukaryotic protein production. This system promotes eukaryotic traits like post-translational modifications and disulfide bond formation. Furthermore, its high-throughput protein synthesis makes it ideal for use in biotechnology and structural biology(Spice et al. 2022).

1.2.3.3.6 *Vibrio natriegens* Lysate

Vibrio natriegens' lysate can produce a large amount of protein due to its rapid growth. It offers an alternative platform for rapid prototyping and high-throughput protein expression in cell-free environments. Furthermore, its short production times and high ribosome density give it an advantage over *E. coli* lysate in some applications(Wiegand et al. 2018).

1.2.4 Limitations of Cell-free Lysates

Cell-free systems are gaining attention in synthetic biology due to their ability to allow biological processes to occur without the need for the complex structures found in living cells. However, with advantages, there are several problems that restrict their broad application. If we follow the limitations that extend from the preparation of the lysate to the characterization of the components, the DNA or RNA template has an important impact on the reaction. Because the reaction results in the production of by-products, accumulation becomes a concern. Quantification of the small molecules will be the final step of discussing the limitations.

One of the major challenges is the difficulty in characterizing the lysates both structurally and functionally (Hunt et al. 2025; Swartz 2018). Cell lysates consist of multiple enzymes and metabolites, which make them complex and often difficult to understand, especially when the conditions are changed while preparing the lysates, such as stress, changes in lysis method, and growth media, or usage of engineered strains (Hunt et al. 2025; Falgenhauer et al. 2021; Contreras-Llano et al. 2020; Henrich et al. 2015). Even when following the same protocol, there can be notable differences in yield between extracts prepared at different times or by different people (Piorino et al. 2023). This creates challenges in standardization and complicates the understanding of reproducibility and scalability of the systems.

A further limitation is the impact of DNA templates on the system. The quality and preparation of the templates used have a direct impact on the efficiency of protein production (E. Romantseva et al. 2022; McManus et al. 2021; E. F. Romantseva et al. 2022). Additionally, when several genetic cassettes are included in the same reaction, the available transcription and translation resources need to be shared. This competition results in unpredictable changes, even without any regulatory connection between genes.

Another limitation of these systems is the duration of the reaction. Reactions often stop quickly because of changes in pH, by-product production, or fast depletion of crucial energy

molecules (Silverman et al. 2019; Karim et al. 2020; Garamella et al. 2016). Although generally protocols have been created to prolong reaction times, these solutions may not be appropriate for all applications (Burrington et al. 2021). This issue specifically creates a problem for applications requiring long-term stability.

Quantification is another important concern. Measuring the amount of small molecules accurately is still difficult, such as toxins (Silverman et al. 2020). The differences among various extract batches, the presence of inhibitory substances in samples accumulated through the reaction, might reduce the accuracy of measurements (Chipman et al. 2025; Dudley et al. 2015; Borkowski et al. 2020).

In summary, although cell-free systems have considerable potential, they encounter important challenges. The complexity, unpredictability, and difficulties in measurement restrict the wide use of this technology. Cell-free systems should be considered not only as simplified extracellular environments, but also as independent systems that have their own unique regulations and functioning mechanisms.

1.3 Biotechnology Applications of Cell-Free Systems

1.3.1 Protein Synthesis

Cell-free system is widely used to produce difficult-to-express proteins like toxins and complex proteins, membrane proteins, and virus-like particles (VLP) and proteins that are incorporated with non-canonical amino acids (Gregorio et al. 2019; Khambhati et al. 2019). Virus-like particles are gaining importance since they are playing an important role in vaccine development, drug delivery, gene therapy, and immunotherapies (Bundy et al. 2008). Production of these particles requires long and complex optimization and characterization processes when they are produced in cell-based systems(Spice et al. 2020). Thus, Armero-Gimenez and colleagues manufactured hepatitis B core antigen (HBc) variants in tobacco BY-2 lysate (BYL) and successfully scaled the reaction from 50 µL to 1L without having any decrease in production yield(Armero-Gimenez et al. 2023). Another example is the production of norovirus VLPs for the first time in *E.coli*-based lysates. Norovirus particles are produced in 4 hours to assemble the Human noroviruses (Sheng et al. 2017). In summary, cell-free systems have become attractive due to their structural stability, rapid production, and high optimizability (Hu and Kamat 2023).

Cell-free systems provide a directly controlled environment, a more flexible and efficient platform to produce therapeutic proteins that can be toxic, difficult to express, or that

require high purity. It also provides advantages by eliminating time-consuming steps in the transfection, clone selection, and expansion protocol (Dondapati et al. 2020). Cell-free platforms support drug analysis by facilitating labeling applications (Zemella et al. 2015; Dondapati et al. 2020). Cell-free system platforms with the integration of artificial intelligence and machine learning (AI/ML) methods offer powerful technology in the field areas of proteome engineering, prototyping acceleration, and de novo biotherapeutic designs (Caschera 2025).

CFPS enables the incorporation of non-canonical amino acids (ncAA) other than the 20 natural amino acids into the protein, thanks to the direct intervention in the reaction (Hunt et al. 2025). This enables the redesign of protein functions. The precise control of peptide sequence modifications, whether natural or synthetic, is critical to the efficacy of many protein-based therapeutic developments (Tinafar et al. 2019). On the other hand, the whole codon table could be reprogrammed, which would make it possible to add non-natural amino acids and make completely new codon tables (Tinafar et al. 2019).

Membrane proteins are found in the cell membrane and are critical for biological functions. However, their production can be challenging because they function within the membrane lipid environment and have low water solubility, and they can be toxic to produce in cellular systems. (Seddon et al. 2004). CFPS offers an alternative production system for these specific protein groups (Steinkühler et al. 2024). To enable the membrane proteins to properly fold in the CFPS, model membranes and a detergent-based system are used (Benedicto et al. 2024). Nanodiscs are a new model membrane to use for membrane protein studies and are composed of synthetic lipid rings and apolipoproteins arranged into small lipid disks (Nath et al. 2007). These disks act like their natural lipid environment, helping to stabilize membrane proteins and proteins remain properly folded and processable while binding to the nanodiscs. If they don't have their native membrane structure, they often fold incorrectly or aggregate, and these membrane models help proteins to fold properly. (Benedicto et al. 2024). Production of membrane proteins is important for drug development, vesicle-based biosensors, and synthetic cell studies (Nath et al. 2007; Jacobs et al. 2019; Kuruma and Ueda 2015).

1.3.2 Synthetic Biology and Genetic Circuits

Since cell-free system usage is widely expanding, the design of the genetic circuits gains importance for the system. Characterizing genetic components, including promoters, ribosome binding sites, and terminators, is crucial, and this process is labour-intensive and time-consuming in living cells (McManus et al. 2021). CFPS may significantly fasten the

design-test-build process by allowing high-throughput screening. High-throughput characterization of genetic fragments is possible by screening libraries containing thousands of variants in 96- or 384-well plates(GAN et al. 2022).

By incorporating genetic circuits, these systems gain programmability. Another exciting application of cell-free systems is the development of artificial cells, which hold potential in diverse areas ranging from biosensors to space exploration (Rothschild et al. 2024). Recently, a circuit operating on a single DNA molecule in a biochip was presented, which they considered an important step for the development of a miniaturized biological system (Hunt et al. 2025; Greiss et al. 2024). However, it has to be noted that cell-free systems still suffer from resource competition and batch-to-batch variability (Hunt et al. 2025).

1.3.3 Drug Discovery and Development

Given the cell-free system's capacity for rapid production, it makes it possible to produce protein within hours (Caschera 2025). This gives an advantage for the identification and validation of drug targets. With the high-throughput screening, thousands of protein variants can be expressed in parallel (GAN et al. 2022). This makes protein engineering and enzyme screening faster than cell-based systems. For example, in one study for discovering antimicrobial peptides, more than 3,000 variants of salivaricin B were tested with cell-free systems (Park et al. 2024). Cell-free systems also offer new opportunities in biological drug development in addition to identifying. In *E. coli*-based cell-free system, unnatural amino acids can be added to produce site-specific and uniform antibody-drug conjugates(Tinafar et al. 2019; Zimmerman et al. 2014).

In combinatorial biosynthesis, they make it possible to test different biosynthetic pathways together, which speeds up the design of new molecules (Bogart et al. 2021). Cell-free systems can also be combined with genetic circuits and membrane-based vesicles to design programmable drug production and delivery systems (Kim et al. 2025). The main advantages of cell-free systems include speed, flexibility, lower cost, reduced risk of contamination from cells (like endotoxins), and suitability for structural studies with isotopic or fluorescent labeling.

1.3.4 Biosensors

Biosensors are analytical tools that take the biological elements, such as enzymes, antibodies, or nucleic acids, and combine them with a proper transduction mechanism to detect the target molecule's existence, concentration, or activity (Wang and Lu 2022; Ali1 et al.

2017). They are becoming an important focus of synthetic biology due to their portability, low cost, rapid response, and real-time monitoring (Xing et al. 2025; Zhang et al. 2022). Biosensors are generally composed of 3 main parts: the recognition part, the transducer, and the signal processing unit (Shafiee et al. 2018). The recognition elements interact with the target molecule, triggering a specific reaction that is converted into a physical, measurable signal (optical, electrical, fluorescent, colorimetric, or luminescent (Wang et al. 2025).

The living cells have been used to develop biosensors for decades, since they are capable of self-sustaining systems (Green et al. 2025). With all the advances of cell-based biosensors, they also have some limitations, such as requiring continuous viability and membrane transport (Green et al. 2025; Zhang et al. 2020). Cell-free systems are adding advantages here since they are free from these limitations.

Cell-free biosensors operate through different recognition mechanisms, which can be categorized into transcriptional regulation-based systems, aptamers, CRISPR-based systems, and toehold switches(Zhang et al. 2020).

The transcriptional regulation-based systems detect the input molecule with the transcription factors and activate or block reporter gene activity, and produce a detectable output with the help of shifting gene activity(Jeon et al. 2022). In one study, Pellinen and colleagues used transcription regulation-based biosensors in *E. coli* lysate in order to detect mercury, which is toxic for living cells (Pellinen et al. 2004).

The aptamers are short, single-stranded, designed nucleotide sequences that bind to a target molecule with high affinity (Duchardt-Ferner et al. 2020; Zhang et al. 2019). Comparing this feature with antibodies, which also bind the target molecule with affinity, aptamers are advantageous in terms of stability, faster and cheaper synthesis, size, and flexibility in modifications(Zhang et al. 2019). Harbaugh and colleagues generated RNA aptamers against dopamine and integrated them directly into a riboswitch scaffold to create a cell-free biosensor to detect dopamine in urine samples as a proof of concept (Harbaugh et al. 2022).

CRISPR-Cas systems have become an important tool for cell-free biosensors with their ability to recognize target nucleic acids with high specificity and their cleavage features(Kellner et al. 2019; K. Chen et al. 2022). After recognizing target genetic material, enzymes such as Cas12 and Cas13 can activate a signal production mechanism with secondary "collateral cleavage" activity (Li et al. 2023; Cecchetelli, n.d.; Wu et al. 2024). This feature, when combined with cell-free systems, enables the development of biosensors that provide rapid and cost-effective field-applicable diagnostics. Cell-free CRISPR biosensors are

especially useful in the diagnosis of infectious diseases (Kellner et al. 2019; B. Chen et al. 2022; Huang et al. 2023). For example, the SHERLOCK and DETECTR platforms can detect RNA or DNA targets in a cell-free environment in minutes and visualize the results using simple fluorescence or colorimetric readout systems(Kellner et al. 2019; Cecchetelli, n.d.). This approach is used not only in clinical diagnosis, but also in a variety of other applications, such as food safety, environmental monitoring(B. Chen et al. 2022). Mahas and colleagues have designed a Cas12a-based cell-free biosensor in order to detect small molecules and as a proof of concept, they detect the different levels of tetracycline(Mahas et al. 2022).

Toehold switches are RNA-based regulators developed in synthetic biology that are commonly used in cell-free biosensor applications (Green et al. 2014). Their structures include a hairpin region and a ribosome binding site (RBS). In the absence of a target RNA molecule, the hairpin structure prevents translation by closing the RBS and start codon (OFF state)(Pardee et al. 2014). In the presence of target RNA, the hairpin opens, allowing the ribosome to access the RBS and begin translation of the reporter protein (ON state)(Pardee et al. 2014). This mechanism has high specificity and sensitivity because the signal is only generated when it interacts with the specific target RNA. Another important feature of toehold switches is their programmability; new switches can be created for various target RNAs, making the platform modular and adaptable(Green et al. 2014). Toehold switch-based biosensors are useful in field testing, viral RNA detection, and portable diagnostic kits because they allow for rapid and controlled protein production in a cell-free environment(Pardee et al. 2014; Hoang Trung Chau et al. 2020).

1.3.5 Metabolic Engineering

Cell-free systems provide a robust platform for metabolic engineering applications. In these systems, metabolic pathways can be reconfigured and optimized independently of living cells' complex regulatory networks(Karim and Jewett 2016). Thus, target metabolites can be produced directly from cell lysates or purified enzymes (Dudley et al. 2015). Cell-free metabolic engineering (CFME) is distinguished by its rapid prototyping capabilities; researchers can quickly test the most efficient production scenario by adjusting enzyme concentrations, cofactor balances, and reaction parameters (Caschera and Noireaux 2015). Cell-free systems also eliminate limitations such as toxic metabolite accumulation and the production of products that impair cell growth (Kay and Jewett 2015). Because of these characteristics, CFME is increasingly being used in the manufacture of biofuels, pharmaceuticals, natural products, and valuable chemicals (Hodgman and Jewett 2012). Cell-

free metabolic engineering has significant potential for biofuel production. Biofuels like ethanol, butanol, and isobutanol have been successfully synthesized in a cell-free environment using reengineered metabolic pathways, offering an alternative and sustainable approach to energy production (Krutsakorn et al. 2013). Another important application is bioplastic production. Polylactic acid (PLA) and similar bioplastic precursors were enzymatically synthesized from cell lysate, demonstrating the efficacy of cell-free platforms for the development of environmentally friendly materials (Bujara et al. 2010). Furthermore, cell-free systems are used in the pharmaceutical industry to produce high-value compounds. High-yield synthesis of pharmaceutical intermediates, such as nucleotide analogs, in a cell-free environment provides a valuable alternative for rapid prototyping and manufacturing in drug development processes (Kay & Jewett, 2015).

1.3.6 High-throughput Screening

Cell-free systems provide support for high-throughput screening (HTS) applications. These systems enable rapid testing of thousands of biosynthetic pathways, enzyme variants, or genetic circuits to identify the best combinations (Sun et al. 2014). Screenings performed in a cell-free environment produce faster and more flexible results than traditional in vivo methods because they are not affected by cell growth or physiological barriers (Hodgman and Jewett 2012). Furthermore, using cell lysates or purified components makes it simple to test various conditions (e.g., pH, temperature, and cofactor balance) in HTS applications (Karim and Jewett 2016). This method can be used to quickly screen large-scale libraries for functional candidates, particularly in ribozyme, aptamer selection, and protein engineering (Martin et al. 2018). Cell-free HTS has numerous applications, including industrial enzyme optimization, biosensor design, and drug discovery (Nirenberg and Matthaei 1961; Laohakunakorn et al. 2020). Cell-free systems are widely used in high-throughput screening applications, particularly in protein engineering research. Large libraries of enzyme variants can be rapidly tested in cell-free environments to identify enzymes with the highest activity or stability (Martin et al. 2018). Ribozyme and aptamer selection are also important for application. Cell-free screening speeds up the development of new biosensor platforms by rapidly identifying RNA-based structures that can bind to specific ligands with high specificity (Laohakunakorn et al. 2020).

1.3.7 Education

Cell-free systems are used as an effective learning tool in synthetic and molecular biology education (Kelwick et al. 2014). Experiments in a cell-free environment enable students to observe molecular processes without the biosafety and technical constraints associated with working with living cells (Silverman et al. 2020). Fundamental concepts such as gene expression, enzyme activities, and biosensor principles can now be tested in a laboratory setting quickly and safely(Shin and Noireaux 2012). Furthermore, cell-free platforms enable students to develop design-thinking and prototyping skills, allowing them to learn the design and optimization of biotechnological circuits (Laohakunakorn et al. 2020).

1.4 Cell-Free Transcriptional Regulation-Based Biosensors: Principles and Designs

1.4.1 Activator-Based Biosensors

Cell-free transcription-translation systems are a suitable platform for implementing regulatory circuits based on activator components such as transcription factors, thus circumventing the permeability limitations and biosafety concerns associated with living cells (Lu 2020; Zhang et al. 2020).

In activator-based biosensors, the binding of a ligand to a transcription factor (or a modified variant) induces a conformational change that allows RNA polymerase access to the promoter region of DNA, thus converting target sequences into signals (D'Ambrosio and Jensen 2017; Hossain et al. 2020; Lee and Maerkl 2024). Regulatory proteins (activators) in this approach are typically composed of two functional modules: a DNA-binding domain (DBD) and a ligand-binding or allosteric regulatory domain (LBD) (D'Ambrosio and Jensen 2017; Hossain et al. 2020; Lee and Maerkl 2024). After the activator binds to the ligand, RNA polymerase or the corresponding transcription machinery in the promoter region initiates or activates transcription. Promoter activation is triggered when ligand samples are added to this mixture; this occurs through the activator-ligand interaction, which produces a reporter (e.g., fluorescent protein, lacZ, luciferase) and thus generates a measurable signal(Lee and Maerkl 2024). Because the activator normally acts as a positive regulator, the signal exhibits a "turn-on" response; in the absence of ligands, basal expression levels are low, whereas in their presence they increase (Lee and Maerkl 2024; Guo et al. 2025). Such systems offer advantages such as tunable sensitivity control, signal amplification, and reversible control. System

dynamics can be studied and optimized, for example, by adjusting parameters such as the activator concentration, the affinity between promoter and activator, the number of operators, and the promoter architecture(Lee and Maerkl 2024; Mahas et al. 2022; Hossain et al. 2020). Progress in the development of activator-based biosensors in cell-free environments has been facilitated in recent years by automated, robotic liquid-handling platforms that enable faster high-throughput screening and circuit optimization (Ekas et al. 2024). However, activator-based systems can face several challenges, such as system leakage, nonspecific binding, optimal signal-to-background ratio tuning, and stability (Wang and Lu 2022; Li et al. 2025).

Activator-based biosensors can also be toehold switches, which can use RNA molecules as activating signal outputs. One of the main advantages of these switches is their modularity which allows the designing biosensor for many different RNA targets (Hoang Trung Chau et al. 2020; McSweeney et al. 2023).

1.4.2 Repressor-Based Biosensors

In repressor-based biosensors, the binding or removal of the ligand controls the binding or removal of the transcription factor from the DNA; this regulation leads to negative control of the reporter gene expression (Pellinen et al. 2004; Gräwe et al. 2019). Generally, the repressor binds to the operator region (either the promoter or the region near the promoter), thus blocking RNA polymerase access to the promoter (Jung et al. 2022). Typically, the repressor has a negative regulatory function; this structure allows for a negative signal-silencing mechanism in the presence of the ligand.

The presence or content of the ligand influences the repressor-operator interaction, resulting in negative regulation of the reporter gene(Barkley et al. 1975; Pellinen et al. 2004). A common example is metal-ion-sensitive repressor proteins, such as metal-regulators, such as ArsR and MerR (Pellinen et al. 2004). These repressors act as metal ion sensors in extracellular environments by dissociating from the operator site upon metal ion binding, thus releasing transcription. Repressor-based systems offer several advantages, such as low basal expression levels, the ability to reverse the response (negative locking), and the development of signal reduction modes(Karig et al. 2012). Parameters such as the number of operators, the affinity between repressor and promoter, and the repressor concentration are crucial for the dynamic range, boundary detection, and contrast performance of a repressor-based biosensor in a cell-free system(Shin and Noireaux 2012; Karzbrun et al. 2014; Chappell et al. 2015).

To compare some characteristics of activator and repressor-based biosensors, see Table 1.1.

Table 1.1 Comparison of characteristics of activator and repressor-based biosensors.

Characteristic	Activator-based Biosensor	Repressor-based Biosensor
Signal polarity	"Turn-on" Ligand binding activates the activator promoter → reporter increase.(Jung et al. 2022)	"Turn-off "(or derepression) Repressor binds to operator; effects the translation→ reporter decrease (Gräwe et al. 2019; Jeong et al. 2019).
Leakiness	Leakage expression depends on promoter and activator level; low basal but high leakage has been reported in well-designed activator systems(Jung et al. 2022; Zhou and Zhang 2023).	It is usually possible to achieve lower basal expression because the repressor directly blocks translation; however, leakage can still occur because operator location/affinity is critical (Gräwe et al. 2019; Jeong et al. 2019).
Dynamic range/ Fold-change	Generally, higher dynamic range can be observed; strong promoter activity upon activator triggering produces large "ON" levels (Voyvodic et al. 2019)	Although fold repression (ON/OFF difference) can be optimized in repressors, in some designs expression of the repressor gene or reporter redundancy may limit the dynamic range(Pandi et al. 2019; Lopreside et al. 2019; Silverman et al. 2019).
Limit of detection (LOD) / sensitivity	Activators provide good LOD if they can trigger low ligand concentrations; however, the LOD system can be further improved with amplification layers(Jung et al. 2022; Li et al. 2024)	The LOD is very sensitive to repressor/promoter affinity and repressor level; pre-expressed repressor or optimal repressor:reporter ratio improves the LOD(Gräwe et al. 2019; Saito et al. 2010b).
Optimization Flexibility	Dynamic range and can be easily adjusted by the promoter binding strength of activators, the number of activator copies, and the amplification layers that can be used(Voyvodic et al. 2019; Jung et al. 2022).	Repressors can be fine-tuned by operator number/position, repressor affinity, and repressor expression source (pre-expressed vs co-expressed); competition for resources (translation resources) should be taken into account(Mannan et al. 2017; Swank et al. 2019; Siegal-Gaskins et al. 2014; Pandi et al. 2019)

1.5 RNA-Binding Proteins

RNA-binding proteins (RBPs) are key regulatory proteins that participate in nearly every stage of RNA metabolism in the cells. These proteins have a conserved structure that allows them to bind specifically to RNA molecules through specific motifs and regulate their processing, transport, stability, and translation (Gerstberger et al. 2014). These motifs are usually found in RNA-interacting regions of proteins and recognize specific RNA sequences or secondary structures. The most common motifs are the RNA Recognition Motif (RRM), the K Homology (KH) region, Zinc Finger motifs, and the RGG box (Gerstberger et al. 2014; Lunde et al. 2007). These structural domains allow RBPs to recognize both sequence and structure-specific RNA. Many RBPs have multiple RNA-binding domains and can interact with multiple RNA targets, which increases their functional diversity and specificity (Lunde et al. 2007). RNA-binding proteins form riboprotein complexes with other proteins and RNA (Glisovic et al. 2008). These complexes help to coordinate processes like RNA processing, transport, and translation. For example, pre-mRNA splicing is carried out by the spliceosome, a large complex in which numerous RBPs interact dynamically(Glisovic et al. 2008).

RBPs' ability to selectively interact with RNA enables post-transcriptional programming of gene expression. This function is used in different applications, including post-transcriptional regulation in synthetic biology, such as designing RNA sensors and artificial circuits (Nguyen et al. 2022). For instance, by identifying particular RNA structural motifs, classical RNA-binding proteins like MS2 coat protein (MS2-CP) have been utilized to create artificial logic gates (like AND, OR, and NOT)(Yang and Ding 2021; Matsuura et al. 2018; Nguyen et al. 2022). Regulating RNA localization is one of the key applications of RBPs in synthetic biology (Mattick 2004).

1.5.1 MS2-cNOT7 and MS2 Loops

The MS2 stem-loop structure consists of a stem region and a loop region. The nucleotide sequence within the loop region typically contains the AUGAAC motif, which serves as the key element that directly interacts with the recognition pockets of the binding protein (Valegård et al. 1997). In terms of RNA folding, the MS2 hairpin exhibits a prefolded conformation, maintaining its secondary structure even before protein binding (Helgstrand et al. 2002). Upon protein binding, however, certain base pairings within the RNA stem undergo

rearrangement, producing a more compact structure through an induced-fit mechanism (Valegård et al. 1997).

The coat protein of the RNA bacteriophage MS2 serves two functions: it is a major structural protein of the viral particle and a translational repressor of the viral replicase gene (Bernardi and Spahr 1972; Peabody and Lim 1996). These functions are based on highly specific protein-protein and protein-RNA interactions. The system is widely used in RNA engineering and molecular biology because the MS2 coat protein (CP or MCP) can specifically bind to a certain RNA stem-loop motif (Johansson et al. 1997). With this specific binding property, it became a great interest for synthetic biology applications, especially as a fusion protein domain (Nakanishi 2021).

When the binding of an RBP does not functionally affect the translation, like in the case with MS2, they can be combined with other proteins. The 5' cap structures and poly(A) tails play an important role in both mRNA stability and translation. Targeted binding of RBPs to mRNAs may promote their degradation and translational reduction by interacting with these crucial structures in RNA (Nakanishi 2021). The cNOT7 protein is an important example to use in combination with the MS2 protein. It is the catalytic de-adenylase subunit of the CCR4-NOT complex and works by shortening the mRNA poly(A) tail, which makes the mRNA less stable (Mauxion et al. 2023). MS2-cNOT7 fusions are used to direct the de-adenylation or degradation of specific RNA through the MS2 domain (Wroblewska et al. 2015). This design gives the possibility to control the translation levels over mRNA stability. To further enhance this control, the fusion constructs include a protease-sensitive cleavage site, such as a TEV protease recognition sequence. This allows the MS2 and cNOT7 domains to be separated in a regulated manner, making repression by MS2–cNOT7 controllable as a protein–protein interaction device (Cella et al. 2018).

1.5.2 L7Ae and Kink-Turn Motifs

The L7Ae protein is a very specific archaeal ribosomal protein that is found in archaeal ribonucleoprotein complexes (Lenk et al. 2024; Suryadi et al. 2005). It is especially well-known for its ability to bind to the RNA secondary structure motif known as kink-turn (k-turn)(Watkins and Bohnsack 2012). L7Ae family proteins are conserved in both Archaea and eukaryotes (e.g., the 15.5K homolog), suggesting that L7Ae has an evolutionarily highly stable RNA recognition mechanism (Rozhdestvensky et al. 2003).

The K-turn motif is characterized by a significant angle (approximately 50–60°) in the RNA double helix, which arises from G-A base pair interactions (Klein et al. 2001). The structure typically comprises three components: (i) the canonical stem (C-stem), characterized by classical Watson-Crick base pairings; (ii) the non-canonical stem (NC-stem), featuring non-standard base pairings such as G-A and A-G; and (iii) the kink region that links the two branches (Turner et al. 2005; Goody et al. 2004).

The K-turn structure imparts an irregular conformation to the native RNA strand; however, this motif alone does not contribute to a stable three-dimensional architecture (Nissen et al. 2001). High-resolution X-ray crystallography studies indicate that RNA remains open and flexible in the absence of L7Ae binding. Upon binding to RNA, L7Ae adopts a more compact and twisted structure. Hydrogen bonds and electrostatic interactions between amino acid residues on the positively charged surface of L7Ae and the RNA phosphate backbone contribute to the stability of this binding (Moore et al. 2004; Vidovic et al. 2000). The RNA recognition site is located on the surface, predominantly composed of positively charged residues (Suryadi et al. 2005).

L7Ae's interaction with RNA alters the three-dimensional conformation of RNA, facilitating a functional fold (Rozhdestvensky et al. 2003). L7Ae functions as a structural chaperone. The interaction between L7Ae and kink-turn has been conserved across evolutionary history in both archaeal and eukaryotic systems (Klein et al. 2001; Rozhdestvensky et al. 2003). Analogous recognition motifs have been identified in archaeal ribosomal RNAs and eukaryotic U4 snRNA(Klein et al. 2001; Moore et al. 2004). Recent research has explored the application of this natural recognition mechanism in biotechnological systems. The L7Ae-kink-turn interaction operates as an RNA-specific conformational switch and is being evaluated as a structural signal transducer module in biosensor designs (Saito et al. 2010b; Wroblewska et al. 2015). This methodology utilizes the structural alteration induced by L7Ae's interaction with RNA as a specific molecular trigger for signal generation or perception. The L7Ae–k-turn interaction is considered a conserved recognition model in nature and serves as a modifiable molecular platform for bioengineering.

1.6 Aim of the Project

In this project, I aimed to characterize genetic circuits based on RNA-binding protein (RBP) repressive activity to investigate their performance in cell-free systems for biosensing purposes.

Specifically, with this study I characterized the behavior of the MS2–cNOT7 and L7Ae RNA-binding proteins by testing their repressive efficiency in different cell-free systems (RRL, E. coli lysate, reconstituted TX-TL systems), genetic contexts, and expression protocols. I then selected the best-performing system and experimental conditions in terms of robustness and repression efficiency to implement an additional translational control layer responsive to viral proteases. This work lays the foundations for the construction of in vitro protease biosensors that could be incorporated into next-generation viral detection diagnostic platforms in clinical setups.

Results

2.1 Testing Mammalian Cell-Free Lysate for Optimization of Post-Translational Control Devices

In the first part of this study, the functional capacity of the chimeric RNA-binding protein MS2-cNOT7 was examined, specifically focusing on its ability to recognize and bind target RNA molecules and subsequently repress their translation within the rabbit reticulocyte lysate (RRL) system. This experimental setup was designed to evaluate whether MS2-cNOT7 could serve as a post-transcriptional regulatory mechanism in RRL, thereby providing a controllable system for modulating gene expression at the level of translation in a mammalian model of cell-free system.

The MS2-CNOT7 is a fusion protein that integrates the RNA-binding characteristics of the MS2 coat protein with the deadenylase functions of CNOT7, an essential element of the CCR4-NOT complex. When the MS2 protein binds to the MS2 loops, this interaction leads CNOT7 to the poly-A tail of the transcript, resulting in the removal of the poly(A) tail. This process destabilizes the mRNA and decreases the efficiency of translation of the reporter transcript. Since de-adenylation and its downstream effects on RNA degradation are tightly linked to eukaryotic RNA metabolism, a eukaryotic environment is essential to accurately assess the activity of MS2-cNOT7 on poly(A) tail regulation. For this requirement, RRL was selected as the experimental platform, as it represents a mammalian cell-free system that preserves the core components of eukaryotic translational and post-transcriptional regulatory pathways.

Since RRL is derived from cytoplasmic extracts of reticulocytes and functions as an *in vitro* translation system, experimental constructs must be supplied as RNA. This requires *in vitro* transcription of the DNA templates prior to their use in translation assays. For this purpose, MS2-cNOT7 and a luciferase reporter containing eight tandem MS2-binding hairpin loops were cloned into a destination vector under the control of a T7 promoter (**Fig. 2.1**). In addition, the plasmid backbone was designed to include a 30-nucleotide polyadenine (poly(A)) tail, allowing amplification of a template by PCR that preserves the poly(A) tail.

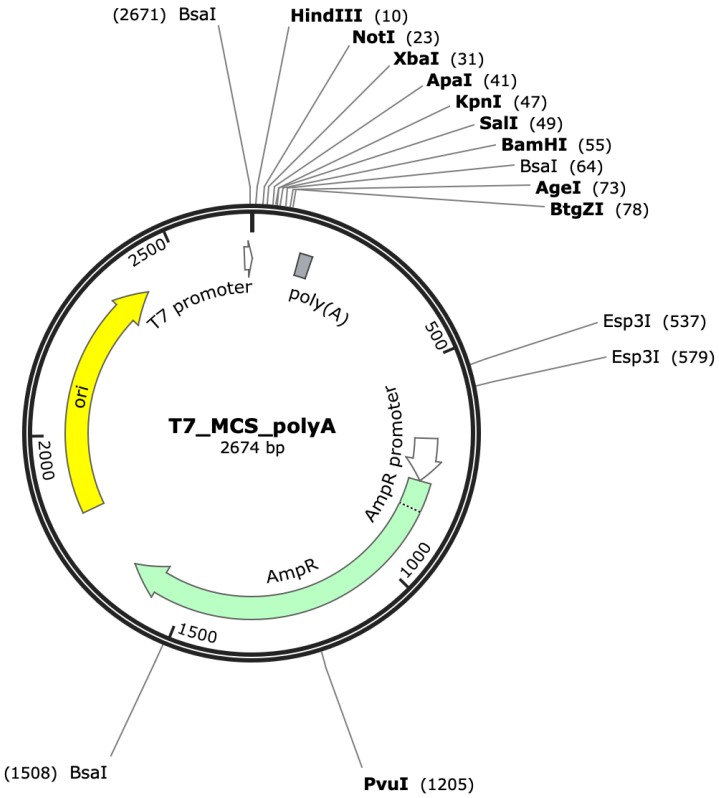

Figure 2. 1 Vector map used for generating MS2-cNOT7 related constructs for in vitro transcription. For the MS2-cNOT7 experiments, MS2-cNOT7, MS2^{mut}-cNOT7, LUCx8MS2-polyA, and Lucx8MS2 constructs; for the L7Ae experiments, L7Ae, L7Ae^{mut} and kt-nLuc constructs were cloned between the T7 promoter and poly(A) in the multiple cloning site (MCS) for flexible cloning of constructs used as templates for in vitro transcription. ori= origin of replication; AmpR=Ampicillin resistance

In addition to wild-type MS2-cNOT7, we added as a control a version of the MS2 domain that was modified with missense mutations (K56D and K58E) to abolish its RNA-binding property, as previously demonstrated in mammalian cells (Peabody 1993). The K-to-D mutation changes the local electrostatic potential in the RNA-binding pocket from positive to negative. This alters the shape of the protein, disrupting the hydrogen bonding interactions required for RNA recognition. Similarly, the K-to-E mutation removes an important positive charge, rendering it less compatible with the negatively charged RNA backbone and significantly reducing its binding to RNA. These mutations prevent MS2 from binding MS2 hairpin loops and, as a result, prevent cNOT7 from getting close proximity to the poly-A tail of the reporter RNA. Equal amounts of the mutant construct were added to the assays to eliminate resource competition as a cause of differences. This design allowed a direct comparison between wild-type MS2-cNOT7, which is expected to repress reporter translation, and mutated MS2-cNOT7 (MS2^{mut}-cNOT7), as a negative control. These mutant variants were cloned into the same plasmid backbone as the wild-type MS2-cNOT7 construct to ensure

comparability. The mutations were verified by Sanger sequencing, and these mutations are taken from an earlier work in the literature.

In vitro transcribed RNA can be generated using different components. To identify the RNA species that are most efficiently translated in *in vitro* translation, transcription of the templates was performed either with or without the Anti-Reverse Cap Analog (ARCA) and using either unmodified or chemically modified nucleotides. To compare the translation level of the produced RNA, the control RNA was supplemented by Promega. The experiments showed that RNA transcribed with uncapped and modified nucleotides resulted in the lowest protein translation efficiency **(Fig. 2.2).** The RNA produced with a cap and unmodified nucleotides showed the closest translation efficiency to that of the control RNA. Next, all constructs were subjected to *in vitro* transcription using an Anti-reverse cap Analog (ARCA) together with unmodified nucleotides.

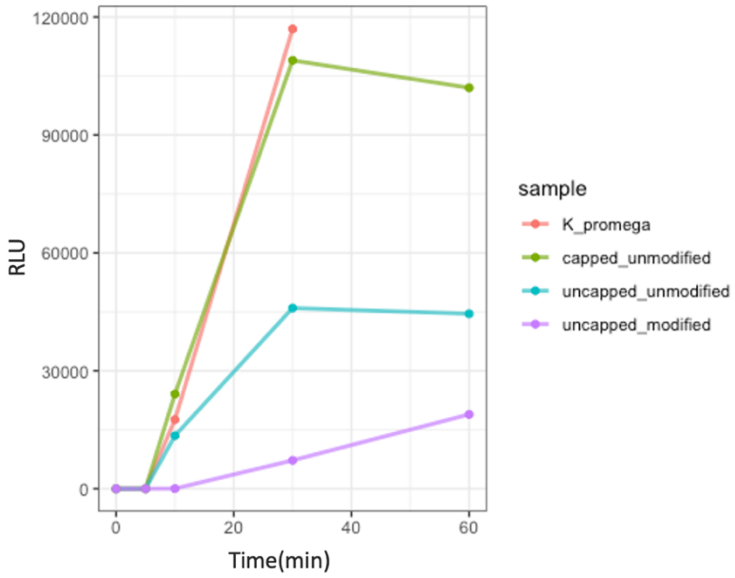

Figure 2. 2 Translation of in vitro transcribed RNA under different conditions.

K_Promega, red line: control template supplemented by Promega. **capped unmodified, green line**: RNA produced with ARCA cap and unmodified nucleotides. **uncapped unmodified, blue line:** RNA produced without ARCA cap and unmodified nucleotides. **uncapped_modified, purple line**: RNA produced without ARCA cap and modified nucleotides.

The transcribed RNAs were subsequently purified and analyzed by agarose electrophoresis to assess their integrity and confirm the absence of degradation **(Fig. 2.3)**.

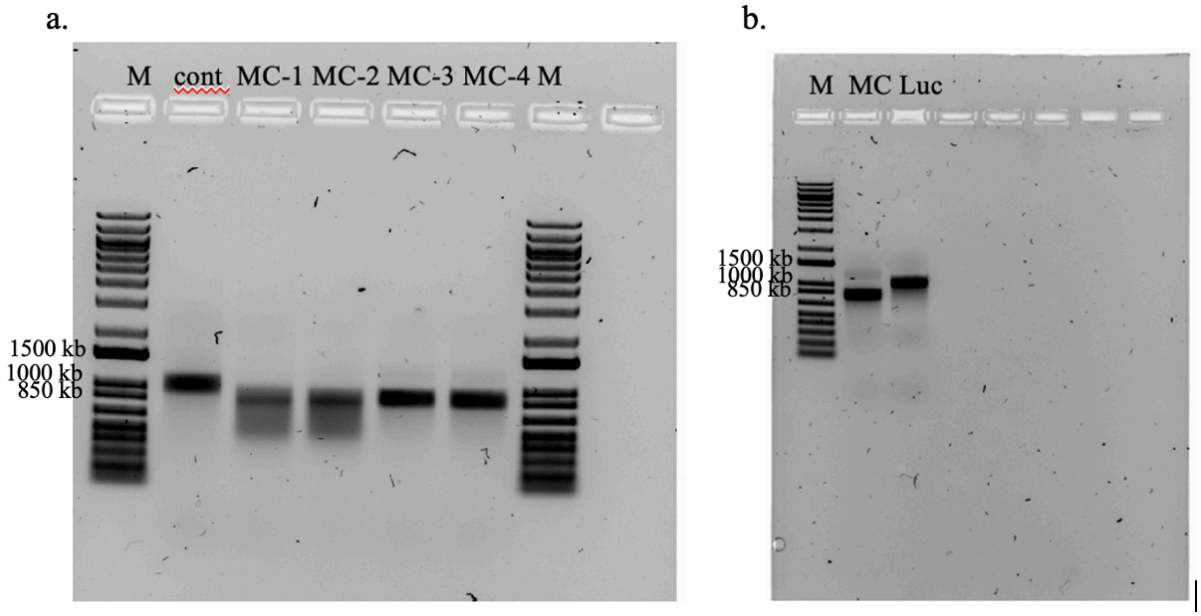

Figure 2. 3 Agarose gel images showing the in vitro transcribed RNA integrity. Representative 1% agarose gel used to assess the integrity of in vitro transcribed RNA. M: molecular marker; cont: control RNA; MC-1 to MC-4: four different RNA preparations for MS2-cNOT7; Luc: luciferase reporter containing MS2 loops.

An agarose gel was run to assess potential degradation, as observed in **Figure 2.3** for MC-1 and MC-2. If the bands appear sharp, as in MC, MC-3, MC-4, and Luc, the samples are then used for testing in the translation system.

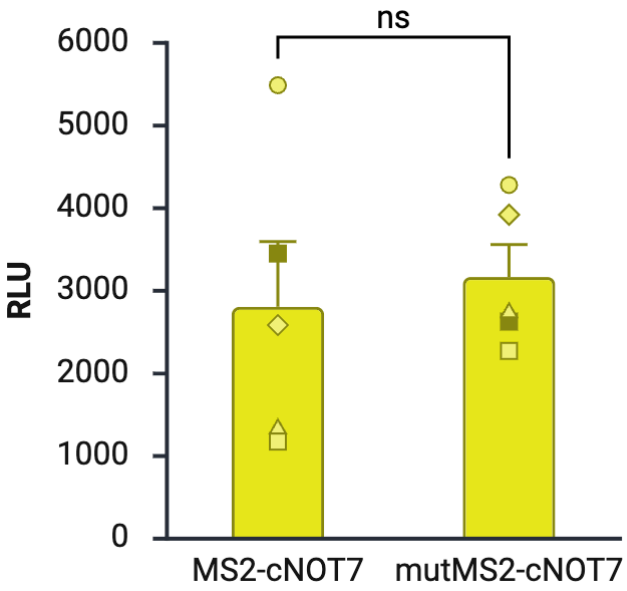

Figure 2. 4 Testing the MS2-cNOT7 repression of the reporter with 8xMS2 loops in RRL. Translation of a luciferase reporter containing MS2 loops in the presence of either MS2-cNOT7 or $MS2^{mut}$–cNOT7 RBP. The bar graph presents the mean luminescence values from five independent experiments, with error bars representing the standard error of the mean. Each data point corresponds to one experiment. ns: not significant; RLU: relative light units; n = 5.

The MS2-cNOT7 showed a trend, but not a robust translational repression of the luciferase reporter in the RRL system (**Fig. 2. 4**) compared to the mutMS2-cNOT7 control, suggesting that it is not a reliable system to carry out these RBP-RNA regulatory experiments. We investigated whether, at the molecular levels, there might be bottlenecks that prevented robust exploitation of RRL for this application (Michel et al. 2000b). Literature reports suggest that RRL can support translation of RNAs lacking a poly(A) tail (Michel et al. 2000a). We thus first analysed the poly(A) effect, by transcribing and testing MS2-cNOT constructs with and without a poly(A) tail in the RRL (**Fig 2. 5**). A slight but not significant repression was observed, indicating that cNOT7 protein activity was negligible in RRL. Additionally, constructs without a poly(A) tail appeared to be translated more efficiently (**Fig. 2. 5**), then their polyadenylated counterparts. The fact that removing the poly(A) tail did not result in a measurable decrease in translation of the reporter suggests that the repression observed in some replicates with the MS2-cNOT7 is most likely due to an alternative mechanism rather than poly(A)-tail-dependent regulation. Thus, due to the lack of effective and robust repression, we stopped testing the MS2-cNOT7 system.

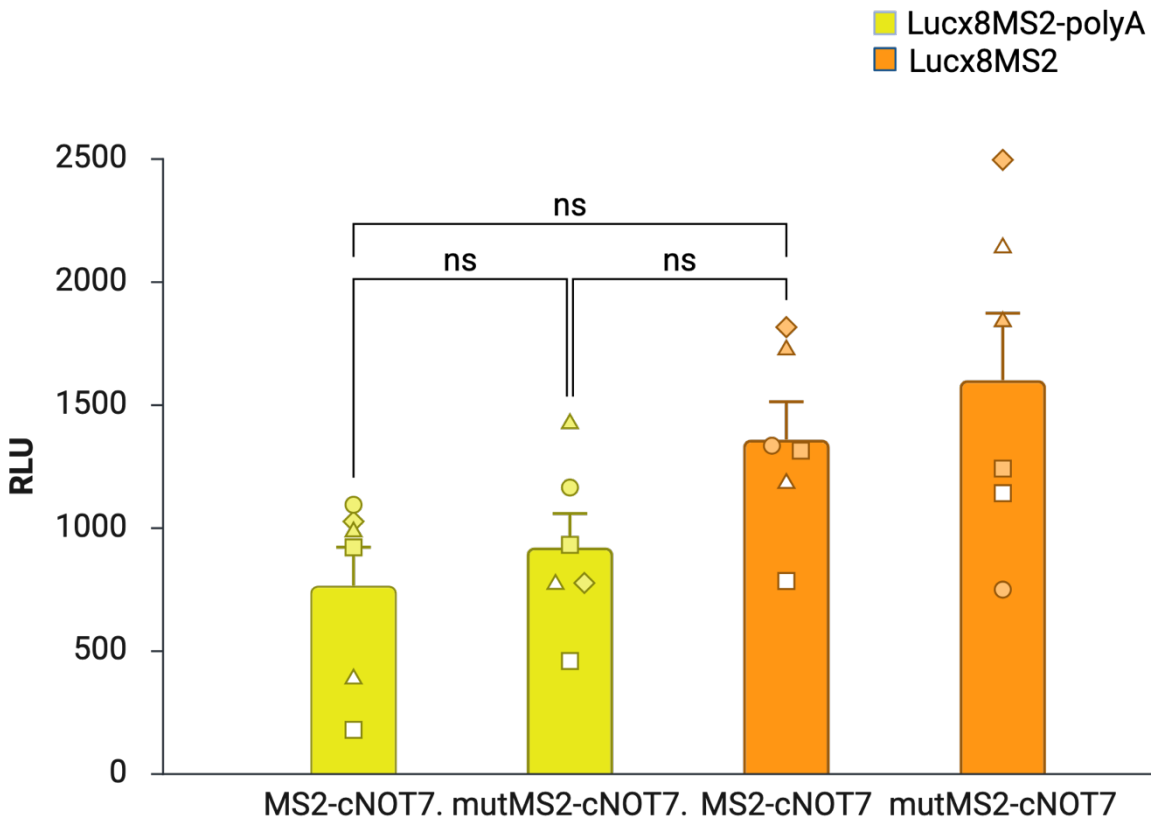

Figure 2. 5 Analysis of reporter RNA repression by MS2–CNOT7s in RRL, with and without a poly(A) tail. Translation of a luciferase reporter including MS2 binding loops, with or without a poly(A) tail, in the presence of either MS2-cNOT7 or MS2^{mut}-cNOT7 RNA-binding protein (RBP). The bar graph displays the mean luminescence values with error bars representing the standard error of the mean. Each data point corresponds to one independent experiment, and for statistical analysis, ANOVA followed by Tukey's multiple comparison tests, ns: not significant; RLU: relative light units. n=6

I next tested repression of L7Ae in the RRL system. L7Ae is an archaeal RNA-binding protein (RBP) that binds the kink-turn structure on RNA and blocks the ribosome binding, resulting in translation repression. Since this system had previously been tested in mammalian cells using two kink-turn (k-turn) structures in the 5′ UTR (Cella et al. 2018), the same construct was cloned into our destination vector for testing in RRL. Initially, L7Ae and the 2 k-turn luciferase reporters were used at a 1:1 molar ratio; we also added a condition to keep the resource competition and added a control RNA. The control RNA encodes nanoluciferase and was used at equimolar or fourfold higher concentrations than the reporter RNA, depending on the experimental condition. Nanoluciferase activity is not detectable using the substrate for Firefly luciferase, which serves as our reporter.

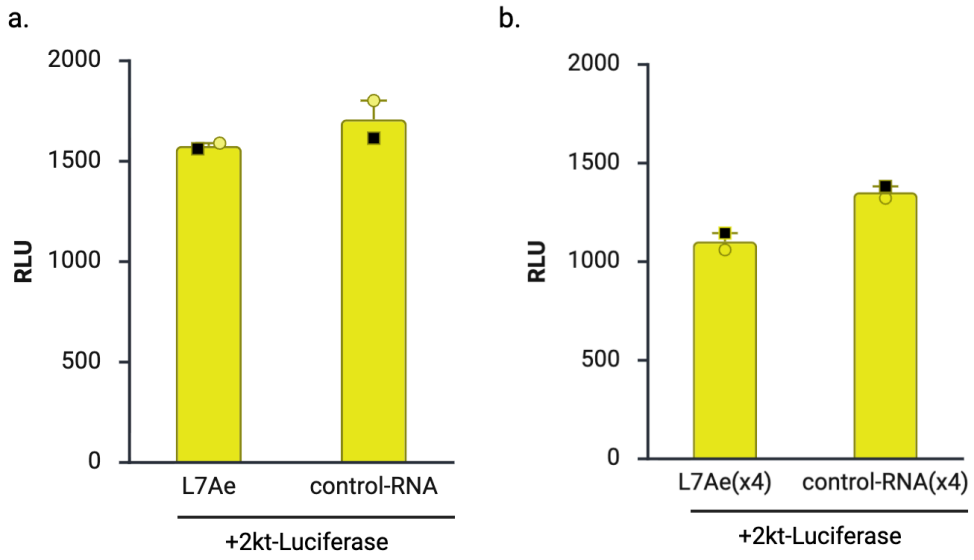

Figure 2. 6 Repression of 2xkt-Luciferase by L7Ae in RRL. a) Bar graph showing the mean luminescence values from two independent experiments, with error bars representing the standard error of the mean. A luciferase reporter containing two kink-turn motifs in the 5′UTR was translated either in the presence of L7Ae encoding RNA or a control RNA which is encoding nanoluciferase protein. The reporter and repressor constructs were mixed in an equimolar ratio (1:1) based on their molar amounts, corresponding to equal femtomole quantities. Each data point corresponds to one experiment. **b)** Bar graph showing the mean luminescence values from two independent experiments, with error bars representing the standard error of the mean. The same reporter was in the presence of L7Ae encoding RNA or a control RNA which is encoding nanoluciferase protein. In the L7Ae(4×) and control-RNA(4×) conditions, the repressor was added at a fourfold excess relative to the reporter plasmid. Each data point corresponds to one experiment, RLU: relative light units.

The luciferase reporter with two k-turn structures at 5' showed no difference in translation in the presence or absence of L7Ae (**Fig. 2.6a**). To increase the expression of the repressor protein, the concentration of L7Ae was increased fourfold relative to the reporter. However, even with an increased repressor, only a slight decrease by L7Ae repression was observed when compared to the control reactions (**Fig. 2.6b**).

In cell-free systems, positioning the kink-turn structure immediately downstream of the start codon results in stronger translational repression (Saito et al. 2010b). Based on this information, we cloned the k-turn directly after the start codon and replaced the reporter with the smaller luminescent protein nanoLuciferase. Nanoluciferase offers several advantages. First, it is smaller in size and requires fewer resources for translation. Additionally, it is an ATP-independent luciferase, meaning it does not consume ATP during its activity, which leaves more ATP available for other processes.

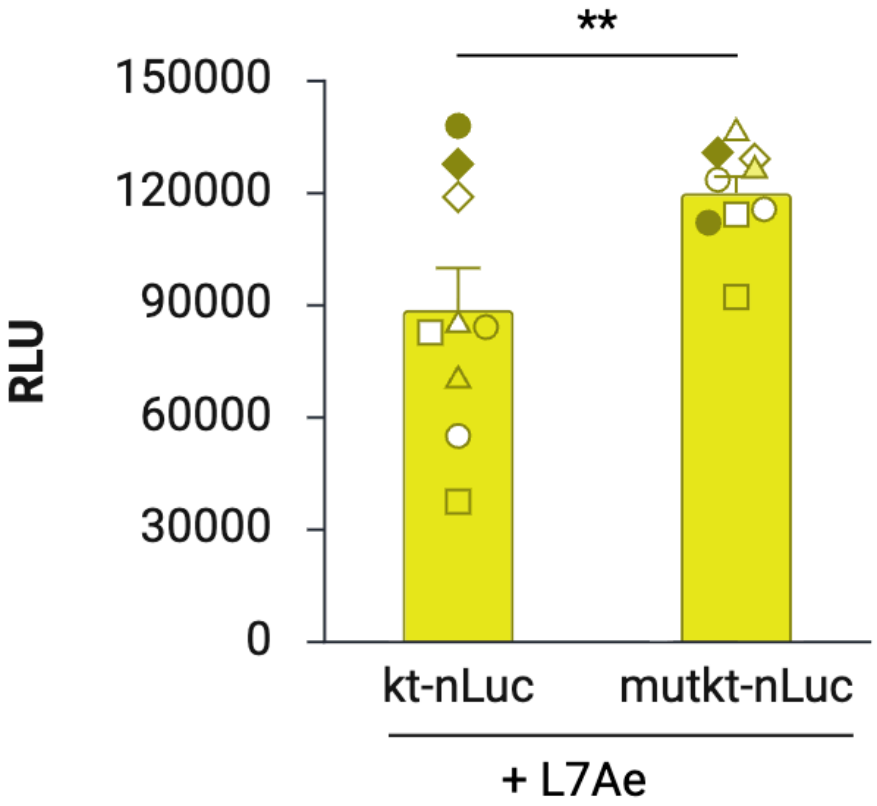

Figure 2.7 Repression of an in-frame kink-turn reporter RNA by L7Ae in RRL Translation of the kt-nLuc or kt^{mut}-nLuc reporter containing the kink-turn structure in the presence of the L7Ae. The bar graph displays the mean luminescence values from nine independent experiments, with error bars representing the standard error of the mean. Each data point corresponds to one experiment. Statistical significance was determined using a one-tailed paired Student's t-test $p < 0.01$, $n = 9$.

The optimized kturn-nanoluc (kt-nLuc) reporter was then tested in RRL. As a control to compare the L7Ae repression, a mutated kink-turn (kt^{mut}nLuc) was cloned with the reporter and used with the L7Ae RBP (**Fig. 2.7**). Although multiple biological replicates showed biological significance of the L7Ae repression, the level of repression was highly variable between replicates (**Fig. 2.7**).

In the Siciliano Lab, an engineered version of L7Ae was previously developed to include a short amino acid sequence sensitive to the tobacco virus protease(Cella et al. 2018). Specifically, a protease recognition and cleavage sequence (ENLYFQ↓G) was added immediately after residue K77 of L7Ae. This design allows for protease-mediated regulation of L7Ae activity through site-specific cleavage. The overall system, based on the interaction between the protease and RNA-binding protein, has previously been shown to effectively modulate target mRNA in the final step of the regulatory cascade in mammalian cells. To further define this regulatory mechanism, I examined its behavior in the rabbit reticulocyte lysate (RRL) system.

Although L7Ae did not exhibit the same robust level of repression in the RRL system as observed in mammalian cells, data showed a significant downregulation of the reporter expression mediated by L7Ae in RRL. Based on this result, I next sought to investigate whether more complex regulatory designs involving protease-RBP and RBP-RNA interactions could be explored. However, it did not exhibit high repression of the reporter, similar to the wild-type L7Ae (**Fig. 2. 8**). While previous data in mammalian cells were showing reduced repression of the target mRNA, the L7Ae-TCS still retained a discrete ON-OFF induction, which we did not observe in the RRL cell-free system.

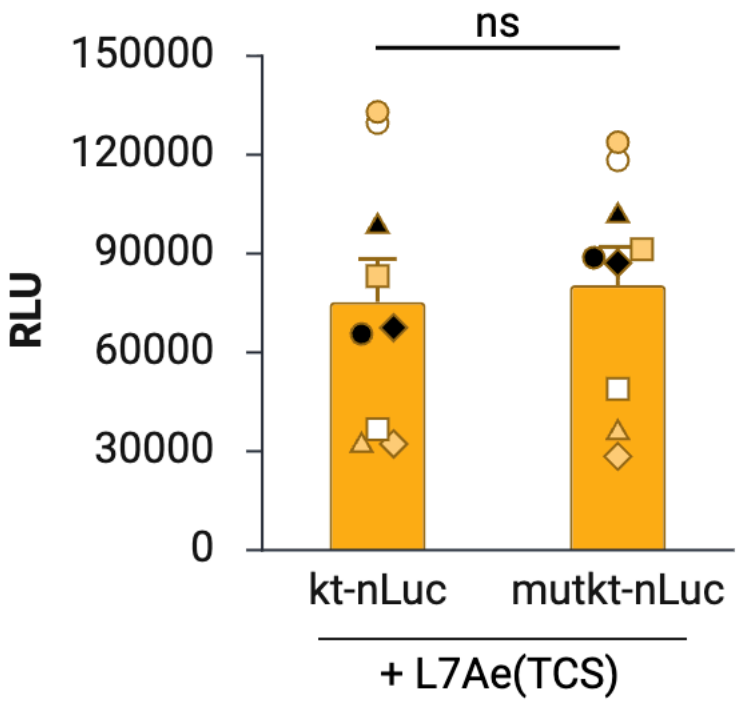

Figure 2. 8 Testing the L7Ae-TCS repression of the kt-nLuc reporter in RRL. Translation of the kt-nLuc or kt^{mut}-nLuc reporter containing the kink-turn structure in the presence of the L7Ae-TCS RBP. The bar graph represents the mean luminescence values from nine independent experiments, with error bars indicating the standard error of the mean. Each data point corresponds to one experiment. Statistical analysis performed using a one-tailed paired Student's t-test (n = 9). RLU: relative light units.

2.2 Testing *E. coli* Cell-Free Lysate for Optimization of Post-Translational Control Devices

Since the RRL cell-free systems did not show robust results, I tested whether L7Ae results in target transcript repression using S30 *E. coli* extract for circular DNA. This system is a transcription/translation (TX/TL) system, meaning that it can transcribe the input DNA into RNA and translate the produced RNA into protein in one reaction. To this end, I employed two different plasmid backbones to understand if there are plasmid-related effects impacting on the results (**Fig. 2.9**).

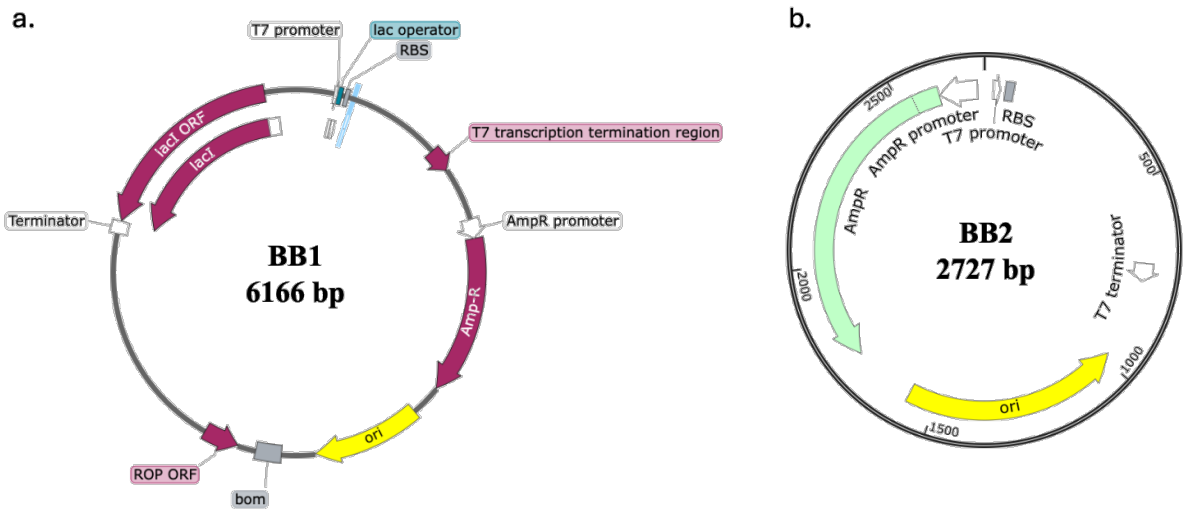

Figure 2.9 Plasmid maps used to test the L7Ae-kt system in E.coli Lysate: a) BB1 plasmid map. This backbone has a T7 promoter, RBS, and T7 Terminator sequence. Additionally, there is an Ampicillin resistance gene, LacI operator, ROP, and bom gene sequences on the backbone. **b)** BB2 plasmid map. This backbone has the same T7 promoter and RBS as the BB1 backbone and a similar T7 terminator sequence to a of BB1 just with one nucleotide different. Additionally, there is an ampicillin resistance gene on the backbone

These backbones differ in both their overall lengths and genetic components. Although both backbones contain the same T7 promoter and the same ribosome binding site (RBS), BB1 is approximately 6 kb in size, whereas BB2 is about 3 kb (**Table 1**).

Table 2.2 Component sequences on BB1 and BB2 backbones.

Component name/ Backbone	BB1 Backbone	BB2 Backbone
T7 promoter	taatacgactcactatagg	taatacgactcactatagg
RBS	tttgtttaactttaagaaggaga	tttgtttaactttaagaaggaga
T7 Terminator Sequence	ctagcataaccccttggggcctct aaacgggtcttgaggAgttttttg	ctagcataaccccttggggcctctaaacgggtcttga ggGgttttttg

Additionally, the distances between the encoded components differ between the two constructs (**Fig**. **2.10**).

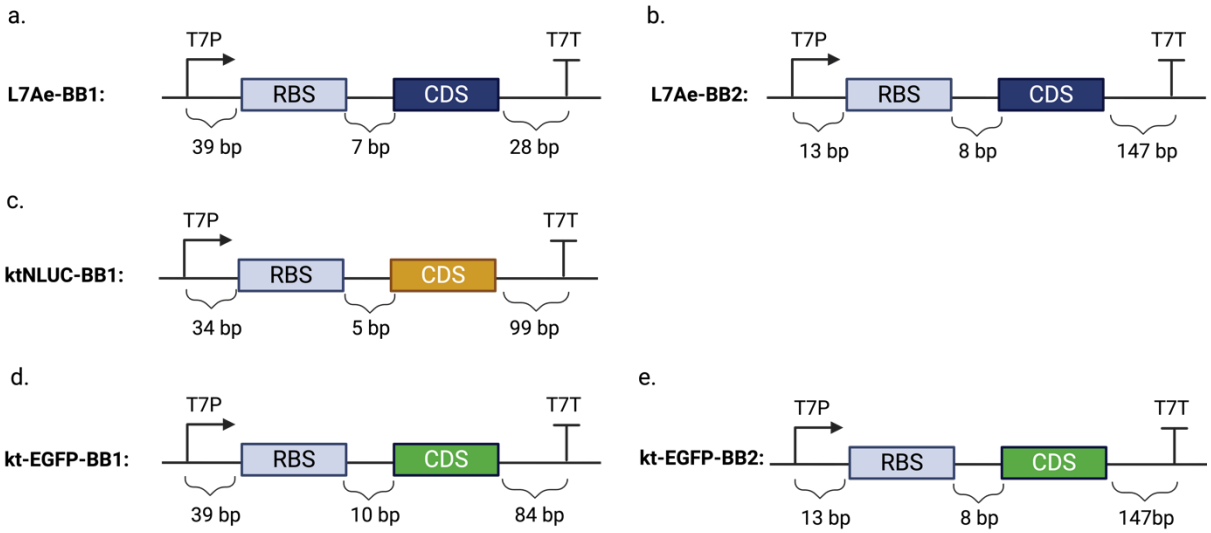

Figure 2. 10 The design of expression cassettes for E.coli and PURE system experiments. a) The expression cassette encoding L7Ae in BB1. **b**) The expression cassette encoding L7Ae in BB2. **c)** The expression cassette encoding ktNLUC in BB1. **d**) The expression cassette encoding kt-EGFP in BB1. **e**) The expression cassette encoding kt-EGFP in BB2. T7P=T7 promoter sequence; RBS= Ribosome binding sites; CDS=Coding sequence; T7T T7 terminator sequence.

First, L7Ae and kturn-nanoluc constructs are inserted into the BB1 backbone with infusion cloning and confirmed via Sanger sequencing. Then, the repression activity of L7Ae on kt-EGFP inserted in backbone BB1 was tested in *E. coli* S30 lysate with a one-step protocol in which the repressor L7Ae was added to the reaction and incubated for 10 minutes. After 10 minutes of incubation, the reporter construct was added, and they were incubated at 37 °C for 1 hour (**Fig. 2.11**).

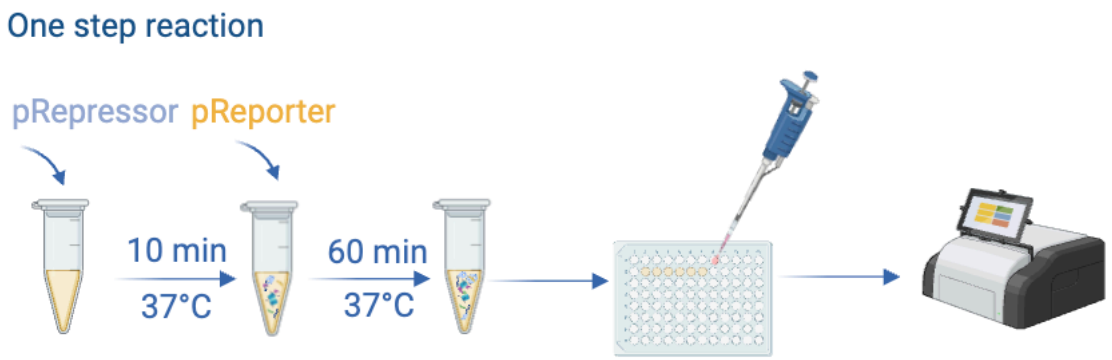

Figure 2. 11 One-step reaction protocol flow for S30 coli E. coli lysate experiment. In one one-step reaction, the repressor-coding construct is introduced into the reaction and incubated for 10 minutes. After this incubation reporter construct is introduced to the reaction, and the complete system is incubated in a thermocycler at 37 °C for an hour. Reaction mixtures are moved to the 96-well plate to measure the reporter activity.

While the repression was observed in some experiments (**Fig. 2.12a**), it was not robust, and similarly to what was shown in RRL lysates in some replicates, luciferase expression was lower in the mutated control condition (**Fig. 2.12b**).

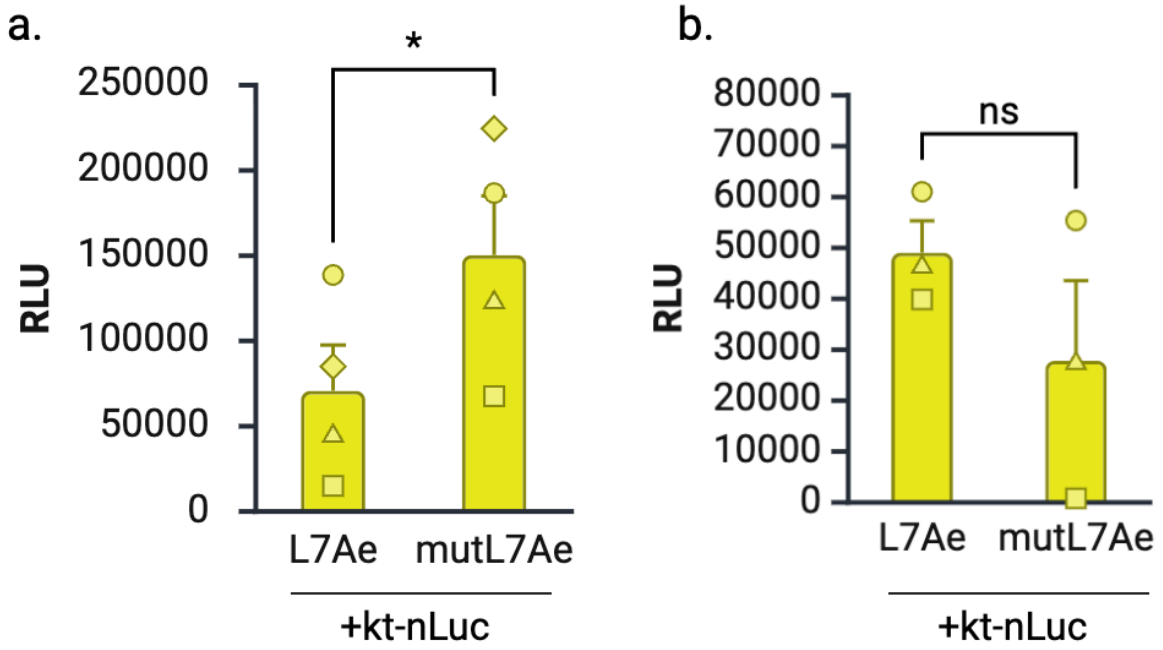

Figure 2.12 Testing L7Ae repression of kt-nLuc reporter encoding in the BB1 backbone in *E.coli* Lysate, a) Bar graph representing the mean luminescence values of four independent experiments, illustrating the repression mediated by L7Ae in comparison to the L7Ae^{mut} on kt-nLuc. Each data point corresponds to one experiment. Statistical significance was assessed using a one-tailed paired Student's t-test $p < 0.02$, ($n = 4$). **b)** Bar graph representing the mean values of the other three independent experiments showing the activity of L7Ae compared to the L7Ae^{mut}. Each data point corresponds to one experiment: ns: not significant; RLU: relative light units.

To better control experimental reproducibility and ensure that a sufficient amount of L7Ae protein was already synthesized and present in the reaction prior to the introduction of the reporter I implemented a two-step protocol (**Fig. 2.13**). To achieve this, L7Ae was added to the reaction mixture and allowed to undergo transcription and translation for 1 hour. After this first incubation step, the kt-nLuc reporter and fresh lysate were introduced, enabling the L7Ae to bind the kink-turn structure on the reporter mRNA immediately upon its transcription.

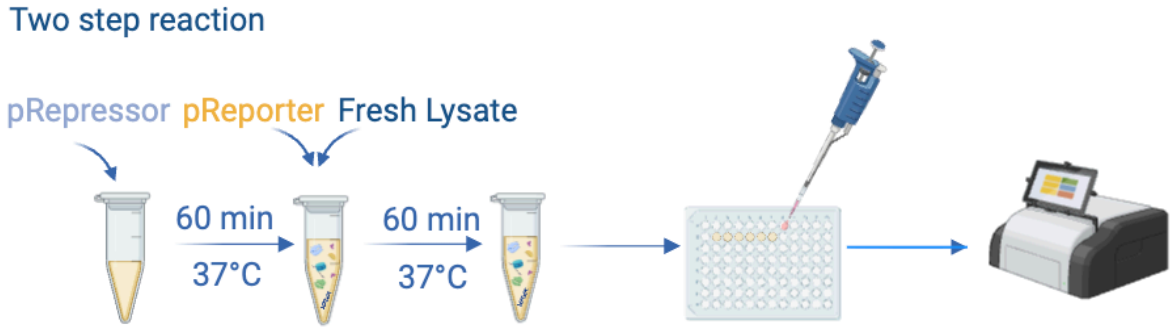

Figure 2. 13 Two-step reaction protocol flow for S30 E.coli lysate experiment. In a two-step reaction, the repressor-coding construct is introduced into the reaction and incubated for 1 hour. After this incubation reporter construct is introduced to the reaction with a fresh lysate, and the complete system is incubated in a thermocycler at 37 °C for 1 additional hour. Reaction mixtures are moved to the 96-well plate to measure the reporter activity.

While testing L7Ae-mediated repression on the kt-nLuc and kt^{mut}-nLuc reporter using the two-step reaction with the BB1 backbone, I observed that single reporter constructs exhibited markedly different translation levels (**Fig. 2.14**).

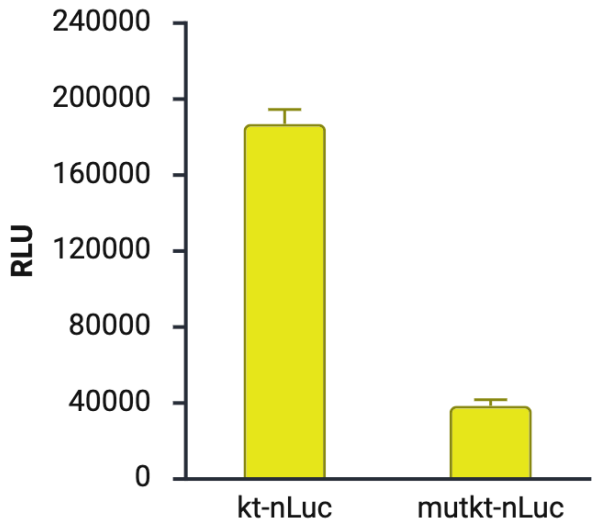

Figure 2.14 Translation of single reporters with the BB1 backbone in *E. coli* lysate. Single reporter constructs encoded in the BB1 backbone were translated in *E. coli* lysate to evaluate their expression levels. The wild-type reporter consistently exhibited higher translation compared to the mutant reporter; however, both constructs showed variability in their expression levels across experiments. Experiments done with one-step protocol, n=3.

To better understand this behavior, I compared the sequence of the k-turn motif I used so far that was demonstrated to be effective in mammalian cells (Cella et al. 2018; Wroblewska et al. 2015) with the sequence that was proven to work in cell-free systems (Saito et al. 2010b), and found pointed nucleotide differences in the motif (**Table 2.2**). Both sequences encode mutated kink-turn structures, each generated by substitutions at two nucleotide positions. Mutated kink-turn sequence 1 was validated in cell-based experiments, whereas mutated kink-turn sequence 2 was tested in a cell-free system.

Table 2. 3 Sequence comparison of the mutated kink turn encoded in the reporter construct

Mutated kink-turn sequence 1	GGGCGTCAT**C**CGAAAG**G**TGCCCCG
Mutated kink-turn sequence 2 (Saito et al. 2010b)	GGGCGTCAT**G**CGAAAG**C**TGCCCCG

Both mutated constructs retained the expected disruption of the kink-turn motif; however, the construct I used translated with lower efficiency. To further investigate this, RNA secondary structures were predicted using RNAfold, revealing distinct folding patterns for the two mutant reporters (**Fig. 2.15 and Fig. 2. 16**).

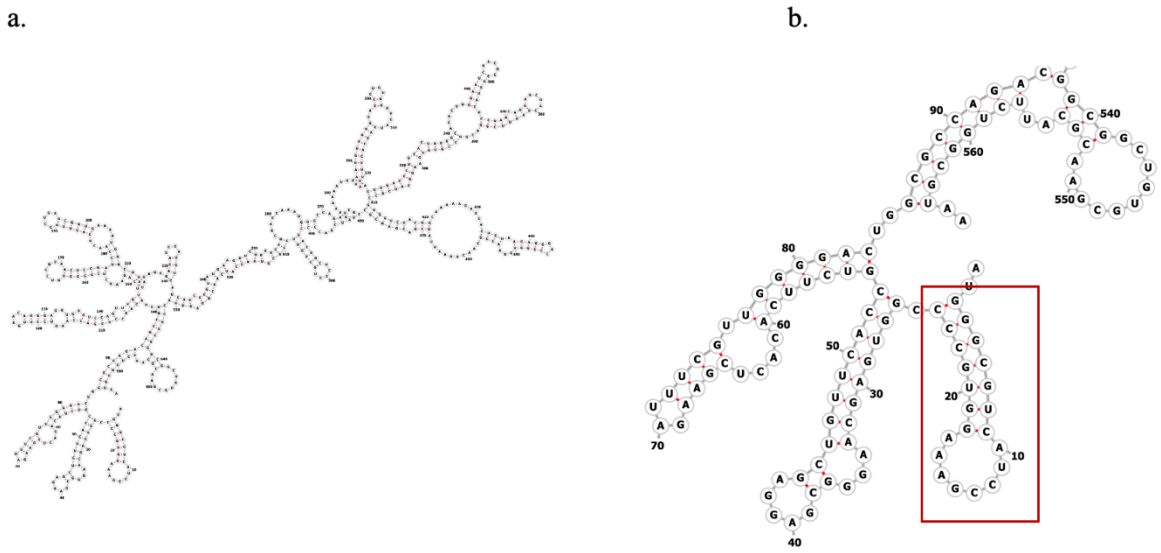

Figure 2.15 Reporter RNA folding prediction encoding the mutation sequence 1 via Vienna RNAWebsuite. a) RNA folding prediction of the reporter construct encoded in BB1 with the NLUC coding sequence with a mutated kink turn sequence 1. **b)** A closer look at the prediction of the mutated k-turn sequence shows two G-U Wobble base pairs and five G-C canonical base pairs. Results have been computed using RNAfold 2.6.3

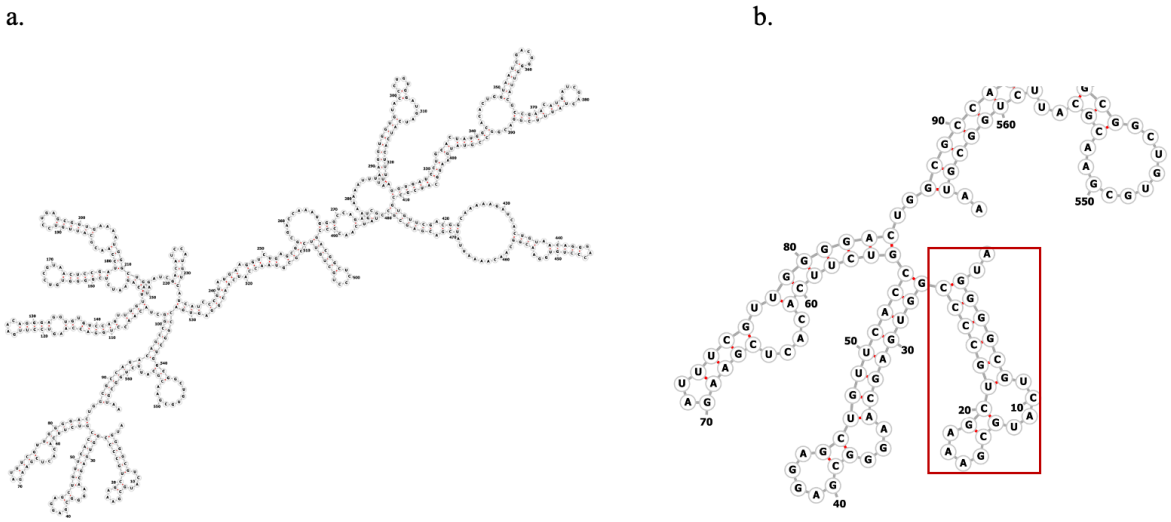

Figure 2. 16 Reporter RNA folding prediction encoding the mutation sequence 1 via Vienna RNAWebsuite. a) RNA folding prediction of the reporter construct encoded in BB1 with the NLUC coding sequence, with a mutated kink turn sequence-2 **b)** A closer look at the prediction of the mutated k-turn sequence shows one G-U Wobble base pair and five G-C canonical base pairs. Results have been computed using RNAfold 2.6.3

For subsequent experiments, the first step was to confirm that the mutated kink-turn-2 sequence is expressed comparably to the wild-type kink-turn sequence. To this end, the mutated kink-turn-2 was cloned into the BB2 backbone containing a EGFP reporter, and single-reporter constructs encoding the wild-type k-turn and optimized mutated k-turn were translated to assess and compare their expression levels (**Fig. 2.17**)

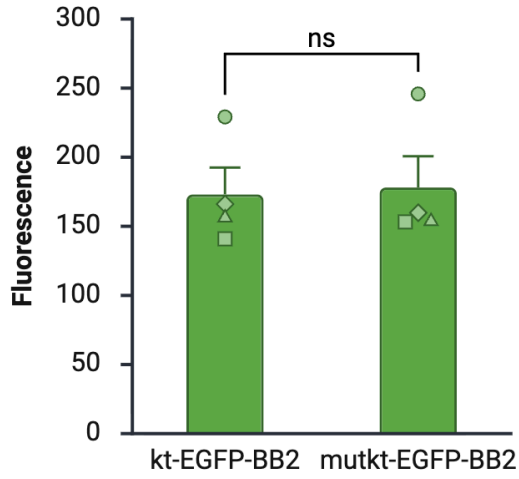

Figure 2. 17 Translation of single reporters with the BB2 backbone in E. coli lysate. Single reporter constructs encoded in the BB2 backbone were translated in E. coli lysate to evaluate their expression levels. kt-EGFP and kt^{mut}-EGFP were expressed at the same level when the mutated sequence 2 was used. n=4. . Statistical significance was assessed using a one-tailed paired Student's t-test, $p < 0.5$, (n = 4).

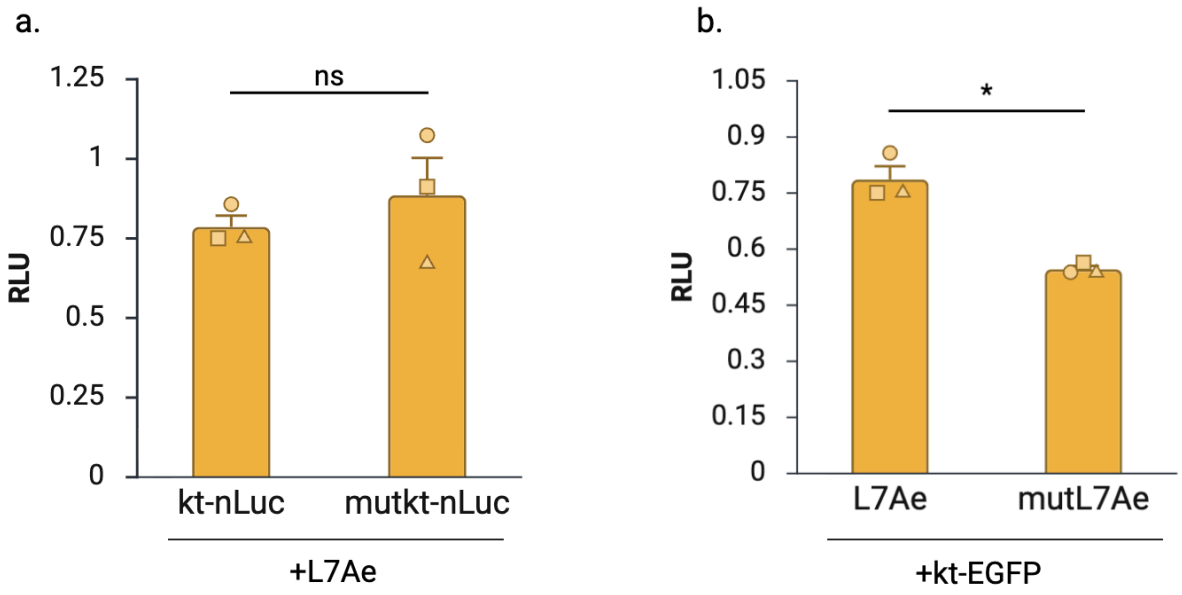

Figure 2. 18 Testing L7Ae repression of kt-nLuc reporter encoding in the BB1 backbone with a one-step reaction protocol in *E.coli* Lysate. a) Bar graph representing the mean values of luminescence of three independent experiments, illustrating the translation of kt-nLuc and kt^{mut}nLuc reporters with L7Ae using a one-step protocol. Each data point corresponds to one experiment. Statistical analysis did not show significance (n = 3). **b)** Bar graph representing the mean values of three independent experiments, showing the repression of kt-nLuc by either L7Ae^{mut} or L7Ae using a one-step protocol. Each data point corresponds to one experiment. ns: not significant; RLU: relative light units. Statistical significance was assessed using a one-tailed paired Student's t-test.

To compare the one-step and two-step protocols in *E. coli*, both were tested using the BB1 backbone, and the following three conditions were tested: L7Ae with kt-nLuc, L7Ae with kt^{mut}nLuc, and L7Ae^{mut} with kt-nLuc. While three biological replicates with the one-step

protocol showed different levels of repression with the L7Ae when comparing the wild-type and mutated reporters, the differences were not statistically significant (**Fig. 2.18a**). Additionally, the kt-nLuc was tested, either the L7Ae or L7Ae^{mut}. The results did not show repression (**Fig. 2. 18b**).

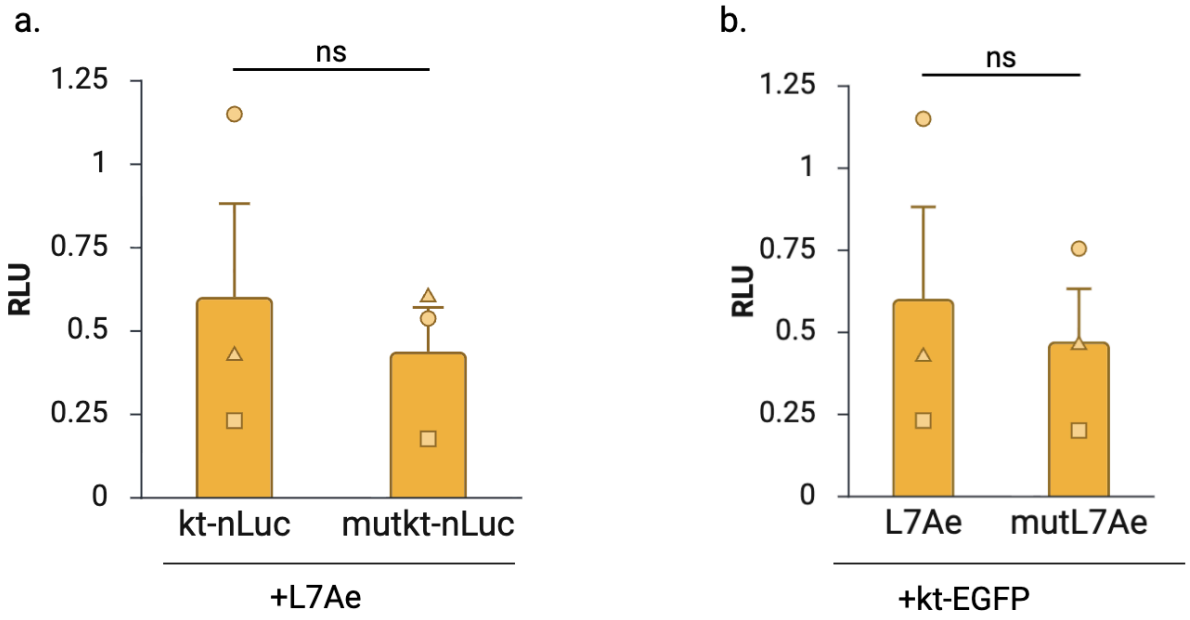

Figure 2. 19 Testing L7Ae repression of kt-nLuc reporter encoding in the BB1 backbone with a two-step reaction protocol in *E.coli* Lysate. a) Bar graph representing the mean luminescence values of three independent experiments, illustrating the translation of kt-nLuc and kt^{mut}nLuc reporters with L7Ae using a two-step protocol. Each data point corresponds to one experiment. Statistical analysis did not show significance (n = 3). **b)** Bar graph representing the mean values of three independent experiments, showing the repression of kt-nLuc by either L7Ae or L7Ae^{mut} using a two-step protocol. Each data point corresponds to one experiment. ns: not significant; RLU: relative light units. Statistical significance was assessed using a one-tailed paired Student's t-test

The BB1 construct was also tested using the two-step protocol to determine whether it could improve variability and repression. However, testing the BB1 backbone in *E. coli* lysate with the two-step protocol did not reduce variability or enhance repression; in fact, it resulted in even more variable outcomes (**Fig 2.19a**). When the activity of L7Ae and L7Ae^{mut} is compared with wild type reporter, L7Ae^{mut} conditions was showing lower luciferase activity than the wild-type conditions (**Fig 2.19b**). It was expected that the L7Ae^{mut} would have a higher RLU value than L7Ae, and with the two-step protocol, it did not show the expected outcome.

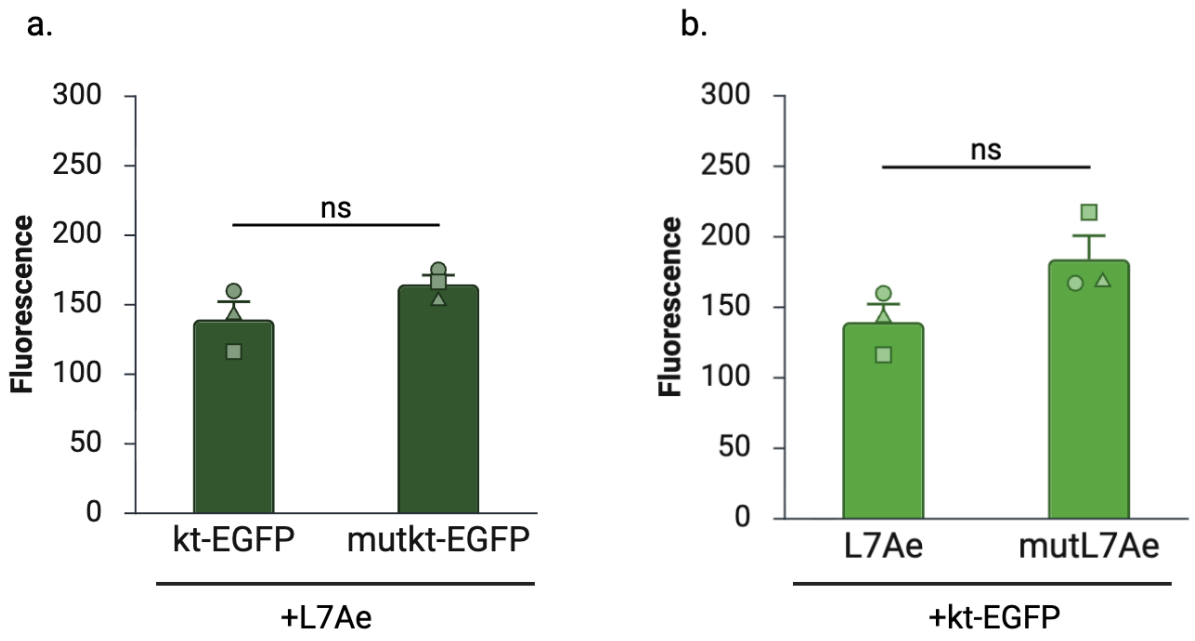

Figure 2. 20 Testing L7Ae repression of the kt-EGFP reporter encoding in the BB2 backbone with a one-step reaction protocol in *E.coli* Lysate. a) Bar graph representing the mean fluorescence values of three independent experiments, illustrating the translation of kt-EGFP and kt^{mut}-EGFP reporters with L7Ae using a one-step protocol. Each data point corresponds to one experiment. Statistical analysis did not show significance (n = 3). **b)** Bar graph representing the mean fluorescence values of three independent experiments, showing the repression of kt-EGFP by either L7Ae or L7Ae^{mut} using a one-step protocol. Each data point corresponds to one experiment (n = 3). ns: not significant. Statistical significance was assessed using a one-tailed paired Student's t-test

To determine whether a different plasmid would exhibit similar behavior or show better response, plasmid BB2 was also tested in *E. coli* lysate using both one-step and two-step reactions. With the one-step reaction, three biological replicates showed repression, but it was not significant. Comparing the wild-type L7Ae and the L7Ae^{mut} the observed different repression was not significant (**Fig. 2.21**).

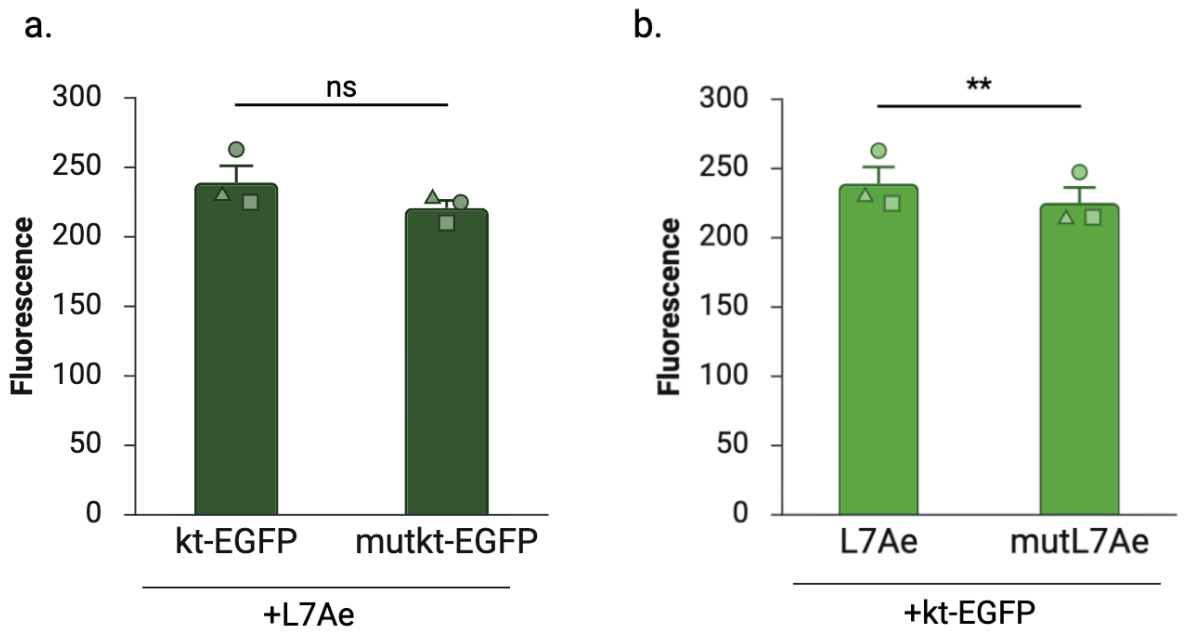

Figure 2. 21 Testing L7Ae repression of the kt-EGFP reporter encoded in the BB2 backbone with a two-step reaction protocol in *E.coli* lysate. a) Bar graph representing the mean fluorescence values of kt-EGFP and kt^{mut}-EGFP reporters with L7Ae using a two-step protocol. **b)** Bar graph representing the mean fluorescence values of kt-EGFP with either L7Ae or L7Ae^{mut} using a two-step protocol. ns: not significant. Statistical significance was assessed using a one-tailed paired Student's t-test. n=3

The repression of the k-turn-EGFP reporter by L7Ae, encoded in the BB2 backbone, was examined via a two-step protocol. Contrary to expectations, this protocol produced an inversion of the reporter's repression behavior **(Fig. 2.21**). Like the BB1, the BB2 results showed different behavior with the two-step protocol. Neither the one-step protocol nor the two-step protocol produced robust and significant repression required to conclude with confidence that L7Ae blocks reporter translation in this system across both backbones and wild-type and mutated reporters. These results showed that rather than the constructions themselves, the variability may be due to restrictions or uncontrollable elements present in the lysate-based system, such as creating byproducts and interfering with the L7Ae-kt system.

As a result, I switched to the PURE cell-free system, a recombinantly generated platform where every component is purified and combined. The PURE system provides a more

regulated biochemical environment than crude lysates, which lowers background variability and makes it easier to control L7Ae-mediated repression.

2.3 Testing the PURE system for Optimization of Post-Translational Control Devices

To evaluate the system in a more controlled and more precise context, I employed a purified and reconstituted cell-free system (PURE), characterized by its precisely and predefined purified components. This defined composition should minimize metabolic side reactions, reduce protease and nuclease contamination, and eliminate the risk of endogenous gene expression, thereby providing a cleaner and more reproducible environment for assessing our control devices (Whittaker 2013; Ohashi et al., n.d.).

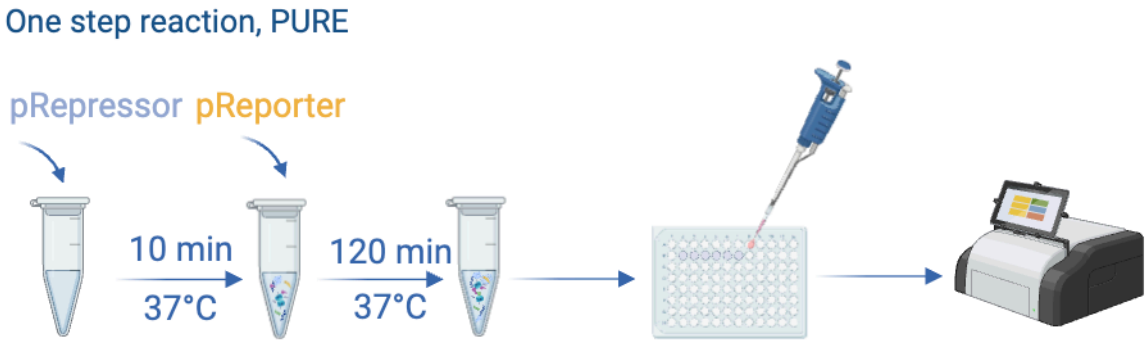

Figure 2. 22 One-step reaction protocol flow for the PURE system experiment. In one-step reaction, the repressor-coding construct is introduced into the reaction and incubated for 10 minutes. After this incubation reporter construct is introduced to the reaction, and the complete system is incubated in a thermocycler at 37 °C for 2 hours. Reaction mixtures are moved to the 384-well plate to measure the reporter activity.

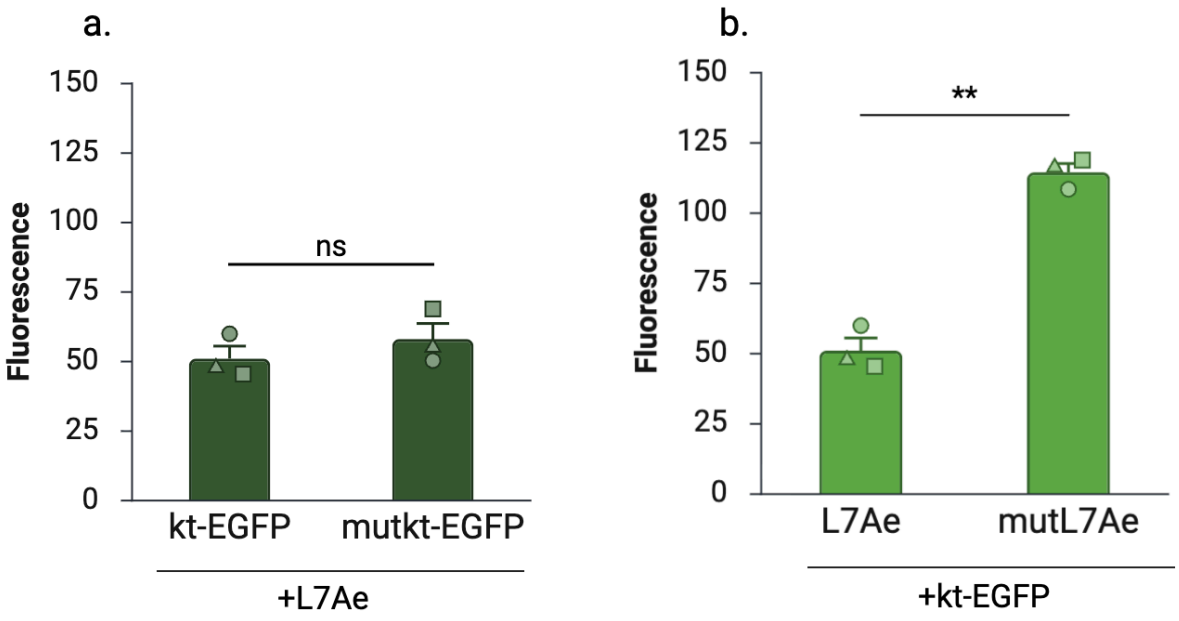

Figure 2. 23 Testing the L7Ae repression of the kt-EGFP reporter encoded in BB1 in the PURE system with a one-step protocol. a) Bar graph representing the mean fluorescence values of kt-EGFP and kt^{mut}-EGFP reporters with L7Ae using a one-step protocol. **b)** Bar graph representing the mean fluorescence values of kt-EGFP by either L7Ae or L7Ae^{mut} using a one-step protocol. Statistical significance was assessed using a one-tailed paired Student's t-test, $p < 0.01$. (n=3)

When comparing the repression levels of kt-EGFP and kt^{mut}-EGFP reporters, no significant repression was observed when the constructs were encoded in the BB1 backbone with the one-step protocol (**Fig. 2.23a**). Different from the BB2 backbone in the PURE system, when L7Ae and L7Ae^{mut} repression of the kt-EGFP tested system with BB1, experiments showed significant repression (**Fig. 2.23b**).

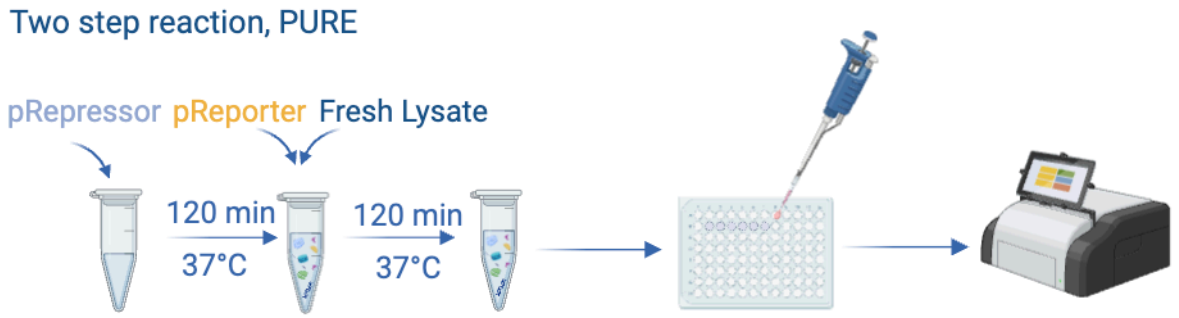

Figure 2. 23 Two-step reaction protocol flow for PURE system experiment. In a two-step reaction, the repressor-coding construct is introduced into the reaction and incubated for 2 hours. After this incubation reporter construct is introduced to the reaction, and the complete system is incubated in a thermocycler at 37 °C for 2 hours. Reaction mixtures are moved to the 384-well plate to measure the reporter activity.

To determine whether pre-translation of the repressor protein could increase the repression fold, a two-step procedure was tested (**Fig. 2.24**). Here, we first incubated L7Ae in the reaction for 2 hours to enable its translation; we then added the reporter and incubated the reaction for 2 more hours.

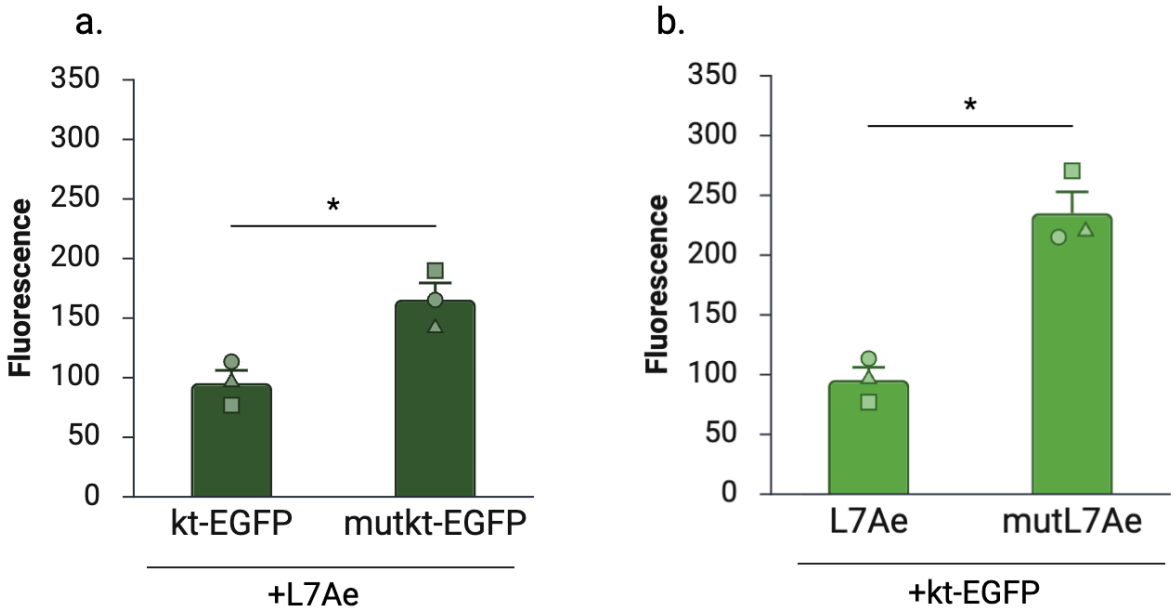

Figure 2. 25 Testing the L7Ae repression of the kt-EGFP reporter encoded in BB1 in the PURE system with a two-step protocol. a) Bar graph representing the mean fluorescence values of independent experiments, illustrating the translation of the kt-EGFP and kt^{mut}-EGFP reporters with L7Ae using a two-step protocol. Statistical significance was assessed using a one-tailed paired Student's t-test, $p < 0.05$. **b)** Bar graph representing the mean fluorescence values of independent experiments showing the repression of kt-EGFP by either L7Ae or $L7Ae^{mut}$ using a two-step protocol. Statistical significance was assessed using a one-tailed paired Student's t-test, $p < 0.02$. (n=3)

Next, L7Ae repression of the kt-EGFP reporter in the BB1 backbone was tested with the two-step protocol. The results indicate significant differences between the wild type and mutkt (**Fig. 2. 25a**), and confirm significant repression of reporter translation by wild type L7Ae as compared to mutL7Ae (**Fig. 2. 25b**).

I further evaluated the system, with the same constructs encoded in the BB2 backbone both with the one-step and two-steps. First, L7Ae repression of the reporter encoded in the BB2 backbone using a one-step protocol (**Fig. 2.22**) and observed a consistent and significant reduction of EGFP expression when embedding the k-turn in the 5'UTR as compared to kt^{mut}-EGFP (**Fig. 2.26a).** However, when the L7Ae and $L7Ae^{mut}$ repression levels of the kt-EGFP reporter were compared, we did not observe any difference in EGFP levels. This was unexpected, since $L7Ae^{mut}$ should not bind to the kink turn structure (**Fig. 2.26b**)

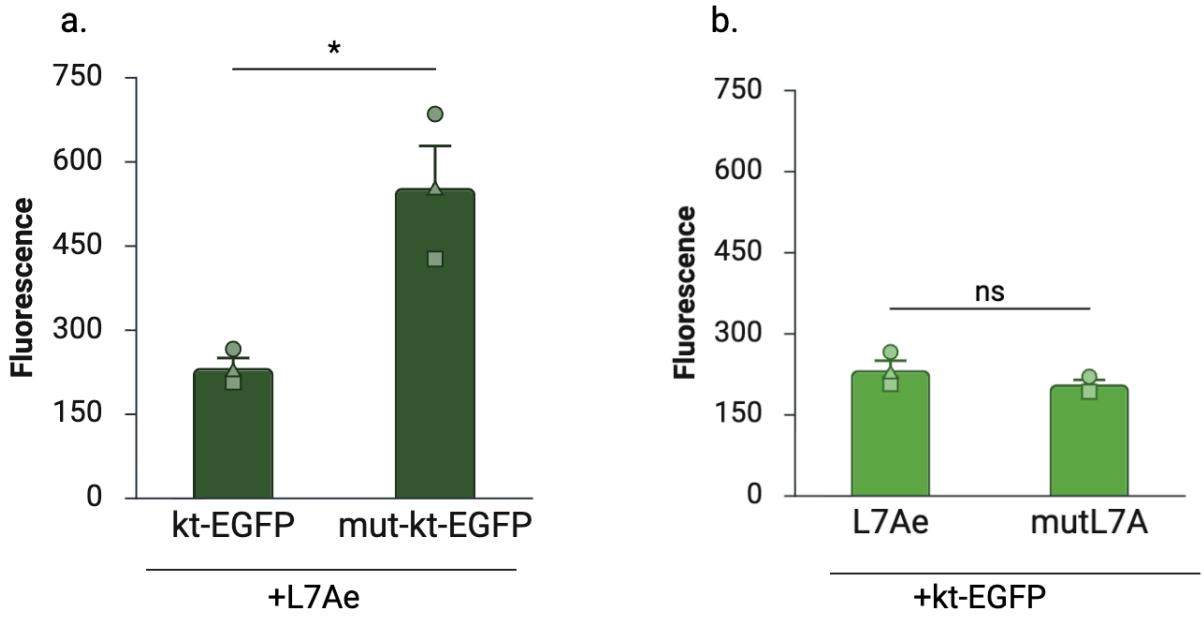

Figure 2. 26 Testing the L7Ae repression of the kt-EGFP reporter encoded in BB2 in the PURE system with a one-step protocol. a) Bar graph representing the mean fluorescence of three independent experiments, illustrating the translation of kt-EGFP and kt^{mut}-EGFP reporters with L7Ae using a one-step protocol. Statistical significance was assessed using a one-tailed paired Student's t-test ($p < 0.04$, $n = 3$). Each data point corresponds to one experiment. **b)** Bar graph representing the mean fluorescence values of three independent experiments, showing the repression of kt-EGFP by either L7Ae or $L7Ae^{mut}$ using a one-step protocol ($n = 3$). ns: not significant.

With the two-step method, we obtained a significant improvement of the repression that was greater than fivefold (**Fig. 2.26**). When the repression of L7Ae was tested by comparing the wild-type and mutant L7Ae constructs, experimental data showed a trend of reduced EGFP expression with wild-type L7Ae, although not statistically significant (**Fig. 2.26b**).

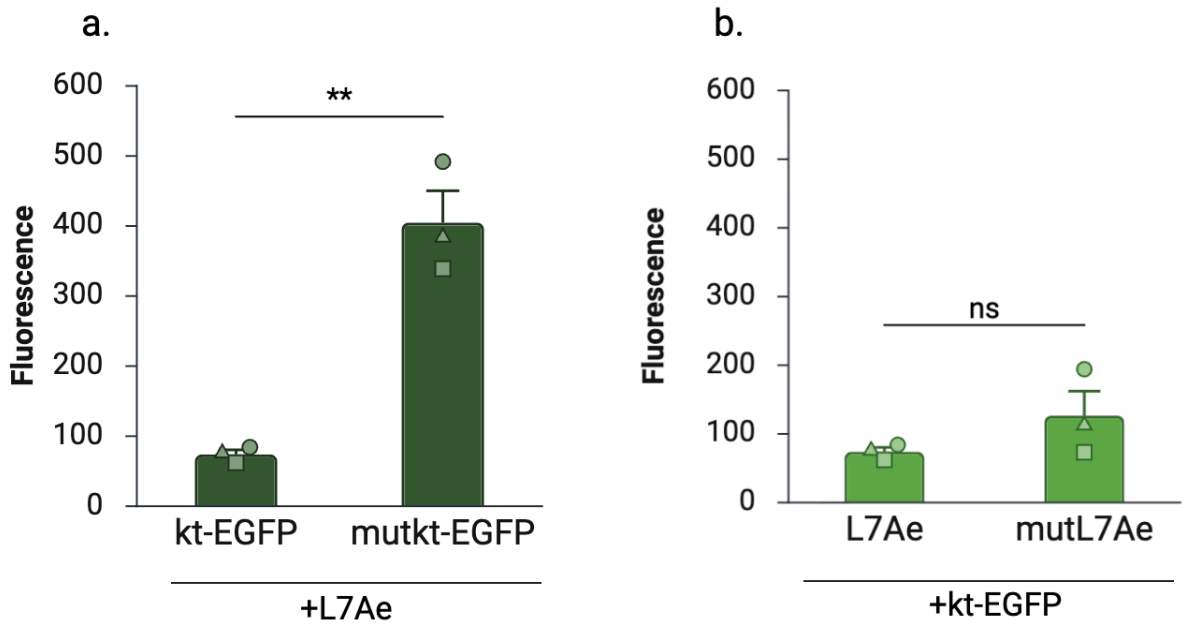

Figure 2. 24 Testing the L7Ae repression of the kt-EGFP reporter encoded in BB2 in the PURE system with a two-step protocol. a) Bar graph representing the mean fluorescence of kt-EGFP and kt^{mut}-EGFP reporters with L7Ae using a two-step protocol. Statistical significance was assessed using a one-tailed paired Student's t-test, $p < 0.01$ ($n = 3$). **b)** Bar graph representing the mean fluorescence of kt-EGFP by either L7Ae or $L7Ae^{mut}$ using a two-step protocol. (n=3) ns: not significant

Overall, I developed a reliable, optimized protocol that enables robust detection of RNA-regulatory circuits in the PURE system using genetically encoded constructs.

2.4. Testing the Purified Repressor Proteins in the PURE system for Optimization of Post-Translational Control Devices

Using the optimized protocol I developed, I aimed to test whether the PURE system can be used to evaluate the functionality of purified proteins. As a model, I used the L7Ae-ktEGFP reporter system. For this purpose, I first overexpressed the L7Ae protein in *E. coli* and purified it using a 6xHis affinity tag. The purified L7Ae protein was then tested for its ability to repress the translation of its target mRNA. The following sections (**Fig. 2.28 and 2.29**) describe each experiment in detail.

The experimental setup included several conditions designed to assess whether the purified L7Ae protein can effectively repress translation in the PURE system.

Functional test of purified L7Ae**:** In this part of the experiment, reporter DNA constructs were added to the PURE system together with the purified L7Ae protein. Translation was carried out to determine whether the presence of L7Ae represses reporter expression, confirming that the purified protein remains functional.

Buffer control experiments**:** To ensure that any observed effects were due to the protein itself and not the buffer used during purification, additional control reactions were performed. In these controls, only the buffer (without protein) was added to the system. Two buffer types were tested: **Buffer 1**: 20 mM Hepes-KOH (pH 7.4), 150 mM KCl, 1.5 mM $MgCl_2$, and 40% glycerol; **Buffer 2:** 10 mM Tris-HCl, 20% glycerol. These controls allowed evaluation of whether the buffer components influenced the translation efficiency in the PURE system.

Purified protein test conditions: Finally, to examine the repression effect of purified L7Ae protein, different concentrations of purified L7Ae (ranging from 2.5 µM to 10 µM). Testes with kt-EGFP and kt^{mut} EGFP reporter constructs.

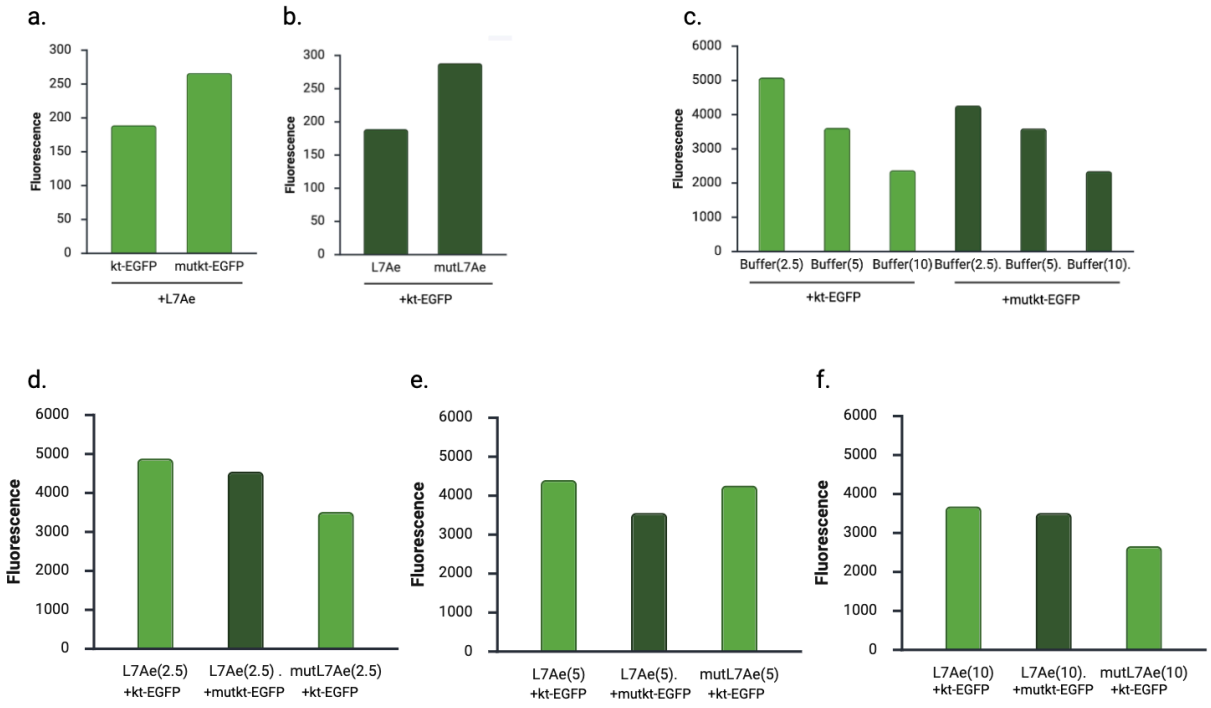

Figure 2. 25 Testing the effectiveness of purified repressor proteins in the PURE system a) Bar graph representing the mean fluorescence of three independent experiments, illustrating the translation of kt-EGFP and kt^{mut}-EGFP reporters with L7Ae using a one-step protocol. **b)** Bar graph representing the mean fluorescence values of three independent experiments, showing the repression of kt-EGFP by either L7Ae or L7Ae^{mut} using a one-step protocol. **c)** Testing L7Ae repression of the kt-EGFP and kt^{mut}-EGFP reporters with the addition of Buffer-1. Different buffer concentrations were used: Buffer(2.5) = 2.5 µM, Buffer(5) = 5 µM, Buffer(10) = 10 µM. All conditions contained the same concentration of the L7Ae plasmid. **d. e. f.** Translation of the kt-EGFP-BB2 reporter in the presence of purified proteins. The kt-EGFP-BB2 plasmid is added 25 fmol for all conditions. Different concentrations of purified L7Ae and mutant L7Ae were tested: L7Ae(2.5) = 2.5 µM of purified L7Ae, L7Ae(5) = 5 µM of purified L7Ae, L7Ae(10) = 10 µM of purified L7Ae; mutL7Ae(2.5) = 2.5 µM of purified L7Ae^{mut}, mutL7Ae(5) = 5 µM of purified L7Ae^{mut}, mutL7Ae(10) = 10 µM of purified L7Ae^{mut}.

For the first experiment, the purified protein in Buffer-1 was used. Initially, repression by L7Ae was tested using genetic constructs to confirm the repression level by the DNA constructs (**Fig. 2.28a and Fig. 2.28b**). To evaluate whether the buffer used for protein purification had any effect on repression, L7Ae-mediated repression was tested with genetic constructs under conditions that included the buffer. Since different concentrations of purified protein were tested, corresponding volume of buffer were also added to maintain consistency.

Data showed that when the buffers are added to the reaction, it boosts the translation of the reporter approximately 20-fold (**Fig. 2.28c**). Later on, purified proteins are tested for repression of the reporter kt-EGFP and kt^{mut}-EGFP under different conditions. For all the protein concentrations (2,5 µM, 5 µM, and 10 µM), purified L7Ae did not show any downregulation of the reporter was not (**Fig. 28d, Fig. 28e, Fig. 28f**).

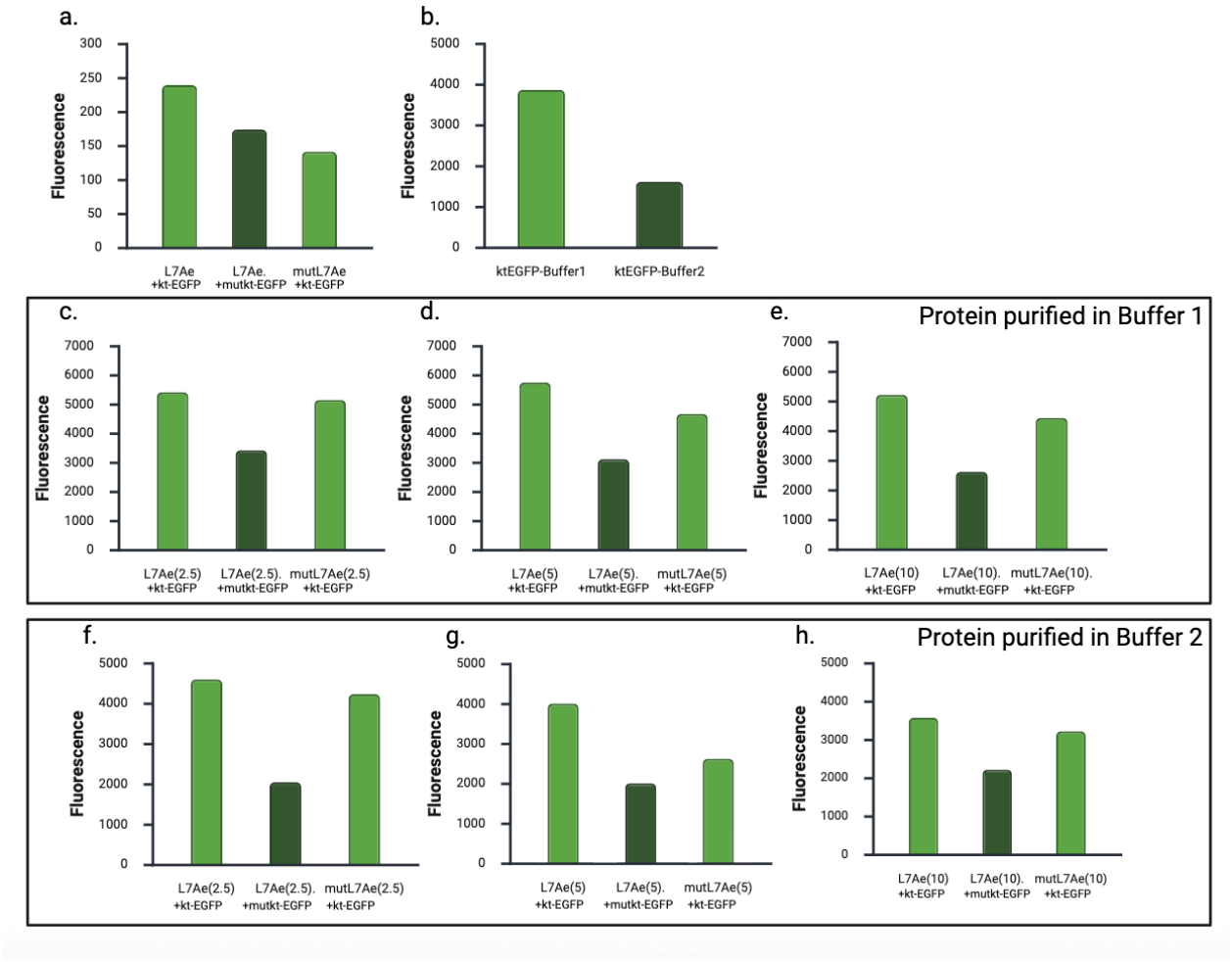

Figure 2. 26 Testing the effectiveness of purified repressor proteins in the PURE system with different buffers. a) Translation of the kt-EGFP reporter with Buffer-1 and Buffer-2 **b)** Translation of the L7Ae+kt reporter system from DNA constructs to verify repression, serving as a control c: Testing L7Ae repression of the kt-EGFP and kt^{mut}-EGFP reporters with the addition of Buffer-1. L7Ae(5) = 5 µM of purified L7Ae, L7Ae(10) = 10 µM of purified L7Ae; mutL7Ae(2.5) = 2.5 µM of purified $L7Ae^{mut}$, mutL7Ae(5) = 5 µM of purified $L7Ae^{mut}$, mutL7Ae(10) = 10 µM of purified $L7Ae^{mut}$. d: Testing L7Ae repression of the kt-EGFP and kt^{mut}-EGFP reporters with the addition of Buffer-2. L7Ae(5) = 5 µM of purified L7Ae, L7Ae(10) = 10 µM of purified L7Ae; mutL7Ae(2.5) = 2.5 µM of purified $L7Ae^{mut}$, mutL7Ae(5) = 5 µM of purified $L7Ae^{mut}$, mutL7Ae(10) = 10 µM of purified $L7Ae^{mut}$.

Next, purified proteins were buffer exchanged into Buffer-2, which does not contain any additional salt ions and only contains Tris-Cl and glycerol, hypothesizing that additional salt amounts in Buffer-1 can be the reason for boosted translation. The system was initially tested using genetic constructs to confirm the repression; however, no repression was observed with the genetic constructs (**Fig. 2. 29a**). This implied that there may have been an issue during the experimental process. Subsequently, the kt-EGFP reporter was employed as a control to test Buffer 1 and Buffer 2 individually. Findings showed that Buffer 1 had a greater degree of translational boosting than Buffer 2 (**Fig. 2. 29b**). The purified protein was subsequently tested at varying concentrations in Buffer 1 (**Fig. 2. 29c, d, e)** and Buffer 2 (**Fig. 2. 29f, g, h**).

Translational boosting was observed in both buffer conditions. L7Ae did not exhibit any repression at any of the concentrations that were tested. The absence of repression with the genetic constructs, despite the fact that repression had been observed in previous experiments, led to the conclusion that an experimental issue had likely occurred. Although no definitive conclusion could be reached, it was postulated that the buffer's inclusion may have obscured the repression effect by improving translation.

2.5. Testing the TEV protease Rescue of the L7Ae repression in the PURE system for Optimization of Post-Translational Control Devices

L7Ae-mediated repression of the kt-reporter was confirmed in the PURE system. The repression efficiency was further optimized by introducing an incubation step, which enhanced the repression fold-change. To examine repression control at the post-translational level, the activity of L7Ae (TCS) was assessed in the PURE system. Since all PURE reactions were initially performed at 37 °C, the repression efficiency of L7Ae(TCS) was first evaluated under these conditions. L7Ae(TCS) exhibited significant repression of reporter expression at 37 °C (**Fig. 2. 30)**.

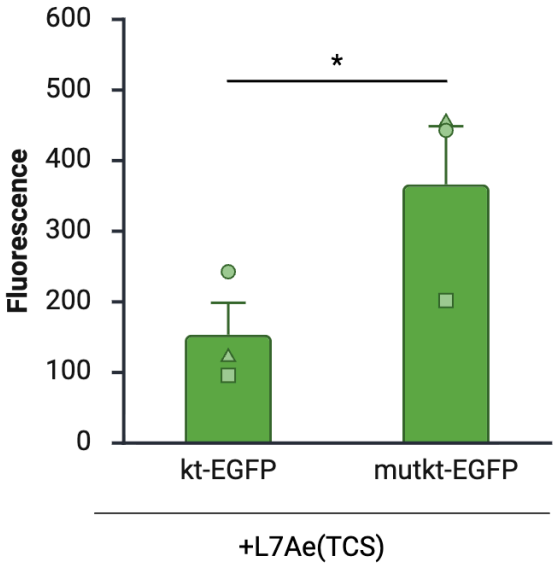

Figure 2. 27 L7Ae(TCS) repression of kt-EGFP-BB2 in the PURE system at 37 °C Bar graph representing the mean fluorescence values of three independent experiments, illustrating the repression of the engineered L7Ae with an insertion of the TEV protease cleavage site was evaluated in the PURE system at 37 °C by comparing the translation level of kt-EGFP-BB2 and kt^{mut}-EGFP-BB2. Statistical significance was assessed using a one-tailed paired Student's t-test, $p < 0.05$. (n=3)

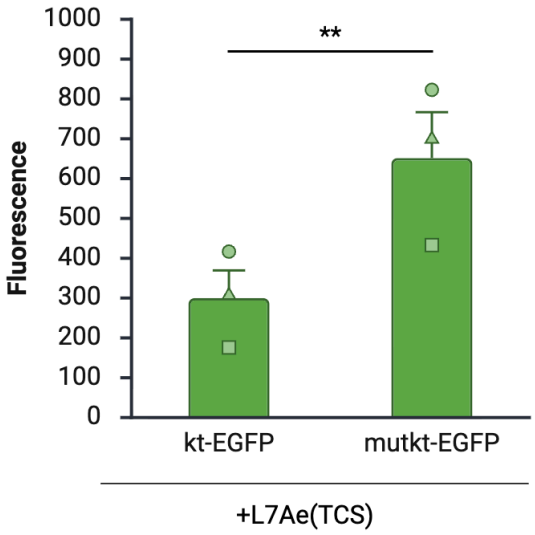

Figure 2. 28 L7Ae(TCS) repression of kt-EGFP-BB2 in the PURE system at 30 °C. Bar graph representing the mean fluorescence values of three independent experiments, illustrating the repression of the engineered L7Ae with an insertion of the TEV protease cleavage site was evaluated in the PURE system at 30 °C by comparing the translation level of kt-EGFP-BB2 and kt^{mut}-EGFP-BB2. Statistical significance was assessed using a one-tailed paired Student's t-test. (n=3)

TEV protease requires a temperature of 30 °C for optimal activity; the repression activity of L7Ae(TCS) was also analyzed at 30 °C to confirm its functionality under these conditions. L7Ae(TCS) also significantly repressed reporter translation (**Fig. 2.31**).

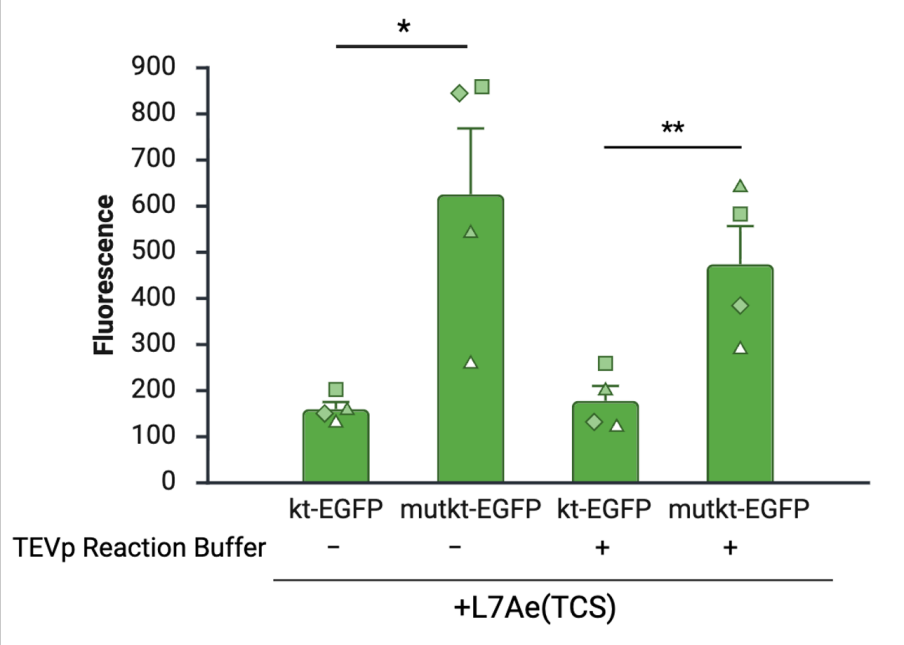

Figure 2. 29 L7Ae(TCS) repression of kt-EGFP-BB2 in the PURE system with or without TEV protease buffer. Bar graph representing the mean fluorescence values of three independent experiments, illustrating the repression of the engineered L7Ae with an insertion of the TEV protease cleavage site was evaluated in the PURE system at 30 °C by comparing the translation level of kt-EGFP-BB2 and kt^{mut}-EGFP-BB2. The first two columns represent the translation of the reporter without any additional buffer. The last two columns represent the repression of the reporter in the presence of TEV protease buffer. Statistical significance was assessed using a one-tailed paired t-test. (n=4)

Once the repression of kt-EGFP by L7Ae(TCS) at 30 °C was established, the next step was to test if TEV protease activity could restore the reporter expression. First, the effect of the TEV protease buffer on repression was tested since TEV protease requires a specific buffer for its activity. To assess this, L7Ae(TCS)-mediated repression of kt-EGFP and kt^{mut}-EGFP was tested in the presence and absence of the TEV protease buffer. The results showed that adding the TEV protease buffer reduced the fold change of repression but maintained the overall repression trend (**Fig. 2.32**).

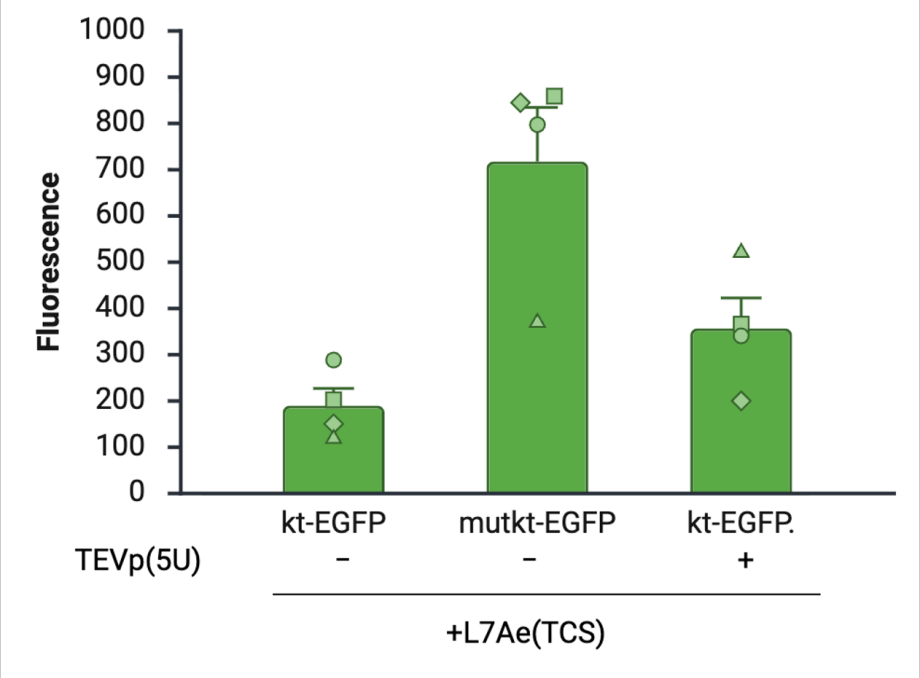

Figure 2. 30 Rescue of the L7Ae(TCS) repression of kt-EGFP-BB2 in the PURE system with 5 units of TEV protease. Bar graph representing the mean fluorescence values of 4 independent experiments, illustrating the repression of the engineered L7Ae with an insertion of the TEV protease cleavage site was evaluated in the PURE system at 30 °C by comparing the translation level of kt-EGFP-BB2 and kt^{mut}-EGFP-BB2. The first two columns represent the translation of the reporter without any protease. The last two columns represent the repression of the reporter in the presence of 5 units of TEV protease. Statistical significance was assessed using one-way ANOVA with the Tukey multiple comparison test. (n=4).

After confirming that the addition of the buffer did not alter the repression pattern, TEV protease was used to test its ability to rescue the L7Ae(TCS)-mediated downregulation of the reporter. Specifically, 5 units of TEV protease were added to the L7Ae(TCS) + kt-EGFP reaction (**Fig. 2.33**). The data indicated that while L7Ae(TCS) significantly repressed kt-EGFP translation, the addition of 5 units of TEV protease led to an increased level of kt-EGFP translation (**Fig. 2.33**). While the repression of the reporter was 2.7-fold when 5 units of TEV were added, it was reduced to 2.3-fold.

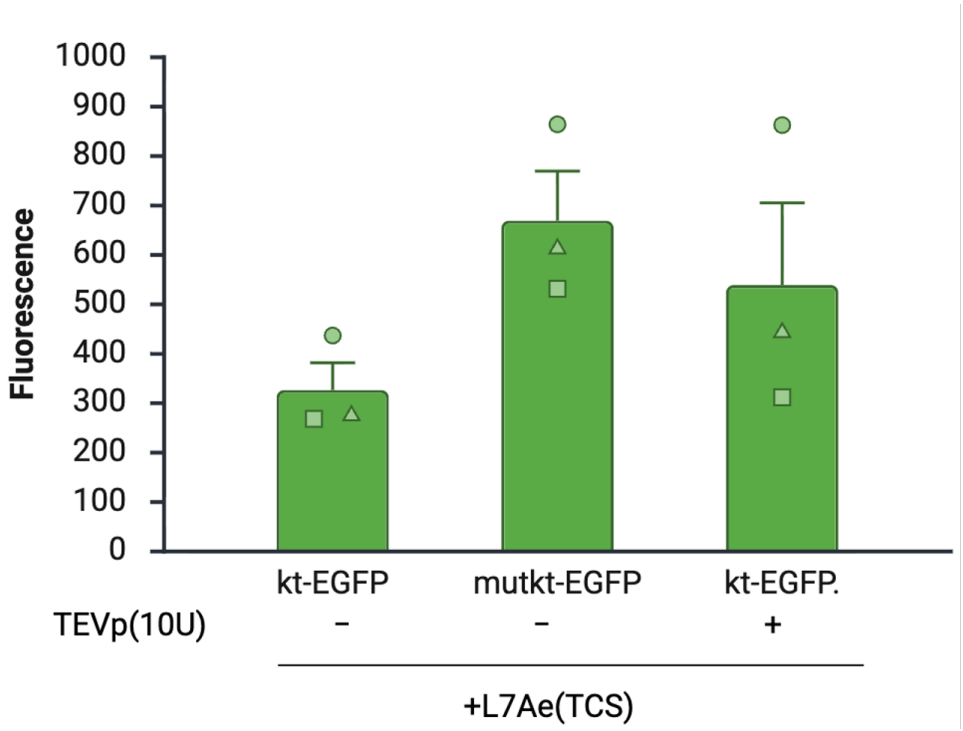

Figure 2. 31 Rescue of the L7Ae(TCS) repression of kt-EGFP-BB2 in the PURE system with 10 units of TEV protease. Bar graph representing the mean fluorescence values of 3 independent experiments, and each experiment's values are the mean of 2 technical replicates, illustrating that the repression of the engineered L7Ae with an insertion of the TEV protease cleavage site was evaluated in the PURE system at 30 °C by comparing the translation level of kt-EGFP-BB2 and kt^{mut}-EGFP-BB2. The first two columns represent the translation of the reporter without any protease. The last two columns represent the repression of the reporter in the presence of 10 units of TEV protease. Statistical significance was assessed using a one-tailed paired Student's t-test. n=3

Aiming to enhance the rescue fold change, the amount of TEV protease was increased to 10 units and tested for its ability to relieve the L7Ae(TCS)-mediated repression. Results showed that the addition of the 10 units of TEV protease led to an increased level of kt-EGFP translation (**Fig. 2.33**). While the repression of the reporter was 2.04-fold when 10 units of TEV were added, it was reduced to 1.2-fold.

In this study, I assessed the activity of RNA-binding protein-based RNA regulation circuits in various cell-free expression systems. The repression activities of the mS2-cNOT7 and L7Ae proteins were analysed using the RRL and *E.coli*-based and PURE systems. The *E.coli* and RRL systems showed inconsistent regulatory response and variable repression efficiencies under the tested conditions. Systematic optimization of the PURE system, including adjustments to reaction parameters, genetic construct backbone, and genetic construct concentration, provided a reproducible and reliable setup for measuring RBP-RNA

regulatory interactions. This optimized PURE-based platform ensures reliable detection of RBP-mediated regulation and provides a solid experimental basis for further quantitative and mechanistic investigations of RNA circuits by using genetically encoded constructs. Additionally, the functionality of the optimized repression system was also tested by adding the RBP-protease interaction. The results confirmed that we established a reliable RBP-based RNA regulatory system, which can be further expanded and layered in cell-free conditions by adding an RBP-protease component.

3. Materials & Methods

3.1 Materials

T4 DNA ligase, Q5 polymerase, and restriction enzymes were purchased from New England Biolabs (Ipswich, MA, USA). Plasmid Mini, Midi, Maxi, and PCR Purification Kits were purchased from QIAGEN.

Enzymes	**Related Experiment**	**#Catalog number**
BamHI- HF	Cloning of the constructs	R0111S, NEB
EcoRI-HF	Cloning of the constructs	R3101S, NEB
NdeI	Cloning of the constructs	R0111S, NEB
NotI-HF	Cloning of the constructs	R3189L, NEB
RNasin inhibitor, recombinant	RRL and PURE experiment	N2511, Promega
T4 ligase	Cloning of the constructs	M0202S
TEV protease	TEV rescue experiment	P8112S, NEB
XbaI	Cloning of the constructs	R0145S
Kits and Chemicals	**Related Experiment**	**#Catalog number**
Amicon® Ultra-15 Centrifugal Filter Unit, Ultracel-3 Membrane	Protein purification	UFC900308
ARCA Cap	*In vitro* transcription assays	S1411L
D-luciferin potassium salt	RRL and *E.coli* lysate experiment	122799, PerkinElmer
Glycerol	Protein purification	15514011, ThermoFisher
Hepes-NaOH	Protein purification	L0180, Biowest
In-Fusion Snap Assembly	Cloning of the construct	638949, Takara Bio
Isopropyl β-D-thiogalactoside (**IPTG**),	Protein purification	I6758, Sigma-Aldrich

Powder, ≥99% (TLC), ≤0.1% Dioxane		
KCl	Protein purification	15514011, Invitrogen
MEGAclear Transcription Clean-Up Kit	*In vitro* transcription assays	AM1908, Thermo Scientific
MEGAscript™ T7 Transcription Kit *in vitro* trascription	*In vitro* transcription assays	AM1334, Thermo Scientific
$MgCl_2$	Protein purification	AM9530, Invitrogen
Mini, midi and MaxiPrep kit	Cloning and plasmid DNA preparation	QIAGEN
Nano-Glo Endurazine Live Cell Substrate	RRL and E.coli lysate translation experiments	N2570, Promega
PURExpress	PURE experiments	E6800L, NEB
Qubit™ dsDNA Quantification Assay Kits	*E.coli* and PURE translation experiments	Q32850, Thermo Scientific
Rabbit Reticulocytes Lysate	RRL translation experiment	L4960, Promega
S30, *E. coli* Lysate for Circular DNA	*E. coli* translation experiment	L1020, Promega
Bacteria Strains	**Related Experiment**	**#Catalog number**
E. coli TOP10	Plasmid DNA preparation	C404006, Thermo Scientific
E. coli Stellar	Cloning experiment	636763, Takara Bio

3.2 Strains and plasmids

Escherichia coli Stellar and TOP10 strains were employed for routine cloning and plasmid DNA amplification.

3.3 Cloning and construct assembly

3.3.1 Cloning design and procedure for Rabbit Reticulocyte Lysate Experiment

For cloning the target gene into an appropriate expression system, a destination vector was used that was specifically designed to include essential regulatory elements, such as a T7 promoter, a multiple cloning site (MCS), and a poly(A) sequence. Because RRL provides only the translational machinery and lacks transcriptional capacity, constructs must be delivered as RNA. To generate these RNAs, *in vitro* transcription was performed using T7 RNA polymerase, which was selected due to its high transcriptional efficiency. For this reason, the gene of interest was cloned downstream of the T7 promoter, ensuring that PCR-amplified templates were immediately compatible for transcription. The MCS was utilized to insert the target gene downstream of the T7 promoter, enabling efficient transcription of the construct. The poly (A) was an important element for different reasons. First, because RRL provides a eukaryotic translation system, the presence of a poly(A) tail enhances the efficiency of translation initiation and overall protein synthesis. Second, the MS2-cNOT7 fusion protein interacts with the reporter RNA through the specific binding of the MS2 protein to the MS2-binding loops on 3' of reporter RNA. This interaction recruits the cNOT7 deadenylase into close proximity to the poly(A) tail of the reporter transcript. The resulting deadenylation leads to the removal of the poly(A) tail, promoting RNA destabilization and degradation, thereby reducing the translation efficiency of the reporter. After the vector design, the insert genes were started to be cloned into the destination vector using the MCS. Some of the cloning was created via T4 ligation. To clone with T4 ligation, first, the target gene was amplified by PCR using specifically designed primers from the plasmid that was used in earlier studies in our laboratory. The resulting products were digested with the appropriate restriction enzymes. The digested products were visualized on 1% agarose gel and extracted. In parallel, the carrier vector was digested with the same enzymes to prepare it for ligation and run on 1% gel and extracted. The T4 ligation reaction was then set up at a 1:3 vector-to-insert ratio by mixing 2 µL of 10× T4 ligation buffer and 1 µL of T4 ligase. The final volume was adjusted to 20 µL

with nuclease-free water, and the mixture was incubated at 16 °C for 15 minutes. For bacterial transformation, 2 µL of the ligation reaction was added to 50 µL of Stellar *E. coli* competent cells. The cells were incubated on ice for 30 minutes, heat-shocked at 42 °C for 45 seconds, and then cooled on ice for 2 minutes. Subsequently, SOC medium was added to the cells, which were incubated at 37 °C for 1 hour to allow recovery and bacterial growth. After incubation, bacteria were spread on an LB Agar plate with a proper antibiotic. Incubated at 37 °C for 16 hours to obtain colonies.

For the cloning with InFusion cloning, the target gene was either amplified with PCR or ordered as gblock (ThermoScientific). If amplification was necessary, the target gene was first amplified by PCR using specifically designed primers. PCR products are run on 1% agarose gel and extracted. The cloning reaction was then set up at a 1:3 vector-to-insert ratio by mixing 2 µL of 5X In-Fusion HD Enzyme Premix and adjusting the volume to 10 µL with nuclease-free water. The reaction was incubated at 50 °C for 15 minutes. Then, the reaction was cooled down at room temperature for 5 minutes. For bacterial transformation, 2.5 µL of the In-Fusion reaction was added to 50 µL of Stellar *E. coli* competent cells. The cells were incubated on ice for 30 minutes, heat-shocked at 42 °C for 45 seconds, and then cooled on ice for 2 minutes. Subsequently, SOC medium was added to the cells, which were incubated at 37 °C for 1 hour to allow recovery and bacterial growth. After incubation, bacteria were spread on an LB Agar plate with a proper antibiotic. Incubated at 37 °C for 16 hours to obtain colonies.

Correct cloning of inserts was confirmed by Sanger sequencing.

Sequencing Primers

Fw: 5’ AGTCAGTGAGCGAGGAAGC 3’

Rv: 5’ AGGAATGGTGCATGCAAGGAG 3’

Additional internal primers for MS2-cNOT7

Fw: 5’ CGGAGGACATGTATGCCCAG 3’

Fw: 5’ CCGCATGGCGTTCGTACT 3’

3.3.2 Construct design for S30 *E. coli* Lysate and PURE Experiment

To clone the construct into backbone-1 (BB1) for the *E. coli* experiments, all inserts L7Ae, mutated L7Ae, kt-NLUC, mutated kt-NLUC, kt-EGFP, and mutated kt-EGFP were ordered as gene blocks, as each sequence was codon-optimized for *E. coli* expression. The constructs were also designed with appropriate overhangs to facilitate In-Fusion cloning. As described before, the BB1 backbone was digested with restriction enzymes (XbaI and EcoRI) and extracted from agarose gel to prepare for cloning. Ordered gene blocks are dissolved in nuclease-free water according to the manufacturer's recommendation and incubated at 50 °C for 10 minutes to obtain properly dissolved gene blocks. Later on, the infusion cloning protocol was followed as it is described above.

To clone the constructs to BB2, the backbone was digested with NdeI-BamHI enzymes and extracted from agarose gel. Later on, the infusion cloning protocol was followed as it is described above.

Constructs are sent for Sanger sequencing and confirmed by sequencing.

Sequencing Primers

Fw: 5' TAATACGACTCACTATAGGG 3'

Rv: 5' GCTAGTTATTGCTCAGCGG 3'

3.4 Design, production, and purification of L7Ae protein

To test the purified repressor protein in the system, L7Ae proteins are cloned into the BB1 backbone with a 6x His tag on the N-terminal of the coding sequence. Brief protocol flow is visualized in Figure 3.1.

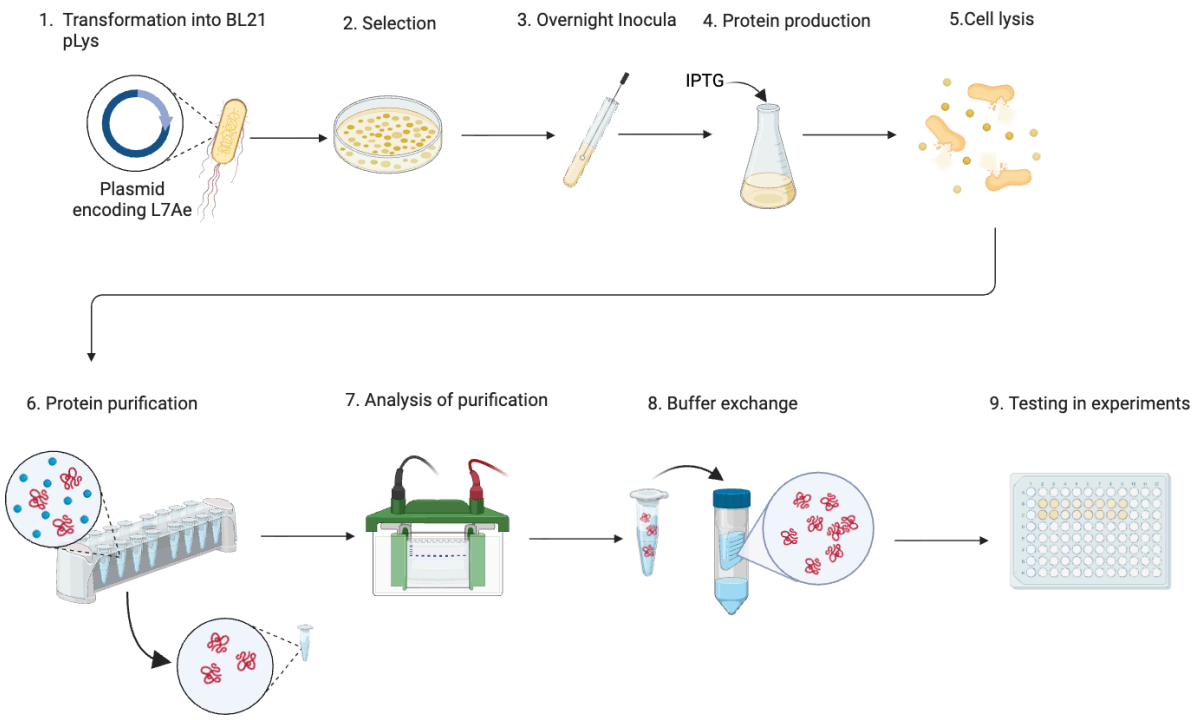

Figure 3. 2 Illustration of the recombinant protein production in BL21 pLys *E.coli* bacteria cells.

The plasmid was transformed into *E. coli* BL21 (DE3) (pLysS) cells with a heatshock transformation. The cells were incubated on ice for 30 minutes, heat-shocked at 42 °C for 45 seconds, and then cooled on ice for 2 minutes. Subsequently, SOC medium was added to the cells, which were incubated at 37 °C for 1 hour to allow recovery and bacterial growth. After incubation, bacteria were spread on an LB Agar plate with a proper antibiotic and incubated at 37 °C for 16 hours to obtain colonies. First to assess the better expressing colonies, single colonies were selected for protein production and growth in 3 mL of LB broth medium overnight at 37 °C. To induce protein expression, 50 mL of LB broth was prepared with 50 µL of antibiotic and 50 µL of overnight inoculum. The culture OD is measured hourly until it reaches 0.2, then it is measured every 30 minutes until it reaches 0.4 at Absorbance at 600 nm. Protein expression was induced with 1 mM IPTG, and the culture was incubated overnight at 25°C.

For purification of the histidine-tagged protein, the MagneHis™ Protein Purification System (V8500) was used. Briefly, cells were lysed in 1X lysis buffer and incubated with DNase I for 15 minutes at room temperature. The lysate was then sonicated for 10 minutes (10 seconds on, 20 seconds off). After sonication, the suspension was incubated at 80°C for 15 minutes and centrifuged at 17,000×g for 30 minutes at 4°C. The supernatant, which contained

the whole cell proteins, was isolated, and this supernatant was used to assess the better expressing colonies at the beginning (**Fig. 3.2**). Before running on the SDS-Page gel, protein concentrations were calculated vis the BCA Assay.

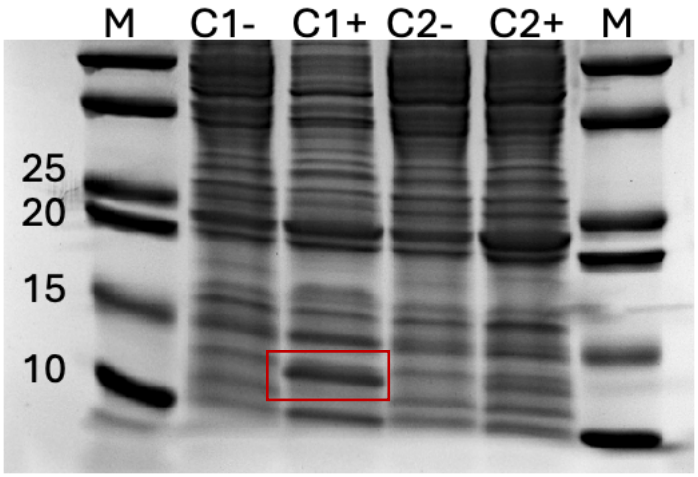

Figure 3.3 SDS Page image of isolated whole-cell proteins from *E.coli* pLys. Two colonies were selected to express the L7Ae protein and protein is 14 kDa. M= Marker, C1-= colony1 culture no induction with IPTG, C1+ = colony1culture induction with IPTG, C2- = colony2 culture no induction with IPTG, C2+ = colony2 culture induction with IPTG.

Isolated proteins from two different colonies showed that colony-1 expressed the target L7Ae protein, and it was selected to continue with protein purification. The resulting supernatant was used for protein purification with Ni particles. Ni particles are vortexed carefully to obtain a uniform suspension, and 30 µL of particles is added to the supernatant obtained. The mix is inverted 10 times carefully and incubated for 2 minutes to bind the proteins onto Ni particles. Tubes were placed in a magnetic stand to separate the Nickel resin. After waiting for 30 seconds, the supernatant was carefully removed and stored as 'supernatant' for SDS-Page analysis. The tubes were removed from the magnetic stand, and the particles were resuspended in 150 µL of binding/wash buffer. After resuspension, the tube was placed on the magnetic stand for approximately 30 seconds to allow the particles to be captured, and the supernatant was carefully removed. This washing procedure was repeated three times in total, and the supernatants removed are stored as 'flow-through' for SDS-Page analysis. Subsequently, the tube was removed from the stand, and the particles were resuspended in 100 µL of elution buffer for protein elution. To compare the protein purified, IPTG non-induced and induced cultures were both purified **(Fig. 3.3**). All the stored samples and eluted protein were run on an SDS-Page gel to see the purified protein. For the eluted proteins from the IPTG non-induced culture, protein concentration was very low and did not run on the gel **(Fig. 3.3**).

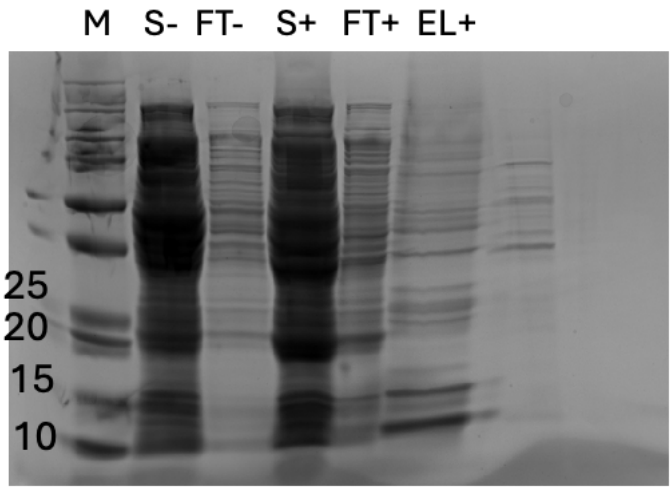

Figure 3.4 SDS Page image of purified proteins from *E.coli* pLys. S- = Supernatant of the non-induced culture. FT- =Flow-through of the non-induced culture, S+ Supernatant of the IPTG induced culture, FT+ Flow through of the IPTG induced culture. EL+ =Eluted proteins from the IPTG-induced culture.

After confirming the eluted protein via SDS-Page gel analysis, the purified proteins were buffer exchanged using the 3 kDa cut-off columns. First, columns were washed with nuclease-free water by adding the water and centrifuging at 4500x*g* for 15 minutes at room temperature. Then, purified proteins were added onto the column and centrifuged at 4500xg for 1 hour at 4 °C. Later on, 500 µL of exchange buffer, either 10 mM Tris-HCl buffer or storage buffer, was added and centrifuged again at 4500x*g*. This step is repeated twice to make sure the elution buffer is removed as much as it is possible. Storage buffer prepared as follows: 20 mM Hepes-KOH (pH 7.4), 150 mM KCl, 1.5 mM MgCl2, containing 40 % glycerol.

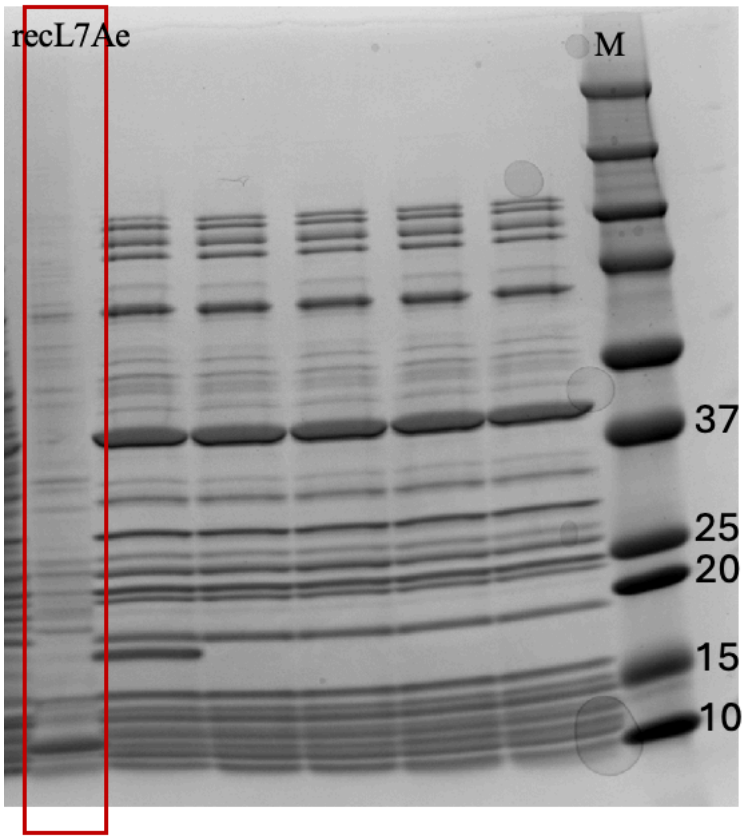

Figure 3.5 SDS Page visualization of buffer exchange recombinant L7Ae protein. Other wells represent different samples. M= marker. L7Ae is a 14 kDa protein.

Buffer exchanged L7Ae, run on SDS-Page after calculating the protein concentration via BCA assay (**Fig. 3. 4**). After producing the wild type L7Ae successfully, different variants of the protein were also purified.

To purify different variants of L7Ae for testing post-translational control in the cell-free system, the L7Ae(TCS) variant was also produced in *E. coli* BL21(DE3)pLysS cells. Purified proteins were run on SDS-Page gel to confirm, and purified proteins contained unspecific protein contamination (**Fig. 3.5**).

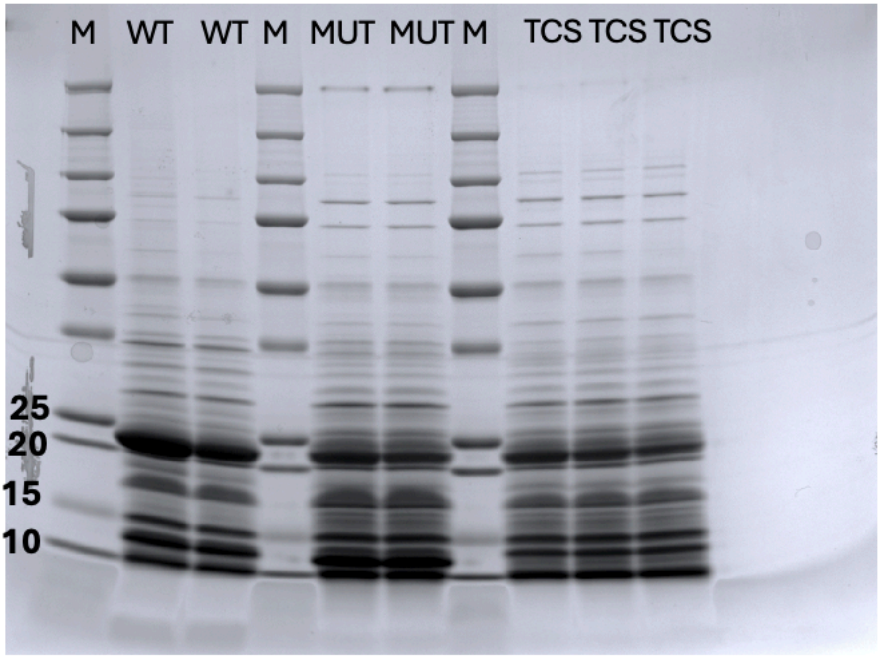

Figure 3.5 SDS Page visualization of purified proteins in elution buffer. M= Marker, WT= purified wild type L7Ae, MUT= purified mutated L7Ae protein, TCS= purified L7Ae(TCS) protein.

3.5 *In Vitro* transcription of templates

All the steps for *in vitro* transcription and translation were done under RNA-free sterile conditions. The cloned templates were amplified using primers specifically designed for *in vitro* transcription. These primers contained both a T7 promoter sequence and a poly(A) tail and were designed to anneal to the backbone region. This design enabled the use of the same primer set for amplification of all cloned constructs. PCR products were separated on a 1% agarose gel. Although the working conditions were not strictly RNase-free, maximum precautions were taken to ensure cleanliness for the agarose gel running. The gel tray and cassette were thoroughly cleaned with RNaseZap, and the agarose gel was prepared in an RNase-free space, and all the used equipment was only used in an RNase-free environment to ensure the lowest RNAse-free environment. Similarly, the loading dye was handled exclusively in an RNase-free space to minimize the risk of RNase contamination. For gel extraction, the kit was opened and maintained in an RNAse-free space and was used exclusively for *in vitro* transcription experiments to further reduce the risk of RNase exposure, and all the tubes that were used were nuclease-free. During elution, aliquots of nuclease-free water were used instead of the kit-provided elution buffer to minimize nuclease contamination. The purified PCR product was subsequently used as a template for *in vitro* transcription.

For uncapped RNA synthesis with natural nucleotide, ATP, CTP, UTP, and GTP were each added to a final concentration of 75 mM. A total of 2 µL of 10X reaction buffer was added, and the DNA template concentration was used between 250–1000 ng. The final reaction volume was adjusted to 20 µL with nuclease-free water. The transcription reaction was incubated at 37 °C for 4 h in a thermocycler.

To transcribe the RNA with a cap and natural nucleotide, ATP, CTP, and UTP were added to a final concentration of 75 mM, while GTP was added to a final concentration of 15 mM. This reduction of GTP concentration is important since both Anti-Reverse Cap Analog (ARCA) [3′-O-Me-m^{7}G(5′)ppp(5′)G] (ARCA) and GTP can be equally incorporated in the transcript. If there's too much GTP in the mixture, the polymerase will likely incorporate a GTP as a starting nucleotide, while ARCA will bind to a smaller amount of transcript. This increases the proportion of uncapped transcripts, resulting in a lower transcript stability in *in vitro* translation reactions. After adding the nucleotides, 2 µL of 10X reaction buffer was added, and the DNA template concentration was used between 250–1000 ng. Cap analog, ARCA added to final concentration 6 mM. The final reaction volume was adjusted to 20 µL. The transcription reaction was incubated at 37 °C for 4 h in a thermocycler.

To produce RNA containing modified nucleotides, with or without a cap structure, the same protocol as described above was followed, except that the corresponding nucleotides were replaced with the desired unnatural analogs.

After transcription, 1 µL of TURBO DNase was added to each reaction. The mixture was gently mixed in an RNAse-free space and incubated at 37 °C for 15 min to remove the DNA template. Subsequently, the RNA was purified to eliminate residual proteins and DNA using the MEGAclear™ Purification Kit. Briefly, RNA samples were adjusted to a final volume of 100 µL with the kit's elution buffer and mixed gently. A total of 350 µL Binding Solution was then added, followed by tmixing through gently pipetting. Next, 100 µL of 100% ethanol was added and mixed gently before loading the entire mixture onto the filter cartridge. The column was centrifuged at 10,000 × *g* for 1 min, and the flow-through was discarded. The column containing *in vitro* transcribed RNAs was then washed twice with 500 µL wash solution. Finally, RNA was eluted by adding 50 µL of preheated nuclease-free water (95 °C) directly onto the column, followed by incubation at 65 °C for 5 min. Eluted RNA integrity was checked on a 1 or 2% agarose gel. To evaluate RNA stability, samples were subjected to heat treatment at 85°C for 3 minutes, followed by immediate cooling on ice for 5 minutes. RNA

degradation was assessed by agarose gel electrophoresis, where the presence of smearing patterns indicative of RNA degradation was evaluated. Only RNAs displaying a single, sharp band on agarose gels were considered of sufficient quality in terms of integrity and used in downstream *in vitro* translation reactions.

Fw Primer:

5’ GAAATTAATACGACTCACTATAGGGAGACCCAAGCT 3’

RvPrimer:

5’ TTTTTTTTTTTTTTTTTTTTTTTTTTTTTTGGGAGCTCGCCCCCTCGGAG 3’

Rv Primer for templates without poly-A sequence:

5’ TTGGGAGCTCGCCCCCT 3’

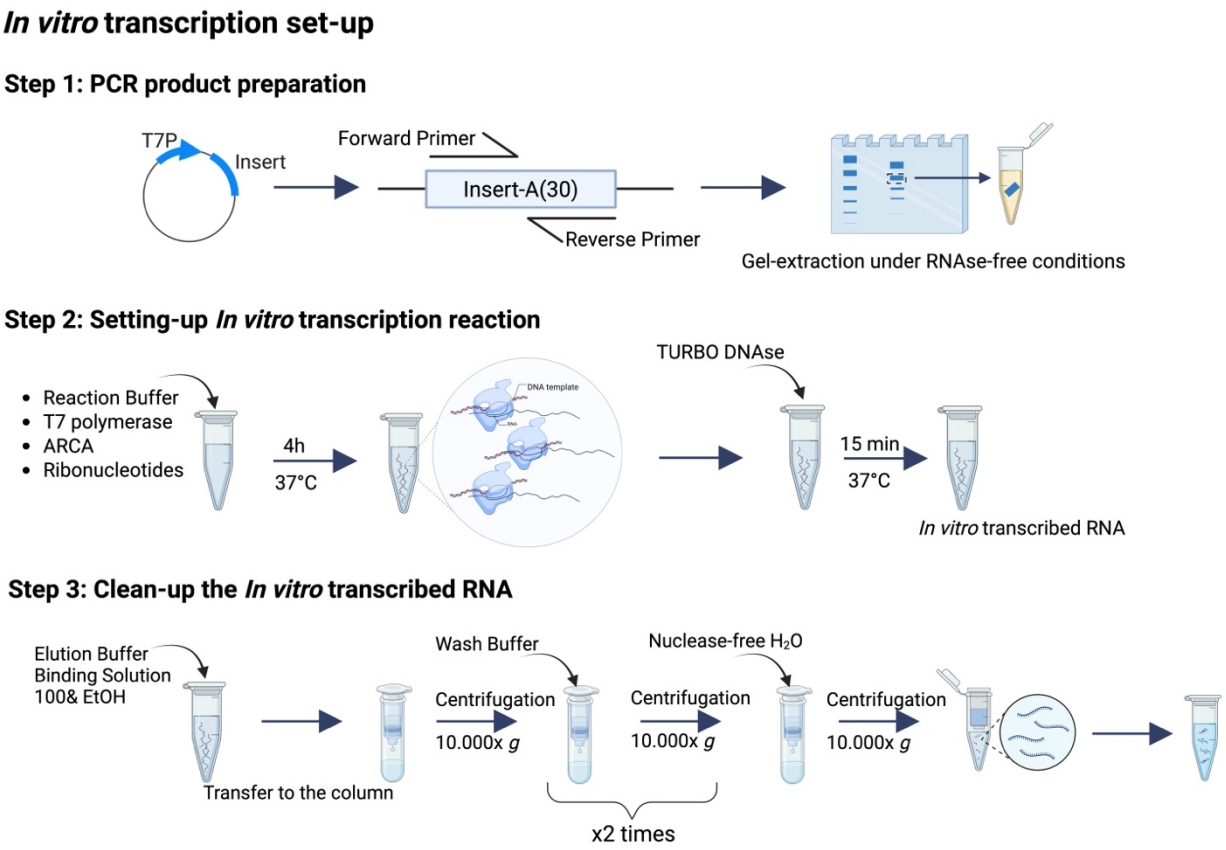

Figure 3. 6 : *In vitro* transcription protocol. Step 1 illustrates the preparation of PCR products used as templates for in vitro transcription. Constructs were cloned into a destination vector, and the gene of interest was amplified by PCR. The resulting PCR products were analyzed on a 1% agarose gel and subsequently extracted. Step 2 depicts the setup of the *in vitro* transcription reaction. Step 3 outlines the RNA purification procedure following in vitro transcription, which enables the use of the *in vitro* transcribed RNA in a cell-free system.

3.5 *In Vitro* Translation in Rabbit Reticulocyte Lysate

In vitro translation assays were performed using nuclease-treated Rabbit Reticulocyte Lysate (RRL) (Promega, L4960). Briefly, 35 µL of lysate was combined with 0.5 µL of 1 mM minus-methionine and 0.5 µL of 1 mM minus-leucine amino acids. To prevent potential RNase-mediated degradation, 20 U of RNase inhibitor (RNasin, Promega) was added to each reaction. For real-time monitoring of luminescence, two different luciferases are used in this study: firefly luciferase and nanoluciferase. Since these two luciferases are orthogonal, they require different substrates to be able to detect. 1 µL of 50 µM D-luciferin was added for firefly luciferase assays, while 0.5 µL of 100× Endurazine was used for Nanoluc-based experiments. Following the addition of RNA templates, the final reaction volume was adjusted to 50 µL with nuclease-free water. To obtain a very well mixed reaction, more robust translation mixtures are prepared in 0.2 µL nuclease-free PCR tubes, mixed well gently, and distributed into white 96-well plates. The protocol flow is illustrated in Figure 3.6.

For the MS2–cNOT7 experiment, each RNA was added at a final concentration of 70 fmol to establish a 1:1 molar ratio. In the experiment where the repressor MS2–cNOT7 protein was used at a fourfold excess relative to the reporter, the final concentration of MS2–cNOT7 was adjusted to 280 fmol. About the addition of the templates first, MS2-cNOT7 RNA was added to the reaction and translated for 10 minutes to allow the construct to be translated into protein prior to the addition of the reporter. Subsequently, Luciferase reporter RNA was added, and translation proceeded at 30°C for 60 minutes. Luminescence was recorded in real time using a GloMax® Discover luminometer.

For the L7Ae–2kt-LUC or kt-NLUC assay, L7Ae was maintained at 70 fmol, while ktNluc and its mutated variant were each used at 0.77 fmol. 70 fmol of L7Ae was pre-incubated with lysate at 30°C for 10 minutes. Subsequently, ktNluc RNA was added, and translation proceeded at 30°C for 60 minutes. Luminescence was recorded in real time using a GloMax® Discover luminometer.

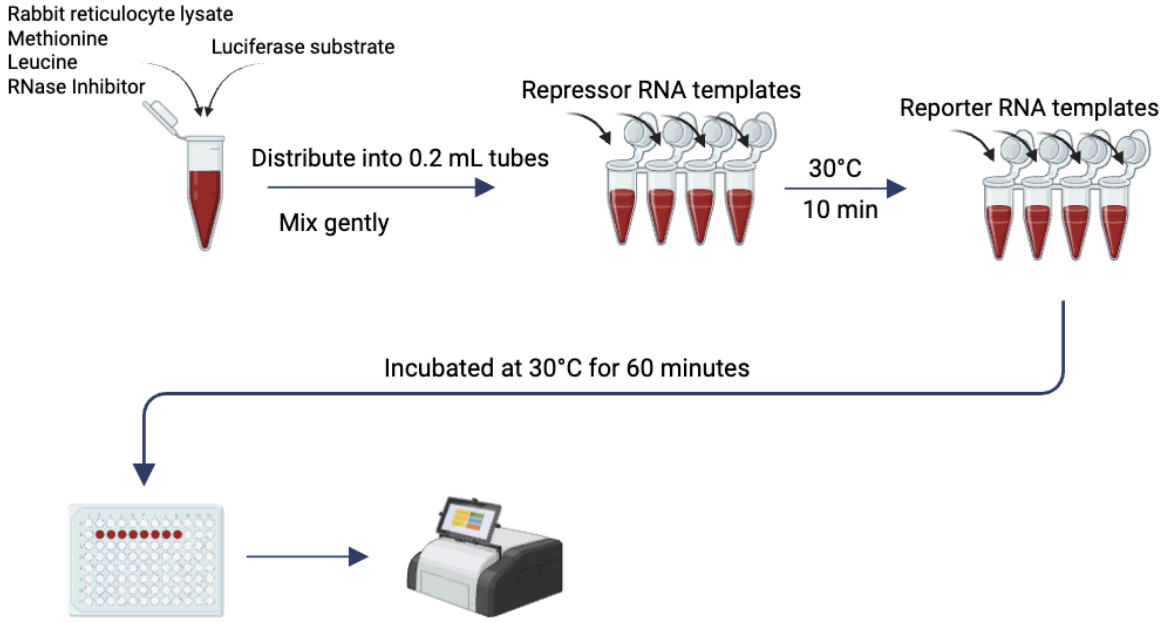

Figure3. 7 : Illustration of *in vitro* translation assays in the RRL system.

3.6 *In Vitro* Translation in *E. coli* Lysate

DNA templates were prepared via midi or maxiprep and quantified with the Qubit™ dsDNA (BR) Quantification Assay Kit. S30 *E. coli* lysate (Promega L1020) is utilized for coupled translation assays, meaning that input can be either DNA or RNA, and the system is able to transcribe the DNA into RNA and translate the RNA into a protein. The protocol flow is illustrated in Figure 3.7.

For the one-step reaction, each reaction includes 5 µL of a complete amino acid mixture, 20 µL of S30 Premix Without Amino Acids, 15 µL of S30 Extract, and 0.5 µL of Endurazine, with the final volume adjusted to 50 µL using nuclease-free water. The prepared master mix is aliquoted into 0.2 mL tubes, and L7Ae (wild-type or mutated) is added.

For the one-step reaction, each reaction is set as described previously, with 535 fmol of L7Ae (wild-type or mutated) added. The mixture is incubated at 37°C for 10 minutes. Then, 65 fmol reporter was added to the reaction and incubated at 37°C for an hour.

For the two-step reaction, each reaction is set as described previously, with 535 fmol of L7Ae (wild-type or mutated) added. The mixture is incubated at 37°C for 60 minutes. To

add the reporter, the same reaction was prepared as described earlier, and 65 fmol of reporter was added to the reaction, mixed with the L7Ae-containing reaction, and incubated for another hour at 37°C.

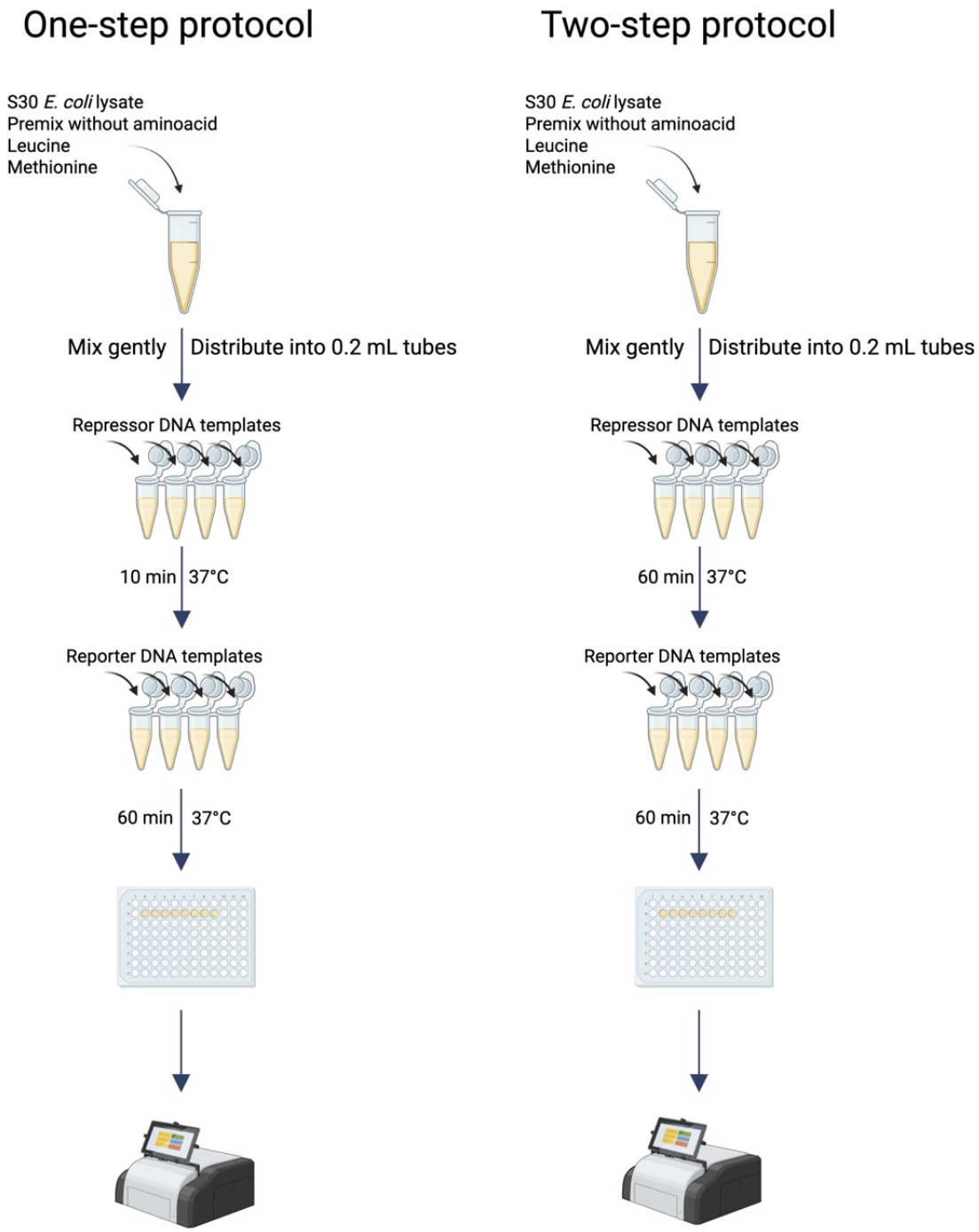

Figure 3.8 Illustration of *in vitro* transcription/translation assays in the *E. coli* system. The left column depicts the setup of the one-step protocol, while the right column shows the workflow of the two-step protocol.

3.7 *In Vitro* Translation assay with the PURE System

All DNA templates used in this system were prepared using either Midi- or Maxiprep procedures to ensure high-quality DNA isolation. The concentration of purified DNA was determined using the Qubit™ dsDNA BR Assay Kit, which provides more accurate quantification compared to spectrophotometric methods. This approach was chosen because residual contaminants such as single-stranded DNA, RNA, proteins, or free nucleotides may remain after DNA purification and can interfere with conventional DNA concentration measurements. To measure DNA concentration using this assay, the Qubit™ working solution was first prepared by diluting the Qubit™ dsDNA BR Reagent 1:200 in the Qubit™ dsDNA BR Buffer. The working solution was then dispensed into RNase-free 0.5 mL thin-wall PCR tubes to a final volume of 200 µL per tube. For calibration of the instrument (Qubit 4 Fluoremeter, ThermoScientific), 10 µL of each Qubit™ standard was added to the respective tubes. For DNA quantification, 2 µL of each sample was added to individual tubes containing the working solution. The tubes were gently mixed by pipetting without touching the tube walls. After incubation at room temperature for 2 minutes, the standards were measured first to calibrate, followed by measurement of the DNA samples. The protocol flow is illustrated in Figure 3.8.

PURExpress (E6800, Promega) was used to test the L7Ae-kt system. Reactions were prepared according to the manufacturer's recommendations. Briefly, 5 µL Solution A was dissolved carefully and mixed well to avoid the formation of precipitates. Solution B (3.75 µL) was always added to Solution A, and it was not diluted unbuffered as per protocol recommendation. 20 units of RNase inhibitor were also added to the reaction mix to reduce the RNase contamination effect on the reaction. The final volume was adjusted with nuclease-free water. L7Ae protein was prepared at a concentration of 75 fmol in a total volume of 2 µL to facilitate accurate adjustment of the DNA template addition, while the reporter was 25 fmol in a total volume of 2 µL.

For the one-step reaction, each reaction is set as described previously in 0.2 mL nuclease-free PCR tubes, with 75 fmol of L7Ae (wild-type or mutated) added. Reaction volumes were adjusted to 14.5 µL and mixed gently. After adjustment, tubes were spun down and incubated at 37°C for 10 minutes in a thermocycler. Then, tubes were removed from the thermocycler, and briefly centrifuged again to collect residual liquid in the bottom of tubes. 25

fmol reporter was added to the reaction, centrifuged, and incubated at 37°C for 120 minutes in a thermocycler. To measure the fluorescence, the reaction volume was adjusted to 30 µL with nuclease-free water and pipetted into a 384-well plate.

For the two-step reaction, each reaction is set as described previously in 0.2 mL nuclease-free PCR tubes. 75 fmol of L7Ae (wild-type or mutated) were added to the mix, and the reaction volume was adjusted to 12.5 µL with nuclease-free water. Reaction mixes were mixed gently, briefly centrifuged, and incubated at 37°C for 120 minutes in a thermocycler. To add the reporter DNA, the same reaction was prepared with a final volume of 12.5 µL, and 25 fmol of reporter was added to the reaction. Tubes were briefly centrifuged again before adding the L7Ae-containing reaction and spun down again before incubating them again for another 120 minutes at 37°C in the thermocycler. To measure the fluorescence, the reaction volume was adjusted to 30 µL with nuclease-free water and pipetted into a black 384-well plate. Fluorescence was assessed with the GloMax® Discover luminometer using the

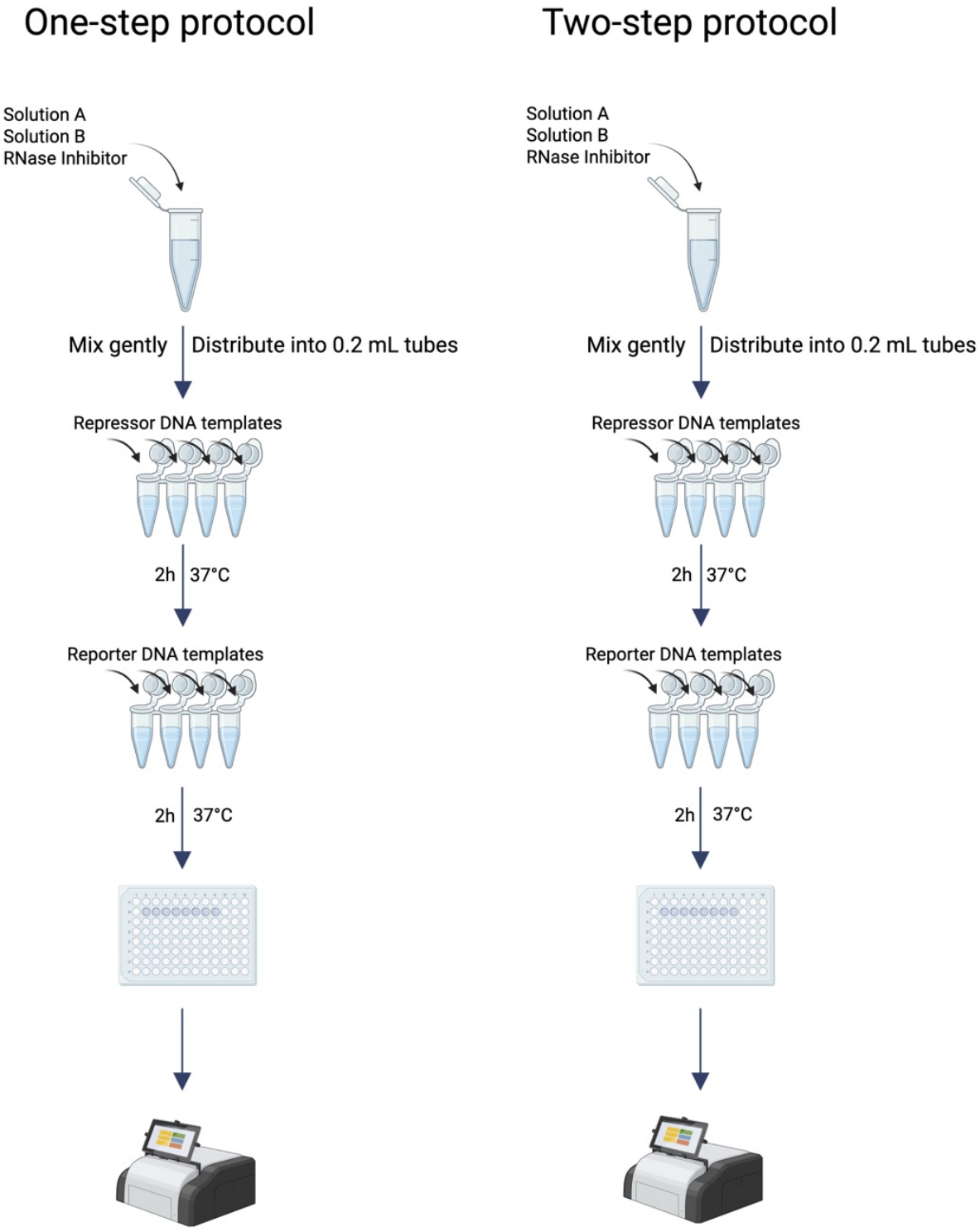

Figure3. 9 Illustration of *in vitro* transcription/translation assays in the PURE system. The left column depicts the setup of the one-step protocol, while the right column shows the workflow of the two-step protocol.

3.8 TEV rescue experiments in PURE System

Prior experiments in the PURE system were conducted to test if L7Ae was repressing the reporter translation. The protocol flow is illustrated in Figure 3.9. After confirming the repressing activity of L7Ae, engineered L7Ae(TCS) was tested. First, L7Ae (TCS) is tested at 37 °C to confirm it is repressing the translation at the temperature at which earlier experiments were performed. The reaction was prepared in a 0.2 mL tube and spun down before incubating in a thermocycler. To test the L7Ae (TCS) repression, 5 µL of Solution A, 3.75 µL of Solution B were mixed with 20 units of RNasin inhibitor. Next, 75 fmol of L7Ae (TCS) was added. DNA dilution used in the experiment was prepared accordingly to have 75 fmol DNA in 2 µL of DNA solution. The reaction was incubated at 37 °C in a thermocycler for 10 minutes, and after incubation, 25 fmol of reporter was added. After the addition of reporter, tubes were again spun down and incubated in a thermocycler at 37 °C for 2 hours.

L7Ae (TCS) repression was tested at 30 °C using the same protocol described above.

To examine TEV protease rescue, 5 µL of Solution A and 3.75 µL of Solution B were mixed with 20 units of RNasin inhibitor. Subsequently, 75 fmol of L7Ae (TCS) was added to the reaction, and the final volume was adjusted to 12.5 µL with nuclease-free water. After briefly spinning down, the reactions were incubated at 30 °C in a thermocycler for 1 hour.

For the DNA-only condition, 1.95 µL of nuclease-free water was added. For the buffer control, 1.45 µL of buffer and 0.5 µL of nuclease-free water were added. For the TEV and inactive TEV conditions, 1.45 µL of buffer and 0.5 µL of protease (5 units) were added, mixed gently, and briefly spun down. The reactions were then incubated for an additional hour. Finally, the reporter mix was prepared as described above, with the total reaction volume adjusted to 12.5 µL.

Inactivating the TEV protease was done by heat inactivation. Protease was incubated at 65 °C for 1 hour and cooled down. Stored at -20 °C.

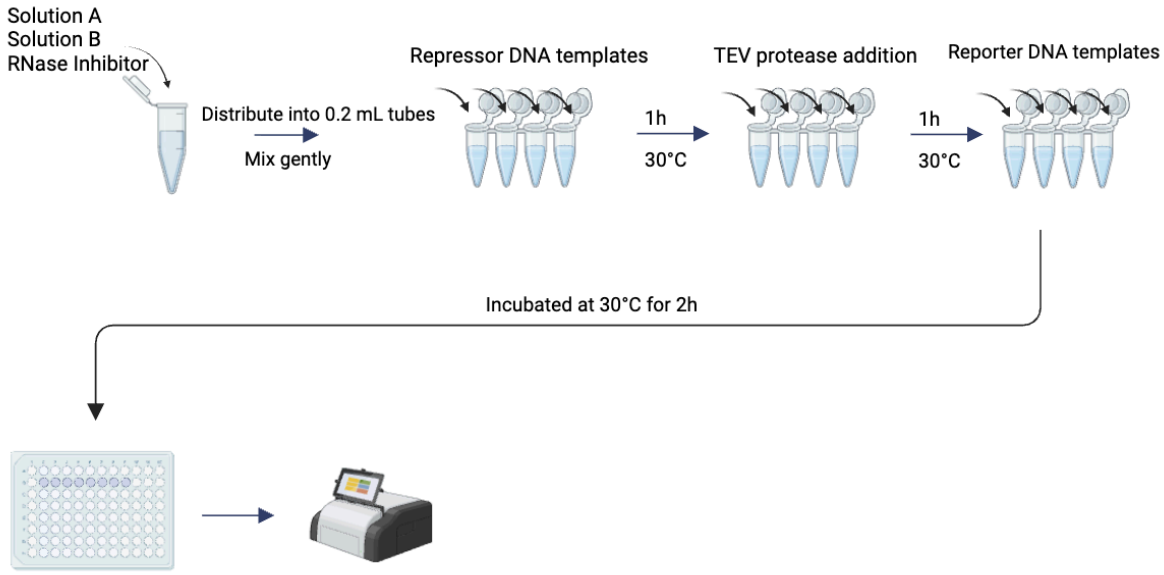

Figure3. 10 Illustration of TEV protease–mediated rescue of L7Ae repression of the kt-EGFP reporter in the PURE system.

3.9 Testing Purified L7Ae protein in PURE System

Purified protein concentrations were quantified using the Bicinchoninic Acid (BCA) Protein Assay Kit (Thermo Fisher Scientific) following the manufacturer's instructions. Absorbance was measured at 562 nm using a microplate reader, and protein concentrations were calculated based on a standard curve generated with bovine serum albumin (BSA).

After quantification, purified protein stocks were adjusted to a final concentration of 1000 ng/µL using the corresponding purification buffer. Working solutions were then prepared at a concentration of 5 µM and used directly in PURE system reactions. The required protein volume was calculated based on the desired final concentration in each reaction mixture.

For buffer control conditions, an equivalent volume of the protein purification buffer was added to the reactions in place of the protein to account for any buffer-related effects. All reactions were prepared on ice and gently mixed before incubation under standard PURE system conditions, as described previously.

3.10 Data Processing and Statistical Analysis

All statistical analyses were done on Biorender or Excel, and statistical tests were chosen according to the experimental design. Excel is used when specifically left or right -or right-tailed analysis is required. For comparisons between groups, statistical tests are mentioned below the related figures. Results are reported as mean ± standard error (SE). The sample size (biological replicates) is indicated for each graph in the respective panel.

4. Discussion

In the RRL part of the study, I investigated the role of MS2-cNOT7 and L7Ae translational repression in the rabbit reticulocyte lysate (RRL) system. MS2-cNOT7 is known to function primarily through de-adenylation of target RNAs, leading to a destabilization of the target mRNA and a consequent reduction of the output protein. Briefly, MS2 protein binds to the MS2 binding loops and brings the cNOT7 protein into close proximity to the poly-(A) tail, and cNOT7 deadenylates the RNA, causing the reduction of the translation. To test the MS2-cNOT7 device in the RRL system, I compared the wild-type and $MS2^{mut}$-cNOT7 proteins with the reporter containing the MS2 binding loop of 3'UTR. I observed that rabbit reticulocyte lysate (RRL) translates reporter RNAs regardless of whether they have a poly(A) tail, and cNOT7 activity is not effective in the system. These results were confirmed by a report discussing that RRL works with a poly(A) independent mechanism (Michel et al. 2000a). Given the lack of effective and reproducible repression observed in the assays, I conclude that RRL is not a suitable system for investigating MS2-cNOT7 activity.

One of the critical factors underlying this result is the nature of RRL. Unlike many eukaryotic cellular systems, where poly(A) tails play a central role in enhancing translation efficiency, our findings support previous reports that poly(A) tails are not effective in RRL. This observation is consistent with the fact that RRL supports poly (A)-independent translation and instead relies on cap-dependent initiation mechanisms that bypass canonical poly(A)-tail-poly(A)-binding protein (PABP) interactions (Michel et al. 2000a). Consequently, repression pathways that may be due to the disruption of poly(A)-mediated translation are unlikely to be captured in this system since RRL is optimized to rapidly produce maximum protein output from exogenous RNA, which may mask subtle regulatory effects such as those mediated by cNOT7. Our findings show that even in the absence of the reporter RNA's poly(A) tail, the RRL system efficiently translates the RNAs. This suggests that the small decrease observed in the MS2-CNOT7 condition is not due to deadenylation, but rather to MS2 protein binding to RNA loops, which might interfere with translation. This interference could be due to several mechanisms. One possibility can be related to ribosome recycling. After the ribosome scans the RNA, it releases the RNA and binds again. When the MS2 protein binds to the MS2 loops on the 3'UTR of the RNA, this binding could affect the recycling process and slow down or block the translation. Another possibility is that the 3' UTR is a region where many regulatory proteins

bind. When MS2 proteins occupy the loops in this region, they might block the binding of these regulatory proteins.

Another critical point to the reliability of the experiment outcomes is RNA integrity and purity, since RNA is the direct input. Taken together, these findings highlight the limitations of using RRL to study post-transcriptional repression mechanisms involving MS2-cNOT7. While the system is highly useful for investigating general aspects of translation, it does not fully reflect the poly(A)-dependent regulation observed *in vivo*. Future experiments should therefore be directed toward alternative systems that more faithfully recapitulate poly(A)-dependent translation and post-transcriptional regulatory processes.

Next, the repression activity of the L7Ae RNA-binding protein on the kt-reporter was tested in the RRL cell-free system. The initial reporter design included two kink-turn structures in the 5′ UTR, positioned at a 16 bp distance from the start codon. With this configuration, L7Ae did not exhibit strong repression of the reporter. A previous study tested the L7Ae's repression of kt-reporter RNA in a PURE system, focusing on how the position of the kink-turn structure influences repression (Saito et al. 2010b). This study showed that when the kink-turn is placed immediately after the start codon, the repression efficacy of L7Ae is higher, and when the distance is increased between the k-turn structure and ATG codon, repression efficiency decreases proportionally. In light of this information, I designed and cloned the reporter by placing the kink-turn structure right after the ATG codon and in frame with the coding sequence of my reporter and kt-reporter construct.

The L7Ae-k-turn translational control system with newly designed constructs was tested in an RRL cell-free system. In experiments with wild-type L7Ae protein, wild-type k-turn, and mutated k-turn reporters, the repression efficiency was not as strong as anticipated, given the results we had collected in mammalian cells (Wroblewska et al. 2015; Cella et al. 2018). The L7Ae and reporter molar ratios (~90:1, 70 fmol L7Ae, 0.77 fmol reporter) and incubation time (10 min with L7Ae first, followed by 60 min with the reporter) were used to ensure sufficient binding in the system, but the measured translational repression was not robust. Even though repression was not robust with wild-type L7Ae, I tested the engineered L7Ae in RRL to proceed with the next steps of the project, aiming to assess whether it could rescue the repression of the reporter. As observed with wild-type L7Ae, engineered L7Ae also exhibited variability in repression, and overall, the system remained inconsistent. Several factors could explain this variability.

Data from the two k-turn reporter constructs indicate that transcription and translation kinetics in cell-free systems differ from those in mammalian cell-based systems. One possible explanation for the lower repression observed when the k-turn is positioned further from the start codon is that ribosomes scan more rapidly in cell-free systems due to reduced regulatory constraints, allowing them to bypass the k-turn structure before initiating translation. Taking into account this potential faster translation process, it might also be possible that L7Ae is not robustly repressing the reporter in RRL. Because the L7Ae protein must be properly folded for effective binding to the k-turn structure to repress translation, and this fast translation process may cause improper folding of L7Ae. Furthermore, it is unknown whether the k-turn motif adopts the expected structure within the reporter mRNA. Finally, k-turn stability is dependent on ions such as Mg^{2+} and K^{+} (Turner et al. 2005); the buffer ion profile of the RRL may limit the motif's stability and ion concentration. Since these ion levels are optimized in RRL to translate the protein, it might be insufficient to support L7Ae-kturn binding.

The timing between the reporter and L7Ae may also be effective. In the current experimental design, L7Ae is incubated for 10 minutes before the reporter is added; before the L7Ae protein can bind to the k-turn motif, it needs to be correctly folded and in a stable conformation. The binding is time-dependent because the complex can't form until the protein and RNA structures interact and change, since the k-turn structure is forming only when L7Ae binds to it. If the reporter RNA is added before the protein is fully folded or in a transient conformational state, the complex may not form efficiently.

In the future, different methods such as electrophoretic mobility shift assay (EMSA) can be used to directly measure the L7Ae-k-turn interaction. The results may help understand whether the sensitivity problem arises because RNA-binding motifs do not always exert as strong effects as predicted in *in vitro* translation systems and whether motif accessibility, binding kinetics, and environmental conditions are critical.

In the *E. coli* lysate part of the study, RNA-binding protein L7Ae was tested in the S30 *E. coli* lysate. L7Ae functions by binding to the kink-turn structure located in the 5′ UTR of the reporter RNA, thereby blocking its translation. To test this activity, I cloned the related construct into two different destination vectors. Both constructs share the same T7 promoter and RBS, but the plasmid backbones in which they are cloned differ in other regulatory elements. BB1 includes additional regulatory elements like the *tet* promoters, the lacI gene and operator, the ROP, and the bom sequences. The *tet* promoter initiates the tetracycline resistance

gene, and it controls tetracycline resistance. The lacI gene and operator encode the lac repressor protein, which binds to the lac operator and suppresses the activity of the lac promoter, which can be controlled by an inducer. The Rop (repressor of primer) sequence, the Rop protein controls plasmid replication, preventing excessive copy number, and it regulates replication initiation by interacting with RNA. The bom (basis of mobility) sequence is essential for mobilization and allows conjugative transfer of the plasmid. Using different backbones allowed me to evaluate the plasmid component factors that may have an impact on transcription and translation efficiency in the cell-free system. Thus, the results obtained can be confirmed as being specific to the L7Ae-kt interaction, independent of vector-related output.

I systematically examined the repressive effect of the L7Ae protein on the kt-reporter. Experiments were designed to include wild-type and mutant versions of both L7Ae and the kt-reporter. This allowed for a comparative assessment of the repressive capacity of the wild-type and mutant versions of the protein. During the experiments, both the repressor (L7Ae) and the reporter (kt-reporter) were encoded and expressed on the same BB1 backbone, thus controlling for the influence of the genetic environment and allowing for the direct measurement of the repressive effect of L7Ae. However, I observed inconsistent behaviour across the experiments, which limits the suitability of this system with the adopted protocol for our studies on RBP-RNA regulation. To address this problem, I tried to optimize the protocol and change the plasmid backbone encoding the components of the system.

Protocol optimization: I reasoned that pre-translating L7Ae could increase the RBP to have increased repression. I thus introduced a two-step variant in which I first pre-translated L7Ae in the reaction, and then I added the reporter gene. However, the two-step protocol with *E. coli* lysate still showed high variability and even reduced repression when compared to the one-step reaction.

Backbone optimization: L7Ae repression was tested with the same one-step protocol with the BB2 backbone. The BB2 backbone is relatively shorter and encodes fewer genes. In addition to the T7 promoter, ribosome binding site (RBS), and T7 terminator sequence, the BB2 backbone also contains the ampicillin resistance gene along with its corresponding promoter.

However, having the RBP encoded in the BB2 vector resulted in the same behavior as BB1. This could be explained by different mechanisms relative to the lysate's environment.

One possibility is that endogenous proteins, RNAs, and other molecules in the lysate may prevent L7Ae from folding correctly or accessing its target RNA. Since these cell-free systems are optimized to translate protein in a short time with a high yield, testing a regulatory system

that requires correctly folded protein and proper secondary structure conformation of RNA might not be efficiently supported by the system. Translation issues in the cell-free system may also arise from resource competition. The presence of these numerous factors can affect translation dynamics; as reported, expressing multiple genes in a cell-free system may cause unexpected variations in protein levels, even if they are not interacting components with each other (Piorino et al. 2023). Possible causes of these results might be related to sharing translational resources, such as ribosomes. However, ribosomes are not the only limiting factors in the cell-free system, as lysates are not self-sustaining like a cell-based system, and each component is present in limited amounts. Some interesting reasons for the unexpected results in the cell-free system might be related to RNA-binding proteins or RNases that may compete with the reporter RNA and reduce repression (Siegal-Gaskins et al. 2014; Piorino et al. 2023). Furthermore, since *E. coli* lysate does not constitute a fully defined system like the PURE system, macromolecular crowding effects may influence the translation of individual components, potentially leading to unanticipated outcomes, such as the observed repression activity of the mutated L7Ae in this lysate.

Furthermore, endogenous mRNA or genomic DNA fragments can contribute to reaction heterogeneity. Also, input DNA molecules may have cryptic promoter activity, which can cause off-target expression or unexpected protein production. Such undesirable products interfere with the action of repressors or other regulators, which may indirectly limit observed protein function.

The combination of these factors may explain why *E. coli* lysate reactions are more variable, and why some regulatory proteins do not function properly. As a result, strategies such as energy source optimization, metabolic waste management, and endogenous nucleic acid clearance can be tested to improve experiment reproducibility in lysate-based systems.

We then examined the efficacy of the L7Ae-k-turn repression mechanism with the PURE cell-free system and explored strategies to obtain robust and strong repression and optimize the rescue of this repression. The PURE system, being entirely synthetic, should ensure a more controllable setting to benchmark the RBP-RNA regulations. To ensure that vector-specific factors did not cause the observed effects of the L7Ae-kt interaction, the system was tested on two different plasmid backbones, BB1 and BB2, as for the *E. coli* lysate.

Using a one-step protocol with the BB2 backbone, the wild-type L7Ae was able to repress reporter expression, while the mutant L7Ae did not, albeit exhibiting minimal residual repression. This outcome is consistent with the hypothesis that the introduced mutation diminishes, albeit does not entirely eliminate the binding affinity of L7Ae to the k-turn motif(Saito et al. 2010a). The low level of repression observed with the one-step protocol is likely due to the fact that the repressor has not been translated sufficiently and efficiently before the initiation of transcription and translation of the reporter.

To improve the ON-OFF ratio, I developed an optimized protocol based again on a two-step reaction that includes (1) a pre-translation stage for L7Ae and (2) the addition of reporter DNA afterward, with the addition of new translation resources. This protocol optimization resulted in a sharp increase in repression with the BB2 backbone, exceeding five-fold compared to the one-step protocol. This was presumably due to the increased availability of functional repressor molecules at the start of reporter translation, as well as the addition of new translational resources from PURE system components. It is important to note that the statistical analysis to compare the wild-type and mutant L7Ae repression did not show any significance with either of the protocols. However, the mutant version showed higher repression in the two-step protocol. This finding suggests that longer incubation periods may influence the kinetics of protein folding and stability in the PURE system.

I also tested an engineered form of L7Ae (TCS) in the BB2 backbone to determine if structural alterations could yield alternate repression properties. The repression by TCS was approximately 2.5-fold less than that of the wild-type, underscoring the known trade-off between designing for novel functionality and preserving robust RNA-binding ability (Cella et al. 2018). However, when the protein was engineered, it was expected to have lower activity compared to the wild-type version, likely by affecting its structure, stability, and binding efficiency.

We investigated further whether the efficiency of repression is affected by the plasmid backbone. In the PURE system, the BB2 backbone consistently exhibited significant repression, whereas the BB1 backbone did not with the one-step protocol. However, implementing the two-step protocol improved the repression of the reporter within the BB1 backbone, which suggests that optimized reaction conditions can mitigate variations in the PURE system. Another important finding was that when constructs were translated within the BB1 backbone, the mutant L7Ae showed the expected pattern of repression, whereas this was not the case with BB2. This suggests that the context of the backbone influences repression,

even though the possible causes of the differences have not been uncovered. These two plasmids differ in their genetic context; the BB1 backbone is longer and contains additional sequences such as the *tet* promoters, *lacI* gene and operator, ROP, and *bom* regions. In contrast, BB2 is shorter and includes only the T7 promoter, ribosome binding site (RBS), T7 terminator, and the ampicillin resistance gene. Since there can be different mechanisms effective on the L7Ae^{mut} repression difference between BB1 and BB2 backbones. These additional sequences on the BB1 backbone, *tet* promoters, the lacI gene and operator, the ROP, and the bom sequences, may modify the overall transcriptional load. By another means, polymerases in the reaction will be 'distracted' by other promoters in BB1, and it will slow down the transcription from the T7 promoter. As a result, the system transcribes less RNA and decreases the translation output. The effects observed are mitigated by regulatory proteins and metabolic buffering in living cells; however, the cell-free system does not possess these compensatory mechanisms. Consequently, even minor alterations can influence the processivity of T7 RNA polymerase and the kinetics of RNA folding. All these points can be the answer to why L7Ae did not show significant repression with the one-step protocol when it was encoded in the BB1 backbone, and the difference between L7Ae and L7Ae^{mut} comparison between BB1 and BB2 backbones. The L7Ae-kt interaction is based on both sequence and secondary structure. I hypothesize that given this structural requirement, minor changes or structural differences in RNA can affect the L7Ae-RNA interaction. Additionally, when the reporter is translated within the BB2 backbone produces more protein than the BB1 backbone in the PURE system. However, when comparing the L7Ae^{mut} repression with L7Ae repression, the L7Ae^{mut} protein expressed from the BB1 backbone shows the expected translation outcome, and it does not repress the kt-EGFP construct. This difference may be due to the variation in the distance between the T7 promoter and the RBS in the constructs. The construct with a 39-bp T7–RBS interval can improve protein co-translational folding by initiating translation more slowly and intermittently. This reduces ribosome density, allowing the polypeptide chain to fold each domain more quickly, increasing the correct folding of the protein. Slower synthesis also reduces the risk of aggregation and misfolding because, during rapid production, polypeptides tend to stick together. Furthermore, the different secondary structure of mRNA with a longer 5′ UTR can create localized slowdowns during translation, facilitating the correct folding. Thus, the resulting correctly folded proteins maintain their function better. As a result, the quality, stability, and functional activity of the resulting proteins are enhanced, even if the total production is low. Also, L7Ae-BB1 exhibited lower fluorescent output compared to the BB2 backbone experiment. This difference may also be related to the additional sequences in BB1.

These extra sequences could be sequestering reaction resources, potentially slowing down translation and affecting the allocation of resources between the system construct and the additional regulatory components in the backbone.(Siegal-Gaskins et al. 2014) The difference in repressive strength that depends on the backbone may not be caused by the L7Ae-kt pair itself, but by small differences in the structure of the DNA, the background of transcription, and the structure of the RNA that are unique to each plasmid. This finding suggests that vector architecture can have a strong impact on the regulation of RNA-protein interactions.

These results confirm that the two-step protocol is broadly applicable and can be useful in the PURE system, offering improved dynamics for post-transcriptional control. Collectively, my results show the benefits of a stepwise reaction in cell-free systems and reveal that repression efficiency is significantly affected by both the technique and the plasmid backbone. Through the optimization of settings for repressor accumulation and resource availability, I obtained substantial control over translation *in vitro*. Future research could focus on measuring the kinetic characteristics of L7Ae–RNA interactions within different backbones, evaluating additional backbones and regulatory elements, and ultimately incorporating the system into more complex synthetic networks.

After optimizing the repression of the reporter by L7Ae in the PURE system, the next step was the optimization of the rescue of the repression. In order to test the rescue, first, L7Ae(TCS) repression was tested in the PURE System at 37°C, which was the reaction temperature for all the experiments performed with the PURE System. L7Ae(TCS) showed a significant repression of the reporter. Next, since TEV protease was the first protease will be tested, repression was tested at 30°C. L7Ae(TCS) shows significant repression of the reporter also at 30 °C. TEV protease was tested in the reaction for rescue. To test the TEV protease activity, TEV protease buffer needs to be used in the reaction to obtain optimized TEV protease activity. Notably, adding buffer alone reduced the repression fold change compared to samples without buffer. This modest effect could be attributed to subtle changes in the chemical environment, such as ionic strength or the presence of stabilizing agents in the buffer, which could partially affect L7Ae-RNA interactions. This observation, although small, highlights the sensitivity of the L7Ae-mediated repression mechanism to experimental context.

TEV protease treatment successfully alleviated L7Ae-induced translational repression. Both 5-unit and 10-unit TEV protease treatments led to an increase in translation, indicating that proteolytic cleavage effectively attenuates the repressive role of L7Ae.

The findings indicate that L7Ae-mediated repression is reversible and can be modulated through proteolytic cleavage. These findings further support the idea that L7Ae-mediated translational regulation may depend on structural integrity or specific sites amenable to selective targeting. Future research could continue with studies on optimizing TEV protease-mediated rescue and testing different proteases to study orthogonality and multiplexity.

To obtain better repression by L7Ae of the kt-reporter in the PURE system, I produced and purified the repressor protein L7Ae from *E. coli* BL21 cells. Adding the repressor protein as a purified protein form leaves all the resources to translate the reporter and might eliminate the possible disadvantages of translating two constructs in the cell-free system.

In experiments using purified L7Ae proteins, the k-turn reporter was not repressed; instead, fluorescence output unexpectedly increased by approximately 10 to 25-fold. This result differs markedly from the previous experiment conducted with DNA constructs. According to the literature, purified L7Ae has been previously tested in the recombinant cell-free system PURExfrex (Saito et al. 2010a). Several factors may explain the observed results. First, the protein may have lost its proper folding or active conformation during purification or storage. Additionally, differences in protein concentration and buffer composition, particularly those affecting the ionic environment of the PURE reaction, could have influenced RNA-protein interactions. It is also known that magnesium ions enhance translation efficiency in cell-free systems up to a certain concentration. Therefore, elevated Mg^{2+} levels that are contained in the purified L7Ae buffer, might have overstimulated translation, counteracting the expected repression of the reporter. In other words, the added buffers may have boosted translation excessively, thereby masking the repression effect. However, the available data are not sufficient to support any hypothesis. Therefore, those observations need to be examined in more detail with additional analyses, such as using the commercial recombinant L7Ae as a positive control to understand if the repression is happening in the reaction. Here, the purified proteins are buffer exchanged into the buffer with $MgCl_2$ and later on exchanged into Tris-Cl buffer, which can carry the residual buffer from the $MgCl_2$ buffer, and it can interfere with the translation.

In this study, the performance of the RNA-regulatory circuits across different cell-free systems is explored. The MS2-cNOT7 and L7Ae RNA-binding proteins were first tested for their repression activities on reporter RNA in RRL, *E.coli,* and PURE systems. In rabbit lysate

and *E. coli*-based systems, the regulatory responses were variable and lacked consistent repression under the tested conditions. To address this, I optimized both the experimental framework and the construct design within the PURE system. Through iterative adjustment of reaction conditions, backbone architecture, and assay parameters, I developed a reliable and reproducible protocol that enables robust detection of RNA-regulatory interactions using genetically encoded constructs. This optimized PURE-based platform provides a controlled environment for dissecting RNA-mediated regulation and establishes a foundation for future quantitative and mechanistic studies of RNA circuits.

Bibliography

Alberts, Bruce. 2011. 'A Grand Challenge in Biology'. *Science* 333 (6047): 1200–1200. https://doi.org/10.1126/science.1213238.

Ali1, Jazib, Jawayria Najeeb2, Muhammad Asim Ali1, Muhammad Farhan Aslam1, and Ali Raza1. 2017. 'Biosensors: Their Fundamentals, Designs, Types and Most Recent Impactful Applications: A Review'. *Biosensors & Bioelectronics* 8 (1): 1–9. https://doi.org/10.4172/2155-6210.1000235.

Armero-Gimenez, Jorge, Ruud Wilbers, Arjen Schots, Charles Williams, and Ricarda Finnern. 2023. 'Rapid Screening and Scaled Manufacture of Immunogenic Virus-like Particles in a Tobacco BY-2 Cell-Free Protein Synthesis System'. *Frontiers in Immunology* 14 (January). https://doi.org/10.3389/fimmu.2023.1088852.

Atkins, J. F., J. B. Lewis, C. W. Anderson, and R. F. Gesteland. 1975. 'Enhanced Differential Synthesis of Proteins in a Mammalian Cell-Free System by Addition of Polyamines'. *The Journal of Biological Chemistry* 250 (14): 5688–95.

Baiersdörfer, Markus, Gábor Boros, Hiromi Muramatsu, et al. 2019. 'A Facile Method for the Removal of dsRNA Contaminant from In Vitro-Transcribed mRNA'. *Molecular Therapy Nucleic Acids* 15 (April): 26–35. https://doi.org/10.1016/j.omtn.2019.02.018.

Barkley, Mary D., Arthur D. Riggs, Alan Jobe, and Suzanne Bourgeois. 1975. 'Interaction of Effecting Ligands with Lac Repressor and Repressor-Operator Complex'. *Biochemistry* 14 (8): 1700–1712. https://doi.org/10.1021/bi00679a024.

Benedicto, Vernon Gil Laylo, Zahraa Haguar, Abbas Abdulhasan, and Vasanthy Narayanaswami. 2024. 'Apolipoprotein E3 Containing Nanodiscs as Vehicles for Transport and Targeted Delivery of Flavonoid Luteolin'. *ACS Omega* 9 (2): 2988–99. https://doi.org/10.1021/acsomega.3c09120.

Bernardi, Alberto, and Pierre-François Spahr. 1972. 'Nucleotide Sequence at the Binding Site for Coat Protein on RNA of Bacteriophage R17'. *Proceedings of the National Academy of Sciences* 69 (10): 3033–37. https://doi.org/10.1073/pnas.69.10.3033.

Bogart, Jonathan W., Maria D. Cabezas, Bastian Vögeli, Derek A. Wong, Ashty S. Karim, and Michael C. Jewett. 2021. 'Cell-Free Exploration of the Natural Product Chemical Space'. *Chembiochem : A European Journal of Chemical Biology* 22 (1): 84–91. https://doi.org/10.1002/cbic.202000452.

Borkowski, Olivier, Mathilde Koch, Agnès Zettor, et al. 2020. 'Large Scale Active-Learning-Guided Exploration for in Vitro Protein Production Optimization'. *Nature Communications* 11 (1): 1872. https://doi.org/10.1038/s41467-020-15798-5.

Brooks, Sierra M., and Hal S. Alper. 2021. ‘Applications, Challenges, and Needs for Employing Synthetic Biology beyond the Lab’. *Nature Communications* 12 (1): 1390. https://doi.org/10.1038/s41467-021-21740-0.

Brookwell, August, Javin P. Oza, and Filippo Caschera. 2021. ‘Biotechnology Applications of Cell-Free Expression Systems’. *Life* 11 (12): 1367. https://doi.org/10.3390/life11121367.

Bujara, Matthias, Michael Schümperli, Sonja Billerbeck, Matthias Heinemann, and Sven Panke. 2010. ‘Exploiting Cell-Free Systems: Implementation and Debugging of a System of Biotransformations’. *Biotechnology and Bioengineering* 106 (3): 376–89. https://doi.org/10.1002/bit.22666.

Bundy, Bradley C., Marc J. Franciszkowicz, and James R. Swartz. 2008. ‘Escherichia Coli-Based Cell-Free Synthesis of Virus-like Particles’. *Biotechnology and Bioengineering* 100 (1): 28–37. https://doi.org/10.1002/bit.21716.

Burrington, Logan R., Katharine R. Watts, and Javin P. Oza. 2021. ‘Characterizing and Improving Reaction Times for E. Coli-Based Cell-Free Protein Synthesis’. *ACS Synthetic Biology* 10 (8): 1821–29. https://doi.org/10.1021/acssynbio.1c00195.

Calhoun, Kara A., and James R. Swartz. 2005. ‘Energizing Cell-Free Protein Synthesis with Glucose Metabolism’. *Biotechnology and Bioengineering* 90 (5): 606–13. https://doi.org/10.1002/bit.20449.

Cameron, D. Ewen, Caleb J. Bashor, and James J. Collins. 2014. ‘A Brief History of Synthetic Biology’. *Nature Reviews Microbiology* 12 (5): 381–90. https://doi.org/10.1038/nrmicro3239.

Caschera, Filippo. 2025. ‘Cell-Free Protein Synthesis Platforms for Accelerating Drug Discovery’. *Biotechnology Notes* 6 (February): 126–32. https://doi.org/10.1016/j.biotno.2025.02.001.

Caschera, Filippo, and Vincent Noireaux. 2015. ‘A Cost-Effective Polyphosphate-Based Metabolism Fuels an All E. Coli Cell-Free Expression System’. *Metabolic Engineering* 27 (January): 29–37. https://doi.org/10.1016/j.ymben.2014.10.007.

Cecchetelli, Alyssa. n.d. ‘Finding Nucleic Acids with SHERLOCK and DETECTR’. Accessed 10 September 2025. https://blog.addgene.org/finding-nucleic-acids-with-sherlock-and-detectr.

Cella, Federica, Liliana Wroblewska, Ron Weiss, and Velia Siciliano. 2018. ‘Engineering Protein-Protein Devices for Multilayered Regulation of mRNA Translation Using Orthogonal Proteases in Mammalian Cells’. *Nature Communications* 9 (1): 4392. https://doi.org/10.1038/s41467-018-06825-7.

Chan, S. Hong, Louise Tirole, Daniel Kneller, Theresa M. Kelley, Nan Dai, and G. Brett Robb. 2023. ‘Co-Transcriptional Capping Using an RNA Capping Enzyme-T7 RNA Polymerase Fusion Protein’. Preprint, bioRxiv, October 28. https://doi.org/10.1101/2023.10.28.564488.

Chappell, James, Melissa K. Takahashi, and Julius B. Lucks. 2015. 'Creating Small Transcription Activating RNAs'. *Nature Chemical Biology* 11 (3): 214–20. https://doi.org/10.1038/nchembio.1737.

Chen, Bing, Ya Li, Feng Xu, and Xiaonan Yang. 2022. 'Powerful CRISPR-Based Biosensing Techniques and Their Integration With Microfluidic Platforms'. *Frontiers in Bioengineering and Biotechnology* 10 (February). https://doi.org/10.3389/fbioe.2022.851712.

Chen, Kun, Ziyi Shen, Guanzhen Wang, et al. 2022. 'Research Progress of CRISPR-Based Biosensors and Bioassays for Molecular Diagnosis'. *Frontiers in Bioengineering and Biotechnology* 10 (September). https://doi.org/10.3389/fbioe.2022.986233.

Chipman, Dallin M., Anna C. Woolley, Davu N. Chau, et al. 2025. 'Cell-Free Protein Synthesis Reactor Formats: A Brief History and Analysis'. *SynBio* 3 (3): 10. https://doi.org/10.3390/synbio3030010.

Clubb, Justin D., Torahito A. Gao, and Yvonne Y. Chen. 2023. 'Synthetic Biology in the Engineering of CAR-T and CAR-NK Cell Therapies: Facts and Hopes'. *Clinical Cancer Research : An Official Journal of the American Association for Cancer Research* 29 (8): 1390–402. https://doi.org/10.1158/1078-0432.CCR-22-1491.

Contreras-Llano, Luis E., Conary Meyer, Yao Liu, et al. 2020. 'Holistic Engineering of Cell-Free Systems through Proteome-Reprogramming Synthetic Circuits'. *Nature Communications* 11 (1): 3138. https://doi.org/10.1038/s41467-020-16900-7.

Cross, Andrew R., Richard W. Erickson, Beverly A. Ellis, and John T. Curnutte. 1999. 'Spontaneous Activation of NADPH Oxidase in a Cell-Free System: Unexpected Multiple Effects of Magnesium Ion Concentrations'. *Biochemical Journal* 338 (1): 229–33. https://doi.org/10.1042/bj3380229.

Cui, Yi, Xinjie Chen, Ze Wang, and Yuan Lu. n.d. 'Cell-Free PURE System: Evolution and Achievements'. *Biodesign Research* 2022: 9847014. https://doi.org/10.34133/2022/9847014.

D'Ambrosio, Vasil, and Michael K. Jensen. 2017. 'Lighting up Yeast Cell Factories by Transcription Factor-Based Biosensors'. *FEMS Yeast Research* 17 (7): fox076. https://doi.org/10.1093/femsyr/fox076.

Doerr, Anne, Elise De Reus, Pauline Van Nies, et al. 2019. 'Modelling Cell-Free RNA and Protein Synthesis with Minimal Systems'. *Physical Biology* 16 (2): 025001. https://doi.org/10.1088/1478-3975/aaf33d.

Dondapati, Srujan Kumar, Marlitt Stech, Anne Zemella, and Stefan Kubick. 2020. 'Cell-Free Protein Synthesis: A Promising Option for Future Drug Development'. *Biodrugs* 34 (3): 327–48. https://doi.org/10.1007/s40259-020-00417-y.

Dougherty, W. G., and T. D. Parks. 1991. 'Post-Translational Processing of the Tobacco Etch Virus 49-kDa Small Nuclear Inclusion Polyprotein: Identification of an Internal Cleavage Site and Delimitation of VPg and Proteinase Domains'. *Virology* 183 (2): 449–56. https://doi.org/10.1016/0042-6822(91)90974-g.

Duchardt-Ferner, Elke, Michael Juen, Benjamin Bourgeois, et al. 2020. 'Structure of an RNA Aptamer in Complex with the Fluorophore Tetramethylrhodamine'. *Nucleic Acids Research* 48 (2): 949–61. https://doi.org/10.1093/nar/gkz1113.

Dudley, Quentin M., Ashty S. Karim, and Michael C. Jewett. 2015. 'Cell-Free Metabolic Engineering: Biomanufacturing beyond the Cell'. *Biotechnology Journal* 10 (1): 69–82. https://doi.org/10.1002/biot.201400330.

Ekas, Holly M., Brenda Wang, Adam D. Silverman, Julius B. Lucks, Ashty S. Karim, and Michael C. Jewett. 2024. 'An Automated Cell-Free Workflow for Transcription Factor Engineering'. *ACS Synthetic Biology* 13 (10): 3389–99. https://doi.org/10.1021/acssynbio.4c00471.

Elowitz, Michael B., and Stanislas Leibler. 2000. 'A Synthetic Oscillatory Network of Transcriptional Regulators'. *Nature* 403 (6767): 335–38. https://doi.org/10.1038/35002125.

Falgenhauer, Elisabeth, Sophie von Schönberg, Chen Meng, et al. 2021. 'Evaluation of an E. Coli Cell Extract Prepared by Lysozyme-Assisted Sonication via Gene Expression, Phage Assembly and Proteomics'. *ChemBioChem* 22 (18): 2805–13. https://doi.org/10.1002/cbic.202100257.

Famulok, Michael, Jörg S. Hartig, and Günter Mayer. 2007. 'Functional Aptamers and Aptazymes in Biotechnology, Diagnostics, and Therapy'. *Chemical Reviews* 107 (9): 3715–43. https://doi.org/10.1021/cr0306743.

Favre, Daniel, and Beat Muellhaupt. 2005. 'Reactivation of Creatine Kinase by Dithiothreitol Prior to Use in an in Vitro Translation Extract'. *ALTEX* 22 (4): 259–64.

Fdez-Sanromán, Antía, Nuria Bernárdez-Rodas, Emilio Rosales, Marta Pazos, Elisa González-Romero, and Maria Ángeles Sanromán. 2025. 'Biosensor Technologies for Water Quality: Detection of Emerging Contaminants and Pathogens'. *Biosensors* 15 (3): 189. https://doi.org/10.3390/bios15030189.

Feng, Jinhui, Qiaqing Wu, Dunming Zhu, and Yanhe Ma. 2022. 'Biotransformation Enables Innovations Toward Green Synthesis of Steroidal Pharmaceuticals'. *ChemSusChem* 15 (9): e202102399. https://doi.org/10.1002/cssc.202102399.

GAN, Rui, Maria D. Cabezas, Ming Pan, et al. 2022. 'High-Throughput Regulatory Part Prototyping and Analysis by Cell-Free Protein Synthesis and Droplet Microfluidics'. *ACS Synthetic Biology* 11 (6): 2108–20. https://doi.org/10.1021/acssynbio.2c00050.

Gao, Wei, Ning Bu, and Yuan Lu. 2019. 'Efficient Incorporation of Unnatural Amino Acids into Proteins with a Robust Cell-Free System'. *Methods and Protocols* 2 (1): 16. https://doi.org/10.3390/mps2010016.

Gao, Yangbin, and Yunde Zhao. 2014. 'Self-Processing of Ribozyme-Flanked RNAs into Guide RNAs in Vitro and in Vivo for CRISPR-Mediated Genome Editing'. *Journal of Integrative Plant Biology* 56 (4): 343–49. https://doi.org/10.1111/jipb.12152.

Garamella, Jonathan, Ryan Marshall, Mark Rustad, and Vincent Noireaux. 2016. 'The All E. Coli TX-TL Toolbox 2.0: A Platform for Cell-Free Synthetic Biology'. *ACS Synthetic Biology* 5 (4): 344–55. https://doi.org/10.1021/acssynbio.5b00296.

Gardner, Timothy S., Charles R. Cantor, and James J. Collins. 2000. 'Construction of a Genetic Toggle Switch in Escherichia Coli'. *Nature* 403 (6767): 339–42. https://doi.org/10.1038/35002131.

Garenne, David, Matthew Haines, Eugenia Romantseva, Paul Freemont, Elizabeth Strychalski, and Vincent Noireaux. 2021. 'Cell-Free Gene Expression'. *Nature Reviews Methods Primers* 1 (July): 49. https://doi.org/10.1038/s43586-021-00046-x.

Garner, Kathryn L. 2021. 'Principles of Synthetic Biology'. *Essays in Biochemistry* 65 (5): 791–811. https://doi.org/10.1042/EBC20200059.

Ge, Xumeng, and Jianfeng Xu. 2020. 'Macromolecular Crowding Effects on Transcription and Translation Are Regulated by Free Magnesium Ion'. *Biotechnology and Applied Biochemistry* 67 (1): 117–22. https://doi.org/10.1002/bab.1827.

Gerstberger, Stefanie, Markus Hafner, and Thomas Tuschl. 2014. 'A Census of Human RNA-Binding Proteins'. *Nature Reviews. Genetics* 15 (12): 829–45. https://doi.org/10.1038/nrg3813.

Glisovic, Tina, Jennifer L. Bachorik, Jeongsik Yong, and Gideon Dreyfuss. 2008. 'RNA-Binding Proteins and Post-Transcriptional Gene Regulation'. *FEBS Letters* 582 (14): 1977–86. https://doi.org/10.1016/j.febslet.2008.03.004.

Goody, Terry A., Sonya E. Melcher, David G. Norman, and David M. J. Lilley. 2004. 'The Kink-Turn Motif in RNA Is Dimorphic, and Metal Ion-Dependent'. *RNA (New York, N.Y.)* 10 (2): 254–64. https://doi.org/10.1261/rna.5176604.

Grasemann, Laura, Barbora Lavickova, M. Carolina Elizondo-Cantú, and Sebastian J. Maerkl. 2021. 'OnePot PURE Cell-Free System'. *Journal of Visualized Experiments (JoVE)*, no. 172 (June): e62625. https://doi.org/10.3791/62625.

Gräwe, Alexander, Anna Dreyer, Tobias Vornholt, et al. 2019. 'A Paper-Based, Cell-Free Biosensor System for the Detection of Heavy Metals and Date Rape Drugs'. *PLOS ONE* 14 (3): e0210940. https://doi.org/10.1371/journal.pone.0210940.

Green, Alexander A., Pamela A. Silver, James J. Collins, and Peng Yin. 2014. 'Toehold Switches: De-Novo-Designed Regulators of Gene Expression'. *Cell* 159 (4): 925–39. https://doi.org/10.1016/j.cell.2014.10.002.

Green, Tyler P., Joseph P. Talley, and Bradley C. Bundy. 2025. 'Recent Advances in Developing Cell-Free Protein Synthesis Biosensors for Medical Diagnostics and Environmental Monitoring'. *Biosensors* 15 (8): 499. https://doi.org/10.3390/bios15080499.

Gregorio, Nicole E., Max Z. Levine, and Javin P. Oza. 2019. 'A User's Guide to Cell-Free Protein Synthesis'. *Methods and Protocols* 2 (1): 24. https://doi.org/10.3390/mps2010024.

Greiss, Ferdinand, Nicolas Lardon, Leonie Schütz, et al. 2024. 'A Genetic Circuit on a Single DNA Molecule as an Autonomous Dissipative Nanodevice'. *Nature Communications* 15 (1): 883. https://doi.org/10.1038/s41467-024-45186-2.

Guo, Xinyue, Min Li, and Xiaolei Zuo. 2025. 'Gene Circuit-Based Sensors'. *Fundamental Research* 5 (5): 1876–88. https://doi.org/10.1016/j.fmre.2024.06.011.

Harbaugh, Svetlana V., Adam D. Silverman, Yaroslav G. Chushak, et al. 2022. 'Engineering a Synthetic Dopamine-Responsive Riboswitch for In Vitro Biosensing'. *ACS Synthetic Biology* 11 (7): 2275–83. https://doi.org/10.1021/acssynbio.1c00560.

Harbers, Matthias. 2014. 'Wheat Germ Systems for Cell-Free Protein Expression'. *FEBS Letters* 588 (17): 2762–73. https://doi.org/10.1016/j.febslet.2014.05.061.

Helgstrand, Charlotte, Elin Grahn, Timothy Moss, et al. 2002. 'Investigating the Structural Basis of Purine Specificity in the Structures of MS2 Coat Protein RNA Translational Operator Hairpins'. *Nucleic Acids Research* 30 (12): 2678–85. https://doi.org/10.1093/nar/gkf371.

Henrich, Erik, Christopher Hein, Volker Dötsch, and Frank Bernhard. 2015. 'Membrane Protein Production in Escherichia Coli Cell-Free Lysates'. *FEBS Letters* 589 (15): 1713–22. https://doi.org/10.1016/j.febslet.2015.04.045.

Hoang Trung Chau, Tin, Dung Hoang Anh Mai, Diep Ngoc Pham, Hoa Thi Quynh Le, and Eun Yeol Lee. 2020. 'Developments of Riboswitches and Toehold Switches for Molecular Detection—Biosensing and Molecular Diagnostics'. *International Journal of Molecular Sciences* 21 (9): 3192. https://doi.org/10.3390/ijms21093192.

Hodgman, C. Eric, and Michael C. Jewett. 2012. 'Cell-Free Synthetic Biology: Thinking Outside the Cell'. *Metabolic Engineering* 14 (3): 261–69. https://doi.org/10.1016/j.ymben.2011.09.002.

Hong, Seok Hoon, Yong-Chan Kwon, Rey W. Martin, et al. 2015. 'Improving Cell-Free Protein Synthesis through Genome Engineering of Escherichia Coli Lacking Release Factor 1'. *Chembiochem: A European Journal of Chemical Biology* 16 (5): 844–53. https://doi.org/10.1002/cbic.201402708.

Hossain, Gazi Sakir, Mukesh Saini, Ryoma Miyake, Hua Ling, and Matthew Wook Chang. 2020. 'Genetic Biosensor Design for Natural Product Biosynthesis in Microorganisms'. *Trends in Biotechnology*, Special Issue: Metabolic Engineering, vol. 38 (7): 797–810. https://doi.org/10.1016/j.tibtech.2020.03.013.

Hu, Vivian T, and Neha P Kamat. 2023. 'Cell-Free Protein Synthesis Systems for Vaccine Design and Production'. *Current Opinion in Biotechnology* 79 (February): 102888. https://doi.org/10.1016/j.copbio.2022.102888.

Huang, Chi-Wei, Chitsan Lin, Minh Ky Nguyen, Adnan Hussain, Xuan-Thanh Bui, and Huu Hao Ngo. n.d. 'A Review of Biosensor for Environmental Monitoring: Principle, Application, and Corresponding Achievement of Sustainable Development Goals'. *Bioengineered* 14 (1): 58–80. https://doi.org/10.1080/21655979.2022.2095089.

Huang, Tao, Rui Zhang, and Jinming Li. 2023. 'CRISPR-Cas-Based Techniques for Pathogen Detection: Retrospect, Recent Advances, and Future Perspectives'. *Journal of Advanced Research* 50 (August): 69–82. https://doi.org/10.1016/j.jare.2022.10.011.

Hunt, Andrew C., Blake J. Rasor, Kosuke Seki, et al. 2025. 'Cell-Free Gene Expression: Methods and Applications'. *Chemical Reviews* 125 (1): 91–149. https://doi.org/10.1021/acs.chemrev.4c00116.

Jackson, R. J., and T. Hunt. 1983. 'Preparation and Use of Nuclease-Treated Rabbit Reticulocyte Lysates for the Translation of Eukaryotic Messenger RNA'. *Methods in Enzymology* 96: 50–74. https://doi.org/10.1016/s0076-6879(83)96008-1.

Jacobs, Miranda L., Margrethe A. Boyd, and Neha P. Kamat. 2019. 'Diblock Copolymers Enhance Folding of a Mechanosensitive Membrane Protein during Cell-Free Expression'. *Proceedings of the National Academy of Sciences* 116 (10): 4031–36. https://doi.org/10.1073/pnas.1814775116.

Jain, K. K. 2013. 'Synthetic Biology and Personalized Medicine'. *Medical Principles and Practice: International Journal of the Kuwait University, Health Science Centre* 22 (3): 209–19. https://doi.org/10.1159/000341794.

Jeon, Yangwon, Yejin Lee, Keugtae Kim, Geupil Jang, and Youngdae Yoon. 2022. 'Transcription Factor-Based Biosensors for Detecting Pathogens'. *Biosensors* 12 (7): 470. https://doi.org/10.3390/bios12070470.

Jeong, Dohyun, Melissa Klocke, Siddharth Agarwal, et al. 2019. 'Cell-Free Synthetic Biology Platform for Engineering Synthetic Biological Circuits and Systems'. *Methods and Protocols* 2 (2): 39. https://doi.org/10.3390/mps2020039.

Jia, Longfei, and Shu-Bing Qian. 2021. 'Therapeutic mRNA Engineering from Head to Tail'. *Accounts of Chemical Research* 54 (23): 4272–82. https://doi.org/10.1021/acs.accounts.1c00541.

Jiang, Xiuping, Kazuyo Oohira, Yugo Iwasaki, Hideo Nakano, Shigeyuki Ichihara, and Tsuneo Yamane. 2002. 'Reduction of Protein Degradation by Use of Protease-Deficient Mutants in Cell-Free Protein Synthesis System of Escherichia Coli'. *Journal of Bioscience and Bioengineering* 93 (2): 151–56. https://doi.org/10.1263/jbb.93.151.

Jin, Xing, Weston Kightlinger, and Seok Hoon Hong. 2019. 'Optimizing Cell-Free Protein Synthesis for Increased Yield and Activity of Colicins'. *Methods and Protocols* 2 (2): 28. https://doi.org/10.3390/mps2020028.

Johansson, Hans E., Lars Liljas, and Olke C. Uhlenbeck. 1997. 'RNA Recognition by the MS2 Phage Coat Protein'. *Seminars in Virology* 8 (3): 176–85. https://doi.org/10.1006/smvy.1997.0120.

Jung, Jaeyoung K., Chloé M. Archuleta, Khalid K. Alam, and Julius B. Lucks. 2022. 'Programming Cell-Free Biosensors with DNA Strand Displacement Circuits'. *Nature Chemical Biology* 18 (4): 385–93. https://doi.org/10.1038/s41589-021-00962-9.

Kapasiawala, Manisha, and Richard M. Murray. 2024. 'Metabolic Perturbations to an Escherichia Coli-Based Cell-Free System Reveal a Trade-off between Transcription

and Translation'. *ACS Synthetic Biology* 13 (12): 3976–90. https://doi.org/10.1021/acssynbio.4c00361.

Karig, David K., Sukanya Iyer, Michael L. Simpson, and Mitchel J. Doktycz. 2012. 'Expression Optimization and Synthetic Gene Networks in Cell-Free Systems'. *Nucleic Acids Research* 40 (8): 3763–74. https://doi.org/10.1093/nar/gkr1191.

Karim, Ashty S., and Michael C. Jewett. 2016. 'A Cell-Free Framework for Rapid Biosynthetic Pathway Prototyping and Enzyme Discovery'. *Metabolic Engineering* 36 (July): 116–26. https://doi.org/10.1016/j.ymben.2016.03.002.

Karim, Ashty S, Blake J Rasor, and Michael C Jewett. 2020. 'Enhancing Control of Cell-Free Metabolism through pH Modulation'. *Synthetic Biology* 5 (1): ysz027. https://doi.org/10.1093/synbio/ysz027.

Kartje, Zachary J., Helen I. Janis, Shaoni Mukhopadhyay, and Keith T. Gagnon. 2020. 'Revisiting T7 RNA Polymerase Transcription in Vitro with the Broccoli RNA Aptamer as a Simplified Real-Time Fluorescent Reporter'. *The Journal of Biological Chemistry* 296 (December): 100175. https://doi.org/10.1074/jbc.RA120.014553.

Karzbrun, Eyal, Alexandra M. Tayar, Vincent Noireaux, and Roy H. Bar-Ziv. 2014. 'Programmable On-Chip DNA Compartments as Artificial Cells'. *Science* 345 (6198): 829–32. https://doi.org/10.1126/science.1255550.

Kay, Jennifer E., and Michael C. Jewett. 2015. 'Lysate of Engineered Escherichia Coli Supports High-Level Conversion of Glucose to 2,3-Butanediol'. *Metabolic Engineering* 32 (November): 133–42. https://doi.org/10.1016/j.ymben.2015.09.015.

Kellner, Max J., Jeremy Koob, Jonathan S. Gootenberg, Omar O. Abudayyeh, and Feng Zhang. 2019. 'SHERLOCK: Nucleic Acid Detection with CRISPR Nucleases'. *Nature Protocols* 14 (10): 2986–3012. https://doi.org/10.1038/s41596-019-0210-2.

Kelwick, Richard, James T. MacDonald, Alexander J. Webb, and Paul Freemont. 2014. 'Developments in the Tools and Methodologies of Synthetic Biology'. *Frontiers in Bioengineering and Biotechnology* 2 (November). https://doi.org/10.3389/fbioe.2014.00060.

Khalil, Ahmad S., and James J. Collins. 2010. 'Synthetic Biology: Applications Come of Age'. *Nature Reviews Genetics* 11 (5): 367–79. https://doi.org/10.1038/nrg2775.

Khambhati, Khushal, Gargi Bhattacharjee, Nisarg Gohil, Darren Braddick, Vishwesh Kulkarni, and Vijai Singh. 2019. 'Exploring the Potential of Cell-Free Protein Synthesis for Extending the Abilities of Biological Systems'. *Frontiers in Bioengineering and Biotechnology* 7 (October). https://doi.org/10.3389/fbioe.2019.00248.

Kim, D. M., and J. R. Swartz. 2001. 'Regeneration of Adenosine Triphosphate from Glycolytic Intermediates for Cell-Free Protein Synthesis'. *Biotechnology and Bioengineering* 74 (4): 309–16.

Kim, Wonhee, Jinjoo Han, Shraddha Chauhan, and Jeong Wook Lee. 2025. 'Cell-Free Protein Synthesis and Vesicle Systems for Programmable Therapeutic Manufacturing and

Delivery'. *Journal of Biological Engineering* 19 (1): 55. https://doi.org/10.1186/s13036-025-00523-x.

Klein, D.J., T.M. Schmeing, P.B. Moore, and T.A. Steitz. 2001. 'The Kink-Turn: A New RNA Secondary Structure Motif'. *The EMBO Journal* 20 (15): 4214–21. https://doi.org/10.1093/emboj/20.15.4214.

Kovtun, Oleksiy, Sergey Mureev, WooRam Jung, Marta H. Kubala, Wayne Johnston, and Kirill Alexandrov. 2011. 'Leishmania Cell-Free Protein Expression System'. *Methods (San Diego, Calif.)* 55 (1): 58–64. https://doi.org/10.1016/j.ymeth.2011.06.006.

Krinsky, Nitzan, Maya Kaduri, Janna Shainsky-Roitman, et al. 2016. 'A Simple and Rapid Method for Preparing a Cell-Free Bacterial Lysate for Protein Synthesis'. *PLOS ONE* 11 (10): e0165137. https://doi.org/10.1371/journal.pone.0165137.

Krutsakorn, Borimas, Kohsuke Honda, Xiaoting Ye, et al. 2013. 'In Vitro Production of N-Butanol from Glucose'. *Metabolic Engineering* 20 (November): 84–91. https://doi.org/10.1016/j.ymben.2013.09.006.

Kuhn, A. N., M. Diken, S. Kreiter, et al. 2010. 'Phosphorothioate Cap Analogs Increase Stability and Translational Efficiency of RNA Vaccines in Immature Dendritic Cells and Induce Superior Immune Responses in Vivo'. *Gene Therapy* 17 (8): 961–71. https://doi.org/10.1038/gt.2010.52.

Kuruma, Yutetsu, and Takuya Ueda. 2015. 'The PURE System for the Cell-Free Synthesis of Membrane Proteins'. *Nature Protocols* 10 (9): 1328–44. https://doi.org/10.1038/nprot.2015.082.

Lage, Daniela P., Patrícia A. F. Ribeiro, Daniel S. Dias, et al. 2020. 'A Candidate Vaccine for Human Visceral Leishmaniasis Based on a Specific T Cell Epitope-Containing Chimeric Protein Protects Mice against Leishmania Infantum Infection'. *Npj Vaccines* 5 (1): 75. https://doi.org/10.1038/s41541-020-00224-0.

Laohakunakorn, Nadanai, Laura Grasemann, Barbora Lavickova, et al. 2020. 'Bottom-Up Construction of Complex Biomolecular Systems With Cell-Free Synthetic Biology'. *Frontiers in Bioengineering and Biotechnology* 8 (March). https://doi.org/10.3389/fbioe.2020.00213.

Lavickova, Barbora, and Sebastian J. Maerkl. 2019. 'A Simple, Robust, and Low-Cost Method To Produce the PURE Cell-Free System'. *ACS Synthetic Biology* 8 (2): 455–62. https://doi.org/10.1021/acssynbio.8b00427.

Lee, Pao-Wan, and Sebastian J. Maerkl. 2024. 'Regulatory Components for Bacterial Cell-Free Systems Engineering'. *ACS Synthetic Biology* 13 (12): 3827–41. https://doi.org/10.1021/acssynbio.4c00574.

Lenk, Robin, Werner Kleindienst, Gábor Tamás Szabó, et al. 2024. 'Understanding the Impact of in Vitro Transcription Byproducts and Contaminants'. *Frontiers in Molecular Biosciences* 11 (July): 1426129. https://doi.org/10.3389/fmolb.2024.1426129.

Li, Yi, Linyang Liu, Laicong Qiao, and Fei Deng. 2023. 'Universal CRISPR/Cas12a-Associated Aptasensor Suitable for Rapid Detection of Small Proteins with a Plate

Reader'. *Frontiers in Bioengineering and Biotechnology* 11 (June): 1201175. https://doi.org/10.3389/fbioe.2023.1201175.

Li, Yueyi, Tyler Lucci, Matias Villarruel Dujovne, Jaeyoung Kirsten Jung, Daiana A. Capdevila, and Julius B. Lucks. 2024. 'Engineering a Cell-Free Biosensor Signal Amplification Circuit with Polymerase Strand Recycling'. *bioRxiv*, April 25, 2024.04.25.591074. https://doi.org/10.1101/2024.04.25.591074.

Li, Yueyi, Tyler Lucci, Matias Villarruel Dujovne, Jaeyoung Kirsten Jung, Daiana A. Capdevila, and Julius B. Lucks. 2025. 'A Cell-Free Biosensor Signal Amplification Circuit with Polymerase Strand Recycling'. *Nature Chemical Biology* 21 (6): 949–58. https://doi.org/10.1038/s41589-024-01816-w.

Lopreside, Antonia, Xinyi Wan, Elisa Michelini, Aldo Roda, and Baojun Wang. 2019. 'Comprehensive Profiling of Diverse Genetic Reporters with Application to Whole-Cell and Cell-Free Biosensors'. *Analytical Chemistry* 91 (23): 15284–92. https://doi.org/10.1021/acs.analchem.9b04444.

Lu, Yuan. 2020. 'Cell-Free Biosensing'. In *Cell-Free Synthetic Biology*, edited by Yuan Lu. Springer. https://doi.org/10.1007/978-981-13-1171-0_4.

Lunde, Bradley M., Claire Moore, and Gabriele Varani. 2007. 'RNA-Binding Proteins: Modular Design for Efficient Function'. *Nature Reviews. Molecular Cell Biology* 8 (6): 479–90. https://doi.org/10.1038/nrm2178.

Mahas, Ahmed, Qiaochu Wang, Tin Marsic, and Magdy M. Mahfouz. 2022. 'Development of Cas12a-Based Cell-Free Small-Molecule Biosensors via Allosteric Regulation of CRISPR Array Expression'. *Analytical Chemistry* 94 (11): 4617–26. https://doi.org/10.1021/acs.analchem.1c04332.

Mannan, Ahmad A., Di Liu, Fuzhong Zhang, and Diego A. Oyarzún. 2017. 'Fundamental Design Principles for Transcription-Factor-Based Metabolite Biosensors'. *ACS Synthetic Biology* 6 (10): 1851–59. https://doi.org/10.1021/acssynbio.7b00172.

Martin, Rey W., Benjamin J. Des Soye, Yong-Chan Kwon, et al. 2018. 'Cell-Free Protein Synthesis from Genomically Recoded Bacteria Enables Multisite Incorporation of Noncanonical Amino Acids'. *Nature Communications* 9 (1): 1203. https://doi.org/10.1038/s41467-018-03469-5.

Martorell, Sara, Cristina Santiso-Bellón, Roberto Gozalbo-Rovira, et al. 2025. 'Synthetic Biology-Driven Optoelectronic Biosensor for Rapid and Highly Sensitive Norovirus Detection in Fecal Samples'. *Biosensors and Bioelectronics* 288 (November): 117787. https://doi.org/10.1016/j.bios.2025.117787.

Matsumoto, Rena, Tatsuya Niwa, Kaori Kuno, Yasuhiro Shimane, Yutetsu Kuruma, and Takashi Kanamori. 2025. 'Lipid Modification and Membrane Localization of Proteins in Cell-Free System'. *ACS Synthetic Biology* 14 (7): 2729–38. https://doi.org/10.1021/acssynbio.5c00155.

Matsumoto, Rena, Tatsuya Niwa, Yasuhiro Shimane, Yutetsu Kuruma, Hideki Taguchi, and Takashi Kanamori. 2023. 'Regulated N-Terminal Modification of Proteins Synthesized

Using a Reconstituted Cell-Free Protein Synthesis System'. *ACS Synthetic Biology* 12 (7): 1935–42. https://doi.org/10.1021/acssynbio.3c00191.

Matsuura, Satoshi, Hiroki Ono, Shunsuke Kawasaki, Yi Kuang, Yoshihiko Fujita, and Hirohide Saito. 2018. 'Synthetic RNA-Based Logic Computation in Mammalian Cells'. *Nature Communications* 9 (1): 4847. https://doi.org/10.1038/s41467-018-07181-2.

Mattick, John S. 2004. 'RNA Regulation: A New Genetics?' *Nature Reviews Genetics* 5 (4): 316–23. https://doi.org/10.1038/nrg1321.

Mauxion, Fabienne, Jérôme Basquin, Sevim Ozgur, et al. 2023. 'The Human CNOT1-CNOT10-CNOT11 Complex Forms a Structural Platform for Protein-Protein Interactions'. *Cell Reports* 42 (1): 111902. https://doi.org/10.1016/j.celrep.2022.111902.

McClellan, David A. 2000. 'The Codon-Degeneracy Model of Molecular Evolution'. *Journal of Molecular Evolution* 50 (2): 131–40. https://doi.org/10.1007/s002399910015.

McManus, John B., Casey B. Bernhards, Caitlin E. Sharpes, et al. 2021. 'Rapid Characterization of Genetic Parts with Cell-Free Systems'. *JoVE (Journal of Visualized Experiments)*, no. 174 (August): e62816. https://doi.org/10.3791/62816.

McMinn, Spencer E., Danielle V. Miller, Daniel Yur, et al. 2024. 'High-Throughput Algorithmic Optimization of In Vitro Transcription for SARS-CoV-2 mRNA Vaccine Production'. *Biochemistry* 63 (21): 2793–802. https://doi.org/10.1021/acs.biochem.4c00188.

McSweeney, Megan A., and Mark P. Styczynski. 2021. 'Effective Use of Linear DNA in Cell-Free Expression Systems'. *Frontiers in Bioengineering and Biotechnology* 9 (July). https://doi.org/10.3389/fbioe.2021.715328.

McSweeney, Megan A., Yan Zhang, and Mark P. Styczynski. 2023. 'Short Activators and Repressors of RNA Toehold Switches'. *ACS Synthetic Biology* 12 (3): 681–88. https://doi.org/10.1021/acssynbio.2c00641.

Merrick, William C. 2010. 'Eukaryotic Protein Synthesis: Still a Mystery'. *The Journal of Biological Chemistry* 285 (28): 21197–201. https://doi.org/10.1074/jbc.R110.111476.

Michel, Yanne M., Didier Poncet, Maria Piron, Katherine M. Kean, And Andrew M. Borman. 2000a. 'Cap-Poly(A) Synergy In Mammalian Cell-Free Extracts: Investigation Of The Requirements For Poly(A)-Mediated Stimulation Of Translation Initiation*'. *Journal Of Biological Chemistry* 275 (41): 32268–76. Https://Doi.Org/10.1074/Jbc.M004304200.

Milligan, J. F., and O. C. Uhlenbeck. 1989. 'Synthesis of Small RNAs Using T7 RNA Polymerase'. *Methods in Enzymology* 180: 51–62. https://doi.org/10.1016/0076-6879(89)80091-6.

Moore, Terrie, Yanming Zhang, Marcia O. Fenley, and Hong Li. 2004. 'Molecular Basis of Box C/D RNA-Protein Interactions'. *Structure* 12 (5): 807–18. https://doi.org/10.1016/j.str.2004.02.033.

Mordstein, Christine, Rosina Savisaar, Robert S. Young, et al. 2020. 'Codon Usage and Splicing Jointly Influence mRNA Localization'. *Cell Systems* 10 (4): 351-362.e8. https://doi.org/10.1016/j.cels.2020.03.001.

Nakanishi, Hideyuki. 2021. 'Protein-Based Systems for Translational Regulation of Synthetic mRNAs in Mammalian Cells'. *Life* 11 (11): 1192. https://doi.org/10.3390/life11111192.

Nath, Abhinav, William M. Atkins, and Stephen G. Sligar. 2007. 'Applications of Phospholipid Bilayer Nanodiscs in the Study of Membranes and Membrane Proteins'. *Biochemistry* 46 (8): 2059–69. https://doi.org/10.1021/bi602371n.

Nguyen, MichaelT. A., Georgios Pothoulakis, and Ebbe S. Andersen. 2022. 'Synthetic Translational Regulation by Protein-Binding RNA Origami Scaffolds'. *ACS Synthetic Biology* 11 (5): 1710–18. https://doi.org/10.1021/acssynbio.1c00608.

Nirenberg, M., and P. Leder. 1964. 'RNA CODEWORDS AND PROTEIN SYNTHESIS. THE EFFECT OF TRINUCLEOTIDES UPON THE BINDING OF SRNA TO RIBOSOMES'. *Science (New York, N.Y.)* 145 (3639): 1399–407. https://doi.org/10.1126/science.145.3639.1399.

Nirenberg, M. W., and J. H. Matthaei. 1961. 'The Dependence of Cell-Free Protein Synthesis in E. Coli upon Naturally Occurring or Synthetic Polyribonucleotides'. *Proceedings of the National Academy of Sciences of the United States of America* 47 (10): 1588–602. https://doi.org/10.1073/pnas.47.10.1588.

Nishikawa, Shota, Wen-Chi Yu, Tony Z. Jia, et al. 2024. 'Amino Acid Self-Regenerating Cell-Free Protein Synthesis System That Feeds on PLA Plastics, CO2, Ammonium, and α-Ketoglutarate'. *ACS Catalysis* 14 (10): 7696–706. https://doi.org/10.1021/acscatal.4c00992.

Nissen, Poul, Joseph A. Ippolito, Nenad Ban, Peter B. Moore, and Thomas A. Steitz. 2001. 'RNA Tertiary Interactions in the Large Ribosomal Subunit: The A-Minor Motif'. *Proceedings of the National Academy of Sciences* 98 (9): 4899–903. https://doi.org/10.1073/pnas.081082398.

Ogino, Tomoaki. 2013. 'In Vitro Capping and Transcription of Rhabdoviruses'. *Methods (San Diego, Calif.)* 59 (2): 188–98. https://doi.org/10.1016/j.ymeth.2012.05.013.

Ohashi, Hiroyuki, Takashi Kanamori, Yoshihiro Shimizu, and Takuya Ueda. n.d. 'A Highly Controllable Reconstituted Cell-Free System -a Breakthrough in Protein Synthesis Research'. *Current Pharmaceutical Biotechnology* 11 (3): 267–71. https://doi.org/10.2174/138920110791111889.

Paddon, C. J., P. J. Westfall, D. J. Pitera, et al. 2013. 'High-Level Semi-Synthetic Production of the Potent Antimalarial Artemisinin'. *Nature* 496 (7446): 528–32. https://doi.org/10.1038/nature12051.

Pandi, Amir, Ioana Grigoras, Olivier Borkowski, and Jean-Loup Faulon. 2019. 'Optimizing Cell-Free Biosensors to Monitor Enzymatic Production'. *ACS Synthetic Biology* 8 (8): 1952–57. https://doi.org/10.1021/acssynbio.9b00160.

Pardee, Keith, Alexander A. Green, Tom Ferrante, et al. 2014. 'Paper-Based Synthetic Gene Networks'. *Cell* 159 (4): 940–54. https://doi.org/10.1016/j.cell.2014.10.004.

Park, Hyeongwoo, Haneul Jin, Dayeong Kim, and Joongoo Lee. 2024. 'Cell-Free Systems: Ideal Platforms for Accelerating the Discovery and Production of Peptide-Based Antibiotics'. *International Journal of Molecular Sciences* 25 (16): 9109. https://doi.org/10.3390/ijms25169109.

Peabody, D. S. 1993. 'The RNA Binding Site of Bacteriophage MS2 Coat Protein'. *The EMBO Journal* 12 (2): 595–600. https://doi.org/10.1002/j.1460-2075.1993.tb05691.x.

Peabody, David S., and Francis Lim. 1996. 'Complementation of RNA Binding Site Mutations in MS2 Coat Protein Heterodimers'. *Nucleic Acids Research* 24 (12): 2352–59. https://doi.org/10.1093/nar/24.12.2352.

Pelham, H. R., and R. J. Jackson. 1976. 'An Efficient mRNA-Dependent Translation System from Reticulocyte Lysates'. *European Journal of Biochemistry* 67 (1): 247–56. https://doi.org/10.1111/j.1432-1033.1976.tb10656.x.

Pellinen, Teijo, Tuomas Huovinen, and Matti Karp. 2004. 'A Cell-Free Biosensor for the Detection of Transcriptional Inducers Using Firefly Luciferase as a Reporter'. *Analytical Biochemistry* 330 (1): 52–57. https://doi.org/10.1016/j.ab.2004.03.064.

Perenkov, Alexey D., Alena D. Sergeeva, Maria V. Vedunova, and Dmitri V. Krysko. 2023. 'In Vitro Transcribed RNA-Based Platform Vaccines: Past, Present, and Future'. *Vaccines* 11 (10): 1600. https://doi.org/10.3390/vaccines11101600.

Piorino, Fernanda, Alexandra T. Patterson, Yue Han, and Mark P. Styczynski. 2023. 'Plasmid Crosstalk in Cell-Free Expression Systems'. *ACS Synthetic Biology* 12 (10): 2843–56. https://doi.org/10.1021/acssynbio.3c00412.

Purnick, Priscilla E. M., and Ron Weiss. 2009. 'The Second Wave of Synthetic Biology: From Modules to Systems'. *Nature Reviews Molecular Cell Biology* 10 (6): 410–22. https://doi.org/10.1038/nrm2698.

Rojas-Villacorta, Walter, Segundo Rojas-Flores, Magaly De La Cruz-Noriega, Héctor Chinchay Espino, Felix Diaz, and Moises Gallozzo Cardenas. 2022. 'Microbial Biosensors for Wastewater Monitoring: Mini-Review'. *Processes* 10 (10): 2002. https://doi.org/10.3390/pr10102002.

Romantseva, Eugenia, Nina Alperovich, David Ross, Steven P Lund, and Elizabeth A Strychalski. 2022. 'Effects of DNA Template Preparation on Variability in Cell-Free Protein Production'. *Synthetic Biology* 7 (1): ysac015. https://doi.org/10.1093/synbio/ysac015.

Romantseva, Eugenia F., Drew S. Tack, Nina Alperovich, David Ross, and Elizabeth A. Strychalski. 2022. 'Best Practices for DNA Template PreparationDNA Template Preparation Toward Improved Reproducibility in Cell-Free Protein ProductionCell-Free Protein Production'. In *Cell-Free Gene Expression: Methods and Protocols*, edited by Ashty S. Karim and Michael C. Jewett. Springer US. https://doi.org/10.1007/978-1-0716-1998-8_1.

Rooke, Jenny. 2013. 'Synthetic Biology as a Source of Global Health Innovation'. *Systems and Synthetic Biology* 7 (3): 67–72. https://doi.org/10.1007/s11693-013-9117-3.

Rothschild, Lynn J., Nils J. H. Averesch, Elizabeth A. Strychalski, et al. 2024. 'Building Synthetic Cells─From the Technology Infrastructure to Cellular Entities'. *ACS Synthetic Biology* 13 (4): 974–97. https://doi.org/10.1021/acssynbio.3c00724.

Rozhdestvensky, Timofey S., Thean Hock Tang, Inna V. Tchirkova, Jürgen Brosius, Jean-Pierre Bachellerie, and Alexander Hüttenhofer. 2003. 'Binding of L7Ae Protein to the K-Turn of Archaeal snoRNAs: A Shared RNA Binding Motif for C/D and H/ACA Box snoRNAs in Archaea'. *Nucleic Acids Research* 31 (3): 869–77.

Ruder, Warren C., Ting Lu, and James J. Collins. 2011. 'Synthetic Biology Moving into the Clinic'. *Science (New York, N.Y.)* 333 (6047): 1248–52. https://doi.org/10.1126/science.1206843.

Sahin, Ugur, Katalin Karikó, and Özlem Türeci. 2014. 'mRNA-Based Therapeutics--Developing a New Class of Drugs'. *Nature Reviews. Drug Discovery* 13 (10): 759–80. https://doi.org/10.1038/nrd4278.

Saito, Hirohide, Tetsuhiro Kobayashi, Tomoaki Hara, et al. 2010a. 'Synthetic Translational Regulation by an L7Ae–Kink-Turn RNP Switch'. *Nature Chemical Biology* 6 (1): 71–78. https://doi.org/10.1038/nchembio.273.

Saito, Hirohide, Tetsuhiro Kobayashi, Tomoaki Hara, et al. 2010b. 'Synthetic Translational Regulation by an L7Ae-Kink-Turn RNP Switch'. *Nature Chemical Biology* 6 (January): 71–78. https://doi.org/10.1038/nchembio.273.

Samnuan, Karnyart, Anna K. Blakney, Paul F. McKay, and Robin J. Shattock. 2021. 'Design-of-Experiments In Vitro Transcription Yield Optimization of Self-Amplifying RNA'. Preprint, bioRxiv, January 8. https://doi.org/10.1101/2021.01.08.425833.

Sawasaki, Tatsuya, Tomio Ogasawara, Ryo Morishita, and Yaeta Endo. 2002. 'A Cell-Free Protein Synthesis System for High-Throughput Proteomics'. *Proceedings of the National Academy of Sciences of the United States of America* 99 (23): 14652–57. https://doi.org/10.1073/pnas.232580399.

Schinn, Song-Min, Andrew Broadbent, William T. Bradley, and Bradley C. Bundy. 2016. 'Protein Synthesis Directly from PCR: Progress and Applications of Cell-Free Protein Synthesis with Linear DNA'. *New Biotechnology* 33 (4): 480–87. https://doi.org/10.1016/j.nbt.2016.04.002.

Seddon, Annela M., Paul Curnow, and Paula J. Booth. 2004. 'Membrane Proteins, Lipids and Detergents: Not Just a Soap Opera'. *Biochimica et Biophysica Acta (BBA) - Biomembranes*, Lipid-Protein Interactions, vol. 1666 (1): 105–17. https://doi.org/10.1016/j.bbamem.2004.04.011.

Shafiee, Ashkan, Elham Ghadiri, Jareer Kassis, Nima Pourhabibi Zarandi, and Anthony Atala. 2018. 'Biosensing Technologies for Medical Applications, Manufacturing, and Regenerative Medicine'. *Current Stem Cell Reports* 4 (2): 105–15. https://doi.org/10.1007/s40778-018-0123-y.

Sheng, Jiayuan, Shaohua Lei, Lijuan Yuan, and Xueyang Feng. 2017. 'Cell-Free Protein Synthesis of Norovirus Virus-like Particles'. *RSC Advances* 7 (46): 28837–40. https://doi.org/10.1039/C7RA03742B.

Shields, D., and G. Blobel. 1978. 'Efficient Cleavage and Segregation of Nascent Presecretory Proteins in a Reticulocyte Lysate Supplemented with Microsomal Membranes'. *The Journal of Biological Chemistry* 253 (11): 3753–56.

Shimizu, Yoshihiro, Akio Inoue, Yukihide Tomari, et al. 2001. 'Cell-Free Translation Reconstituted with Purified Components'. *Nature Biotechnology* 19 (8): 751–55. https://doi.org/10.1038/90802.

Shin, Jonghyeon, and Vincent Noireaux. 2012. 'An E. Coli Cell-Free Expression Toolbox: Application to Synthetic Gene Circuits and Artificial Cells'. *ACS Synthetic Biology* 1 (1): 29–41. https://doi.org/10.1021/sb200016s.

Shrestha, Prashanta, Troy Michael Holland, and Bradley Charles Bundy. 2012. 'Streamlined Extract Preparation for Escherichia Coli-Based Cell-Free Protein Synthesis by Sonication or Bead Vortex Mixing'. *BioTechniques* 53 (3): 163–74. https://doi.org/10.2144/0000113924.

Siavashy, Saeed, M. Soltani, Shayan Rahimi, Mehraveh Hosseinali, Zahra Guilandokht, and Kaamran Raahemifar. 2024. 'Recent Advancements in Microfluidic-Based Biosensors for Detection of Genes and Proteins: Applications and Techniques'. *Biosensors and Bioelectronics: X* 19 (August): 100489. https://doi.org/10.1016/j.biosx.2024.100489.

Siegal-Gaskins, Dan, Zoltan A. Tuza, Jongmin Kim, Vincent Noireaux, and Richard M. Murray. 2014. 'Gene Circuit Performance Characterization and Resource Usage in a Cell-Free "Breadboard"'. *ACS Synthetic Biology* 3 (6): 416–25. https://doi.org/10.1021/sb400203p.

Silverman, Adam D., Ashty S. Karim, and Michael C. Jewett. 2020. 'Cell-Free Gene Expression: An Expanded Repertoire of Applications'. *Nature Reviews Genetics* 21 (3): 151–70. https://doi.org/10.1038/s41576-019-0186-3.

Silverman, Adam D., Nancy Kelley-Loughnane, Julius B. Lucks, and Michael C. Jewett. 2019. 'Deconstructing Cell-Free Extract Preparation for in Vitro Activation of Transcriptional Genetic Circuitry'. *ACS Synthetic Biology* 8 (2): 403–14. https://doi.org/10.1021/acssynbio.8b00430.

Sokolova, Nika, Bo Peng, and Kristina Haslinger. 2023. 'Design and Engineering of Artificial Biosynthetic Pathways—Where Do We Stand and Where Do We Go?' *FEBS Letters* 597 (23): 2897–907. https://doi.org/10.1002/1873-3468.14745.

Spice, Alex J., Rochelle Aw, Daniel G. Bracewell, and Karen M. Polizzi. 2020. 'Synthesis and Assembly of Hepatitis B Virus-Like Particles in a Pichia Pastoris Cell-Free System'. *Frontiers in Bioengineering and Biotechnology* 8 (February): 72. https://doi.org/10.3389/fbioe.2020.00072.

Spice, Alex J., Rochelle Aw, and Karen M. Polizzi. 2022. 'Cell-Free Protein Synthesis Using Pichia Pastoris'. *Methods in Molecular Biology (Clifton, N.J.)* 2433: 75–88. https://doi.org/10.1007/978-1-0716-1998-8_4.

Steinkühler, Jan, Justin A. Peruzzi, Antje Krüger, et al. 2024. 'Improving Cell-Free Expression of Model Membrane Proteins by Tuning Ribosome Cotranslational Membrane Association and Nascent Chain Aggregation'. *ACS Synthetic Biology* 13 (1): 129–40. https://doi.org/10.1021/acssynbio.3c00357.

Sun, Zachary Z., Clarmyra A. Hayes, Jonghyeon Shin, Filippo Caschera, Richard M. Murray, and Vincent Noireaux. 2013. 'Protocols for Implementing an Escherichia Coli Based TX-TL Cell-Free Expression System for Synthetic Biology'. *Journal of Visualized Experiments: JoVE*, no. 79 (September): e50762. https://doi.org/10.3791/50762.

Sun, Zachary Z., Enoch Yeung, Clarmyra A. Hayes, Vincent Noireaux, and Richard M. Murray. 2014. 'Linear DNA for Rapid Prototyping of Synthetic Biological Circuits in an Escherichia Coli Based TX-TL Cell-Free System'. *ACS Synthetic Biology* 3 (6): 387–97. https://doi.org/10.1021/sb400131a.

Suryadi, Jimmy, Elizabeth J. Tran, E. Stuart Maxwell, and Bernard A. Brown. 2005. 'The Crystal Structure of the Methanocaldococcus Jannaschii Multifunctional L7Ae RNA-Binding Protein Reveals an Induced-Fit Interaction with the Box C/D RNAs',. *Biochemistry* 44 (28): 9657–72. https://doi.org/10.1021/bi050568q.

Swank, Zoe, Nadanai Laohakunakorn, and Sebastian J. Maerkl. 2019. 'Cell-Free Gene-Regulatory Network Engineering with Synthetic Transcription Factors'. *Proceedings of the National Academy of Sciences of the United States of America* 116 (13): 5892–901. https://doi.org/10.1073/pnas.1816591116.

Swartz, James R. 2018. 'Expanding Biological Applications Using Cell-Free Metabolic Engineering: An Overview'. *Metabolic Engineering*, Metabolic Engineering Host Organism Special Issue, vol. 50 (November): 156–72. https://doi.org/10.1016/j.ymben.2018.09.011.

Tan, Xiao, Justin H. Letendre, James J. Collins, and Wilson W. Wong. 2021. 'Synthetic Biology in the Clinic: Engineering Vaccines, Diagnostics, and Therapeutics'. *Cell* 184 (4): 881–98. https://doi.org/10.1016/j.cell.2021.01.017.

Thoring, Lena, Doreen A. Wüstenhagen, Maria Borowiak, Marlitt Stech, Andrei Sonnabend, and Stefan Kubick. 2016. 'Cell-Free Systems Based on CHO Cell Lysates: Optimization Strategies, Synthesis of "Difficult-to-Express" Proteins and Future Perspectives'. *PLoS ONE* 11 (9): e0163670. https://doi.org/10.1371/journal.pone.0163670.

Thoring, Lena, Anne Zemella, Doreen Wüstenhagen, and Stefan Kubick. 2019. 'Accelerating the Production of Druggable Targets: Eukaryotic Cell-Free Systems Come into Focus'. *Methods and Protocols* 2 (2): 30. https://doi.org/10.3390/mps2020030.

Tinafar, Aidan, Katariina Jaenes, and Keith Pardee. 2019. 'Synthetic Biology Goes Cell-Free'. *BMC Biology* 17 (1): 64. https://doi.org/10.1186/s12915-019-0685-x.

Turner, ben, sonya e. Melcher, timothy j. Wilson, david g. Norman, and david m.j. lilley. 2005. 'induced fit of rna on binding the l7ae protein to the kink-turn motif'. *Rna* 11 (8): 1192–200. Https://doi.org/10.1261/rna.2680605.

Tusup, Marina, Lars E. French, Mara De Matos, David Gatfield, Thomas Kundig, and Steve Pascolo. 2019. 'Design of in Vitro Transcribed mRNA Vectors for Research and Therapy'. *CHIMIA* 73 (5): 391–391. https://doi.org/10.2533/chimia.2019.391.

Valegård, Karin, James B Murray, Nicola J Stonehouse, Sjoerd van den Worm, Peter G Stockley, and Lars Liljas. 1997. 'The Three-Dimensional Structures of Two Complexes between Recombinant MS2 Capsids and RNA Operator Fragments Reveal Sequence-Specific Protein-RNA Interactions1'. *Journal of Molecular Biology* 270 (5): 724–38. https://doi.org/10.1006/jmbi.1997.1144.

Vidovic, I., S. Nottrott, K. Hartmuth, R. Lührmann, and R. Ficner. 2000. 'Crystal Structure of the Spliceosomal 15.5kD Protein Bound to a U4 snRNA Fragment'. *Molecular Cell* 6 (6): 1331–42. https://doi.org/10.1016/s1097-2765(00)00131-3.

Vilkhovoy, Michael, Abhinav Adhikari, Sandra Vadhin, and Jeffrey D. Varner. 2020. 'The Evolution of Cell Free Biomanufacturing'. *Processes* 8 (6): 675. https://doi.org/10.3390/pr8060675.

Voyvodic, Peter L., Amir Pandi, Mathilde Koch, et al. 2019. 'Plug-and-Play Metabolic Transducers Expand the Chemical Detection Space of Cell-Free Biosensors'. *Nature Communications* 10 (1): 1697. https://doi.org/10.1038/s41467-019-09722-9.

Wang, Baojun, and Cheemeng Tan. 2023. 'Special Issue "Synthetic Biology for Biosensing in Health and Environmental Applications"'. *Biosensors* 13 (10): 937. https://doi.org/10.3390/bios13100937.

Wang, Ting, and Yuan Lu. 2022. 'Advances, Challenges and Future Trends of Cell-Free Transcription-Translation Biosensors'. *Biosensors* 12 (5): 5. https://doi.org/10.3390/bios12050318.

Wang, Wenjing, Yumin He, Suxiang He, et al. 2025. 'A Brief Review of Aptamer-Based Biosensors in Recent Years'. *Biosensors* 15 (2): 120. https://doi.org/10.3390/bios15020120.

Watkins, Nicholas J., and Markus T. Bohnsack. 2012. 'The Box C/D and H/ACA snoRNPs: Key Players in the Modification, Processing and the Dynamic Folding of Ribosomal RNA'. *Wiley Interdisciplinary Reviews. RNA* 3 (3): 397–414. https://doi.org/10.1002/wrna.117.

Weber, Wilfried, and Martin Fussenegger. 2009. 'Engineering of Synthetic Mammalian Gene Networks'. *Chemistry & Biology* 16 (3): 287–97. https://doi.org/10.1016/j.chembiol.2009.02.005.

Weissman, Drew, Norbert Pardi, Hiro Muramatsu, and Katalin Karikó. 2013. 'HPLC Purification of In Vitro Transcribed Long RNA'. In *Synthetic Messenger RNA and Cell Metabolism Modulation: Methods and Protocols*, edited by Peter M. Rabinovich. Humana Press. https://doi.org/10.1007/978-1-62703-260-5_3.

Whittaker, James W. 2013. 'Cell-Free Protein Synthesis: The State of the Art'. *Biotechnology Letters* 35 (2): 143–52. https://doi.org/10.1007/s10529-012-1075-4.

Wiegand, Daniel J., Henry H. Lee, Nili Ostrov, and George M. Church. 2018. 'Establishing a Cell-Free Vibrio Natriegens Expression System'. *ACS Synthetic Biology* 7 (10): 2475–79. https://doi.org/10.1021/acssynbio.8b00222.

Wroblewska, Liliana, Tasuku Kitada, Kei Endo, et al. 2015. 'Mammalian Synthetic Circuits with RNA Binding Proteins Delivered by RNA'. *Nature Biotechnology* 33 (8): 839–41. https://doi.org/10.1038/nbt.3301.

Wu, Qing, Zhengfei Yi, Haoran Li, et al. 2024. 'Harnessing Noncanonical Trans-Cleavage Characteristics of Cas12 and Cas13a to Enhance CRISPR-Based Diagnostics'. *Communications Biology* 7 (1): 1312. https://doi.org/10.1038/s42003-024-07000-z.

Xiang, Yiyu, Neil Dalchau, and Baojun Wang. 2018. 'Scaling up Genetic Circuit Design for Cellular Computing: Advances and Prospects'. *Natural Computing* 17 (4): 833–53. https://doi.org/10.1007/s11047-018-9715-9.

Xiao, Yi, Zhe Du, Yuqian Li, et al. 2025. 'A Review on the Application of Biosensors for Monitoring Emerging Contaminants in the Water Environment'. *Sensors* 25 (16): 4945. https://doi.org/10.3390/s25164945.

Xing, Enpeng, Hongfei Chen, Xianglin Xin, Haoran Cui, Yanzhi Dou, and Shiping Song. 2025. 'Recent Advances in Smart Phone-Based Biosensors for Various Applications'. *Chemosensors* 13 (7): 221. https://doi.org/10.3390/chemosensors13070221.

Yadav, Surendra, Alexander J. P. Perkins, Sahan B. W. Liyanagedera, Anthony Bougas, and Nadanai Laohakunakorn. 2025. 'ATP Regeneration from Pyruvate in the PURE System'. *ACS Synthetic Biology* 14 (1): 247–56. https://doi.org/10.1021/acssynbio.4c00697.

Yadavalli, Raghavendra, and Tobili Sam-Yellowe. 2015. 'HeLa Based Cell Free Expression Systems for Expression of Plasmodium Rhoptry Proteins'. *Journal of Visualized Experiments : JoVE*, no. 100 (June): 52772. https://doi.org/10.3791/52772.

Yan, Xu, Xu Liu, Cuihuan Zhao, and Guo-Qiang Chen. 2023. 'Applications of Synthetic Biology in Medical and Pharmaceutical Fields'. *Signal Transduction and Targeted Therapy* 8 (1): 199. https://doi.org/10.1038/s41392-023-01440-5.

Yang, Jiong, and Shigang Ding. 2021. 'Chimeric RNA-Binding Protein-Based Killing Switch Targeting Hepatocellular Carcinoma Cells'. *Molecular Therapy. Nucleic Acids* 25 (August): 683–95. https://doi.org/10.1016/j.omtn.2021.08.012.

Youssef, Maryam, Cynthia Hitti, Julia Puppin Chaves Fulber, and Amine A. Kamen. 2023. 'Enabling mRNA Therapeutics: Current Landscape and Challenges in Manufacturing'. *Biomolecules* 13 (10): 1497. https://doi.org/10.3390/biom13101497.

Zawada, James F., Gang Yin, Alexander R. Steiner, et al. 2011. 'Microscale to Manufacturing Scale-up of Cell-Free Cytokine Production--a New Approach for Shortening Protein Production Development Timelines'. *Biotechnology and Bioengineering* 108 (7): 1570–78. https://doi.org/10.1002/bit.23103.

Zemella, Anne, Lena Thoring, Christian Hoffmeister, and Stefan Kubick. 2015. 'Cell-Free Protein Synthesis: Pros and Cons of Prokaryotic and Eukaryotic Systems'. *Chembiochem* 16 (17): 2420–31. https://doi.org/10.1002/cbic.201500340.

Zhang, Junjie, Huixian Huang, Guangchun Song, et al. 2022. 'Intelligent Biosensing Strategies for Rapid Detection in Food Safety: A Review'. *Biosensors and Bioelectronics* 202 (April): 114003. https://doi.org/10.1016/j.bios.2022.114003.

Zhang, Liyuan, Wei Guo, and Yuan Lu. 2020. 'Advances in Cell-Free Biosensors: Principle, Mechanism, and Applications'. *Biotechnology Journal* 15 (9): e2000187. https://doi.org/10.1002/biot.202000187.

Zhang, Liyuan, Xiaomei Lin, Ting Wang, Wei Guo, and Yuan Lu. 2021. 'Development and Comparison of Cell-Free Protein Synthesis Systems Derived from Typical Bacterial Chassis'. *Bioresources and Bioprocessing* 8 (1): 58. https://doi.org/10.1186/s40643-021-00413-2.

Zhang, Yang, Bo Shiun Lai, and Mario Juhas. 2019. 'Recent Advances in Aptamer Discovery and Applications'. *Molecules* 24 (5): 941. https://doi.org/10.3390/molecules24050941.

Zhou, Gloria J., and Fuzhong Zhang. 2023. 'Applications and Tuning Strategies for Transcription Factor-Based Metabolite Biosensors'. *Biosensors* 13 (4): 428. https://doi.org/10.3390/bios13040428.

Zimmerman, Erik S., Tyler H. Heibeck, Avinash Gill, et al. 2014. 'Production of Site-Specific Antibody–Drug Conjugates Using Optimized Non-Natural Amino Acids in a Cell-Free Expression System'. *Bioconjugate Chemistry* 25 (2): 351–61. https://doi.org/10.1021/bc400490z.

APPENDIX A

SPRINGER NATURE LICENSE TERMS AND CONDITIONS

Oct 30, 2025

This Agreement between Dudu Boyvat/ Italian Institute of Technology ("You") and Springer Nature ("Springer Nature") consistsof your license details and the terms and conditions provided by Springer Nature and Copyright Clearance Center.

License Number	6138740325733
License date	Oct 30, 2025
Licensed ContentPublisher	Springer Nature
Licensed ContentPublication	Nature Reviews Genetics
Licensed Content Title	Cell-free gene expression: an expanded repertoire of applications
Licensed Content Author	Adam D. Silverman et al
Licensed Content Date	Nov 28, 2019
Type of Use	Thesis/Dissertation